Recherche de marqueurs biomécaniques améliorant le diagnostic et l'évaluation thérapeutique d'une scoliose idiopathique de l'adolescent

Tristan Langlais

HESAM UNIVERSITÉ

Arts et Métiers Sciences et Technologies

ÉCOLE DOCTORALE SCIENCES DES MÉTIERS DE L'INGÉNIEUR

Institut de biomécanique humaine Georges Charpak – Campus de Paris

THÈSE

Présentée par : **Tristan LANGLAIS**

soutenue le : 16 décembre 2022

pour obtenir le grade de : Docteur d'HESAM Université

préparée à : **École Nationale Supérieure d'Arts et Métiers**

Spécialité : **Biomécanique**

Recherche de paramètres biomécaniques améliorant le diagnostic et l'évaluation thérapeutique d'une scoliose idiopathique de l'adolescent

THÈSE dirigée par Madame Wafa SKALLI

et encadrée par Messieurs Claudio VERGARI et Raphaël VIALLE

Jury

M. Jérôme SALES DE GAUZY, Professeur des universités en orthopédie infantile, Toulouse Université	Rapporteur
M. Pascal SWIDER, Professeur des universités, Institut de mécanique des fluides, Toulouse Université	Rapporteur
Mme Kariman ABELIN-GENEVOIS, Doctorat ès sciences, Chirurgienne, Centres des Massues, Lyon	Examinatrice
Mme Wafa SKALLI, Professeur des universités, IBHGC, HESAM Université, Paris	Examinatrice
M. Claudio VERGARI, Doctorat ès sciences, IBHGC, HESAM Université, Paris	Examinateur
M. Raphaël VIALLE, Professeur des universités en orthopédie infantile, Sorbonne Université, Paris	Examinateur
M. Reinhard ZELLER, Professeur des universités en orthopédie infantile, Sick Kids, Toronto	Examinateur
M. Jean DUBOUSSET, Professeur émérite, Académie Nationale de médecine	Invité

THÈSE

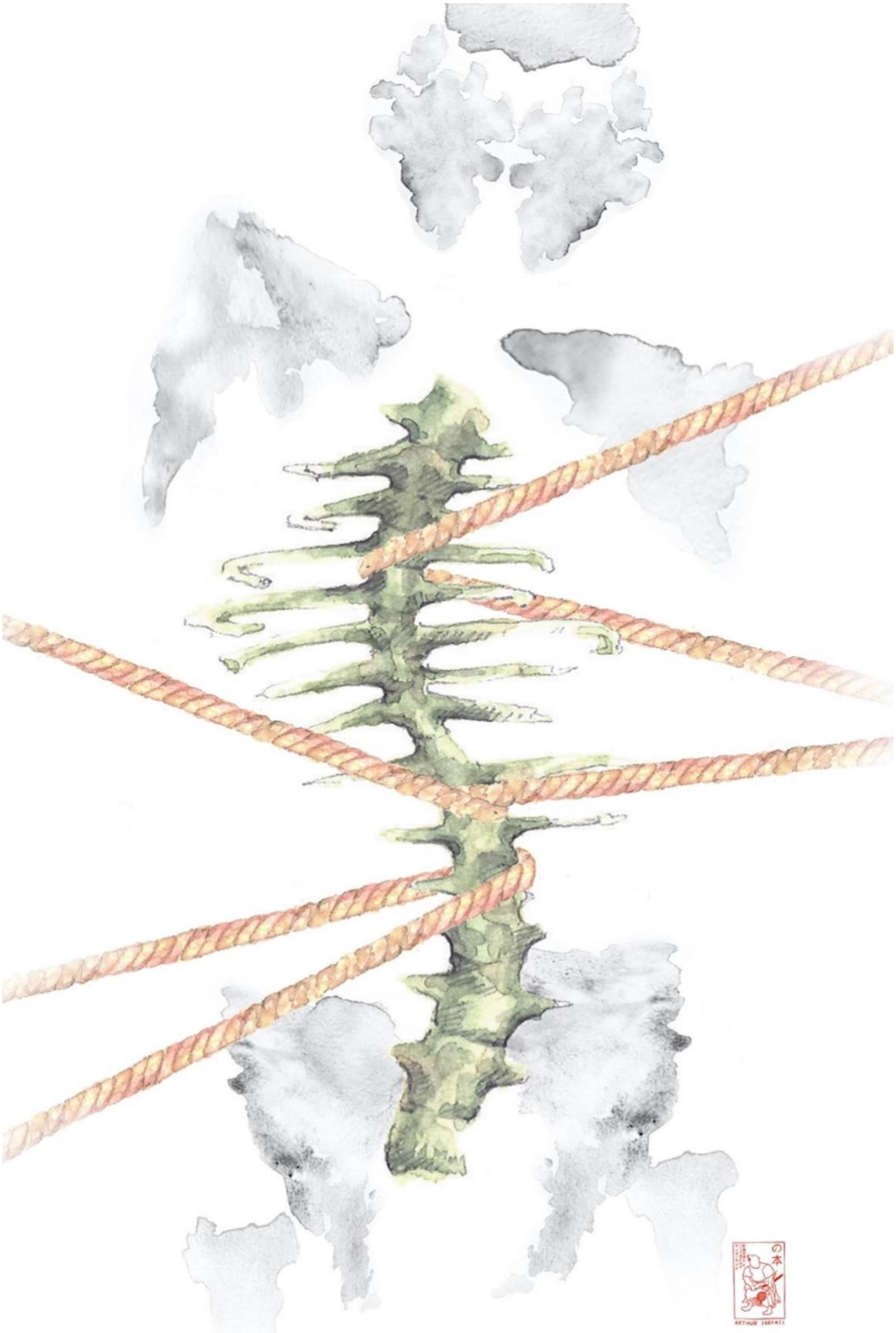

Remerciements

Je voudrais remercier l'ensemble du jury,

Madame le professeur Wafa Skalli pour m'avoir fait l'honneur de diriger cette thèse. Votre recherche permanente vers l'utilité clinique de nos travaux communs m'a permis de garder une vision pratique, critique et clinique. Merci.

Madame le docteur Kariman Abelin-Genevois pour avoir accepté de juger ce travail. C'est un plaisir et un honneur d'avoir ton regard avisé sur ce travail.

Monsieur le professeur Pascal Swider pour avoir accepté de juger ce travail. C'est probablement le début d'une étroite collaboration.

Monsieur le professeur Raphaël Vialle de m'avoir accompagné à la fin de mon internat et durant mes deux premières années de mon clinicat. Votre sens de l'organisation et de l'efficacité m'a permis d'avancer dans mon parcours professionnel avec sang-froid.

Monsieur Claudio Vergari pour m'avoir accompagné et encadré avec rigueur et bienveillance. J'espère que notre collaboration qui a débuté en 2016 se poursuivra car nous formons une solide équipe.

Monsieur le professeur Jérôme Sales de Gauzy pour votre présence au sein du jury. Vos qualités humaines et professionnelles forcent le respect. Je ne vous remercierai jamais assez de votre bienveillance à mon égard. Merci.

Monsieur le professeur Reinhard Zeller pour votre présence au sein du jury. Je vous remercie d'avoir accepté de poser un regard éclairé sur ce travail.

Monsieur le professeur Jean Dubousset pour votre présence au sein du jury. Je vous remercie sincèrement de m'avoir aidé et accompagné tout au long de ses travaux à l'institut. Je suis admiratif de votre expérience clinique et dévouement auprès de nous (« les apprentis chirurgiens »).

Je voudrais associer à ces remerciements,

Monsieur le **docteur Christian Morin**, le **docteur Pierre Mary**, le **docteur Pierre Chrestian**, le **professeur Christophe Glorion** et le **professeur Pascal Boileau** qui à chaque instant de doute ou de questionnement me conseille et me guide sans relâche, avec bienveillance, dans mon parcours clinique et professionnel.

Mes co-chefs et internes de Trousseau et Necker enfants malades qui m'ont permis d'investir du temps dans ce travail. Ainsi que **l'équipe du professeur Stéphanie Pannier** qui m'a accordé du temps libre durant cette dernière année afin de me consacrer aux travaux de cette thèse.

La fondation ParisTech et les différents mécènes du programme de chaire BiomecAM en modélisation biomécanique personnalisée (**Société Générale, COVEA, Société Protéor** et tout particulièrement la **Fondation Yves Cotrel** pour les recherches en pathologie rachidienne), qui ont permis de financer une partie importante des recherches sur lesquelles je me suis appuyé.

Les différents participants et centres investigateurs de la cohorte de l'indice de sévérité.

Mes collègues de l'institut de biomécanique humaine Georges Charpak et tout particulièrement **Marine Souq** qui a été d'une aide et d'une efficacité redoutable depuis le début de notre collaboration.

Le personnel médical et paramédical de tous les centres hospitaliers dont j'ai eu la chance d'intégrer.

Je souhaiterais remercier **mes coéquipiers, ma famille, ma femme et mes fils** qui m'apportent un équilibre, une harmonie, un bonheur et une énergie débordante quotidiennement.

Enfin je tiens à remercier tous **les patients « petits » et « grands »** pour tout ce qu'ils m'apportent dans ma pratique et plus particulièrement tous ceux qui ont participé à l'élaboration de cette thèse.

Table des matières

I - Introduction

La scoliose idiopathique de l'adolescent est une déformation tridimensionnelle de la colonne vertébrale d'origine multifactorielle, propre à l'espèce humaine bipède (Cheng et al. 2015), atteints 1 à 3 % des enfants (Lonstein 1994), préférentiellement les filles (dans 80% de cas) et les adolescents de l'hémisphère nord (Grivas et al. 2006).

L'évolution naturelle d'une courbure scoliotique est de s'aggraver en période de forte croissance rachidienne comme durant la puberté. Certaines scolioses n'évoluent pas ou peu mais le mécanisme de ces deux évolutions reste incompris. L'aggravation d'une scoliose en forte période de croissance impose un dépistage précoce et un suivi régulier clinique et radiographique. La mise en place d'un traitement orthopédique précoce permet de freiner l'aggravation de la courbure et éviter dans de nombreux cas une intervention chirurgicale (Nachemson et Peterson 1995). L'enjeu principal est le dépistage précoce de la scoliose et de sa potentielle aggravation afin d'y adapter un traitement personnalisé. Le second enjeu est l'évaluation du traitement mis en place. La multiplicité et le développement des techniques de traitement orthopédique ou chirurgical nous conduisent à utiliser des paramètres quantitatifs, objectifs et fiables à l'évaluation de nos pratiques.

Les dernières innovations technologiques ont permis une évaluation objective tridimensionnelle de la déformation osseuse, de l'équilibre global, de la barycentremétrie résultant de la reconstruction de l'enveloppe externe mais également des perturbations du disque intervertébral. Les travaux fondamentaux issus de ces techniques ont abouti à l'évaluation de nombreux paramètres biomécaniques personnalisés, fiables, prédicteurs de l'évolution d'une courbure et évaluant l'efficacité d'un traitement correcteur.

L'objectif de cette thèse est de déterminer la pertinence des facteurs biomécaniques issus de la reconstruction tridimensionnelle de la colonne vertébrale osseuse, de l'enveloppe externe et de l'analyse du disque intervertébral par élastographie ultrasonore qui permette d'aider le clinicien au diagnostic et à l'évaluation thérapeutique d'une scoliose idiopathique.

Dans ce but, notre exposé s'articulera autour d'une partie rappelant la définition, la caractérisation et le suivi d'une scoliose idiopathique, une seconde partie où nous passerons en revue les différents facteurs biomécaniques possibles et exposerons les différentes problématiques liées à cette revue. Dans un second temps, nous rapporterons les travaux de

thèse à visée diagnostique dans lequel nous aborderons l'alignement global puis la distribution des masses du patient scoliotique. Enfin, nous terminerons notre exposé dans un chapitre thérapeutique dans lequel nous nous focaliserons sur les changements de la distribution des masses et des propriétés biomécaniques du disque intervertébral après une chirurgie de correction et fusion vertébrale postérieure.

II - Définition et contexte clinique

II.1 Définition

Une scoliose est une déformation tridimensionnelle de la colonne vertébrale définie dans le plan coronal par une courbure d'au moins 10°, une diminution voire une inversion des courbures sagittales et une rotation axiale (Coonrad et al. 1998). Son étiopathogénie est multifactorielle (Kouwenhoven et Castelein 2008) et la responsabilité de ses différents facteurs (telle que la génétique, les systèmes nerveux, osseux, hormonales ou disco-musculo-ligamentaires) reste encore mal compris. L'enjeu de la recherche sur la pathogénie est de faire la distinction entre les facteurs préexistants et inducteurs de la déformation avec les mécanismes de compensation et d'adaptation secondaire. La scoliose est dite « idiopathique » lorsque la cause induisant la déformation est inconnue. Selon la société de recherche pour la scoliose (SRS : Scoliosis Research Society - https://www.srs.org), le terme « adolescent » signifie que la déformation est apparue juste avant ou au début de la puberté et avant la maturation squelettique, ce qui correspond à une fourchette allant de 10 ans à 17 ans.

II.2 Le diagnostic

Le diagnostic d'une scoliose est clinique et repose sur la mise en évidence d'une gibbosité, ce qui traduit une rotation axiale vertébrale (figure 1: test Adams : enfant penché en avant, genou tendu, tête et scapula enroulées en avant). C'est le signe pathognomonique de la scoliose. L'examen physique est complété par l'analyse coronale de l'équilibre de la

ceinture scapulaire, de la taille (figure 2: exemple du signe de la lucarne) et du bassin puis par la mesure des flèches sagittales.

Figure 1: Le test d'Adams (sur l'image de droite) révèle une gibbosité thoracique droite dans le cas d'une scoliose thoracique droite (Langlais et Sales de Gauzy 2019).

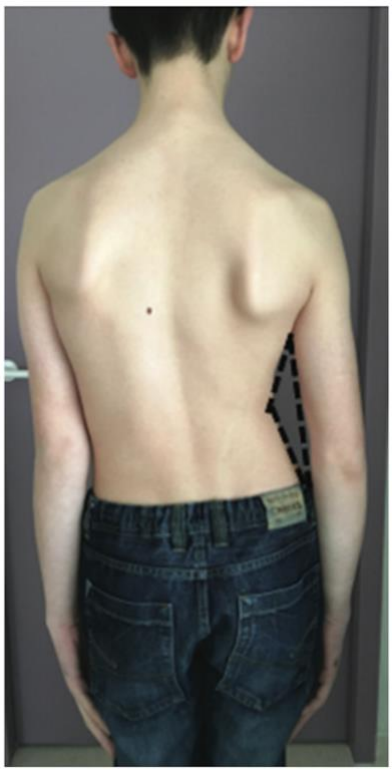

Figure 2: Exemple du signe de la lucarne. La lucarne traduit une asymétrie du pli de la taille et est délimitée sur la figure par des traits discontinus (Langlais et Sales de Gauzy 2019).

Une radiographie du rachis de face et de profil complète le bilan diagnostique. Depuis 2007, le système de radiographie biplanaire basse dose EOS® permet l'acquisition en 20 à 30 secondes d'un cliché numérique du squelette entier face et profil debout, avec une diminution de huit à dix fois du taux d'irradiation (jusqu'à un facteur 15 pour le protocole microdosse) (Dubousset et al. 2007; Ilharreborde et al. 2016) par rapport à une radiographie conventionnelle. Le second intérêt majeur de cette technique acquisition est l'analyse tridimensionnelle personnalisée du rachis, du bassin et ainsi ouvre les perspectives concernant l'analyse du plan axial (figure 3). Cette technique d'imagerie s'est inscrite comme l'examen de référence pour le diagnostic et le suivi des scolioses idiopathiques.

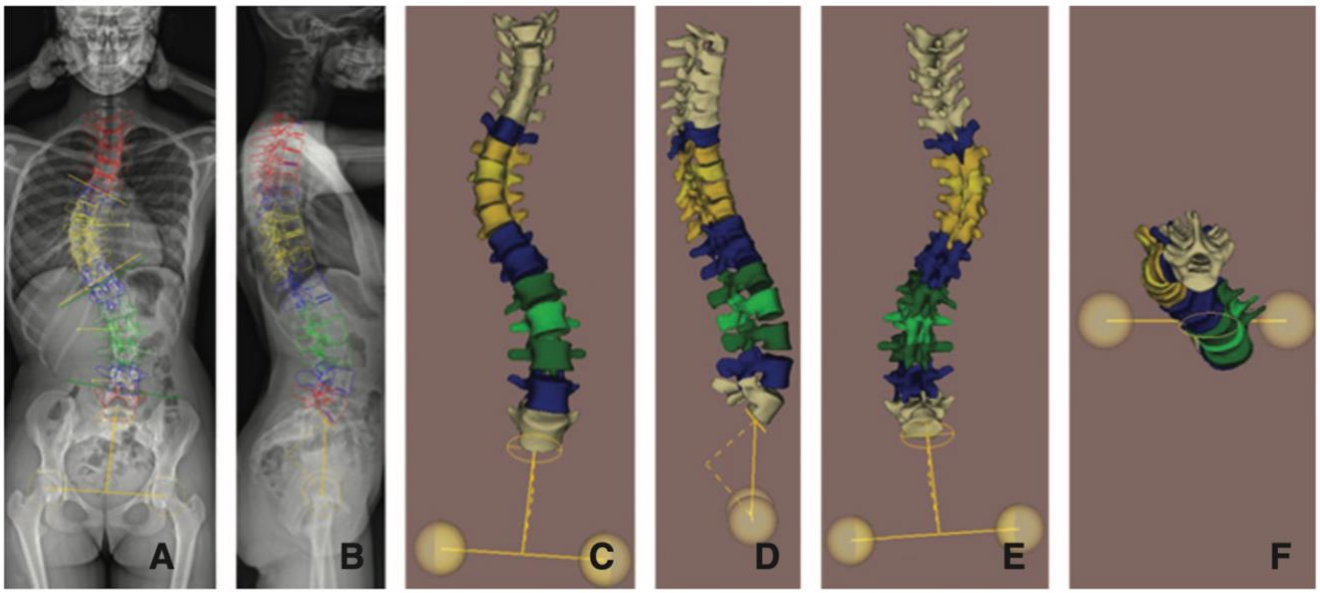

Figure 3: Reconstruction 3D d'une scoliose thoracique droite issue d'une radiographie biplanaire basse dose debout de face (A) et de profil (B). Reconstruction 3D vue de face (C), de profil (D), de derrière (E) et du dessus (F) (Langlais et Sales de Gauzy 2019).

II.3 La caractérisation d'une déformation scoliotique

Une scoliose est décrite selon (figure 4) :

- son côté qui est défini par la convexité de la courbure

- ses vertèbres limites supérieures et inférieures qui correspondent aux vertèbres les plus inclinées dans le plan coronal

- ses niveaux jonctionnels supérieurs et inférieurs qui correspondent :
1) Soit à un disque intervertébral : il est défini comme disque situé entre deux courbures structurales ou entre une courbure structurale et une contre courbure de compensation et peut être soupçonné sur le cliché de face en regardant la rotation axiale de la projection des pédicules.
2) soit à une vertèbre : elle est définie comme la vertèbre qui est surmontée d'un disque qui tourne (ou baille) dans un sens (ou d'un côté) et du disque du dessous qui tourne (ou baille) en sens (ou du côté) inverse du premier disque.

- son sommet qui correspond à la vertèbre ou le disque intervertébral dont la translation latérale est la plus importante dans le plan coronal par rapport à la ligne médiane.

- les vertèbres dites « neutres » supérieure et inférieure correspondent aux vertèbres dont la rotation est quasi nulle.

- sa localisation qui dépend du sommet de la courbure (vertèbre ou disque intervertébral) : une scoliose cervico-thoracique est définie par un sommet entre la vertèbre C7 et le disque intervertébral T1-T2, une scoliose thoracique entre T2 et T11-T12, une scoliose thoraco-lombaire entre T12 et L1, une scoliose lombaire entre L1-L2 et L4.

- le nombre de courbure : unique, double ou triple

- son angle de Cobb (décrit en 1948 par J.R Cobb) qui correspond à l'angle formé par la droite tangentielle au plateau supérieur de la vertèbre limite supérieure avec la droite tangentielle au plateau inférieur de la vertèbre limite inférieure de la même courbure.

- sa rigidité dont l'origine reste inconnue. Elle peut être évaluée à l'examen clinique par une traction manuelle de la tête qui permet au clinicien d'apprécier la réductibilité de la gibbosité, de la courbure et la correction de l'équilibre des épaules et de la taille. Cette appréciation est subjective. La rigidité d'une courbure peut être évaluée par des clichés en suspension (ou en traction) ou en inclinaison latérale maximum (dit « en bending »). L'angle de Cobb frontal est calculé et renseigne ainsi sur la réductibilité d'une courbure.

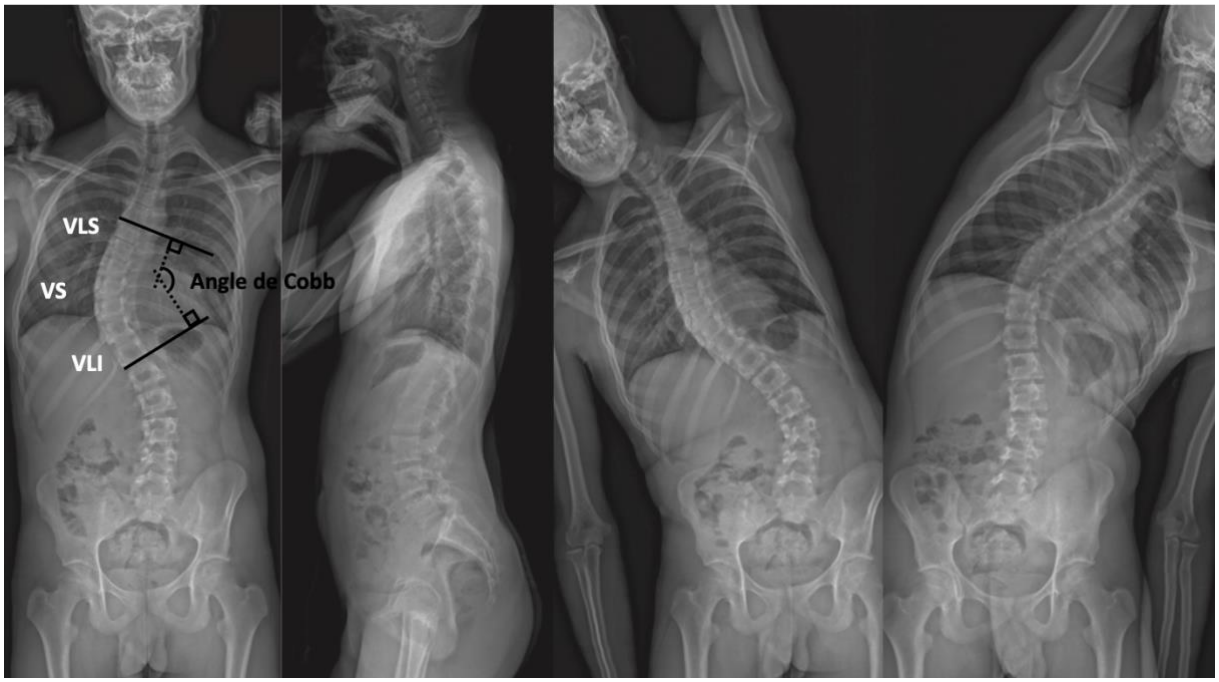

Figure 4: Exemple d'une scoliose thoracique droite à courbure unique. La vertèbre limite supérieure (VLS) correspond à la 6ème vertèbre thoracique (T6), la vertèbre sommet (VS) à T9 et la limite inférieure (VLI) à T12. Le niveau jonctionnel supérieur correspond au disque intervertébral T4-T5 et T12-L1 pour la jonction inférieure. La vertèbre neutre supérieure est la vertèbre T5 alors que l'inférieure est T12. Les clichés en inclinaison latérale maximum sont visibles sur les images de droites (inclinaison droite puis gauche). La contre courbure lombaire est souple alors que la courbure thoracique semble se réduire d'environ 30%.

II.4 L'histoire naturelle d'une scoliose idiopathique de l'adolescent

Chaque courbure suit une évolution qui lui est propre. Cependant, la tendance naturelle d'une courbure est de s'aggraver durant une période de forte croissance rachidienne (Dubousset 1999; Duval-Beaupère et Lamireau 1985). Certaines scolioses sont dites progressives c'est-à-dire une augmentation de l'angle de Cobb d'au moins 6° à deux consultations successives (Richards et al. 2005). A contrario, une scoliose non progressive est dite stable mais le mécanisme de ces deux évolutions possibles reste incompris (Altaf et al. 2013). L'enjeu est de pouvoir prédire, précocement, l'évolution d'une scoliose car il permettrait la mise en place d'une stratégie thérapeutique précoce et ainsi limiter la progression de la déformation durant la période de croissance rachidienne. Il convient d'ajouter un enjeu économique car la possibilité d'identifier, précocement, une scoliose stable permettrait de proposer uniquement une simple surveillance clinique et ainsi limiter le nombre de radiographie et de la mise en place d'un corset à tort.

II.5 La prise en charge thérapeutique

L'objectif du traitement est de contenir l'aggravation de la scoliose durant la croissance et d'obtenir en fin de croissance une (des) courbure(s) équilibrée(s), et harmonieuse(s) durant l'âge adulte permettant une vie normale.

- *La surveillance simple*

Une simple surveillance clinique et radiologique peut être proposée dans deux situations : 1) au décours d'un premier bilan pour déterminer le caractère évolutif de la courbure ; 2) pour des scolioses évolutives d'angulation entre 10 et 20° en dehors de la période pubertaire. La surveillance est espacée de six mois mais ce délai peut être ramené à trois mois lorsque la période pubertaire approche. Il consiste à un examen physique (mesure de la gibbosité, évaluation de l'équilibre) et une radiographie biplanaire du rachis en entier et debout.

- *Le traitement orthopédique*

L'objectif du traitement orthopédique est de « freiner » l'évolution de la courbure

pendant la phase de croissance sans entraver le bon développement de la cage thoracique. Ce traitement a pour but de terminer la croissance avec une courbure résiduelle équilibrée dans le plan coronal et sagittal et ne nécessitant pas de traitement chirurgical. Le plâtre élongation, dérotation et flexion (EDF) de Cotrel et Morel garde une place dans certaine indication « coup de frein », le corset est le traitement orthopédique utilisé par l'ensemble de la communauté internationale (Nachemson et Peterson 1995; Weinstein et al. 2013). La décision de la mise en place d'un corset repose sur des critères quantitatifs, conformément aux directives de la société internationale du traitement et par réhabilitation de la scoliose (SOSORT), c'est-à-dire un angle de Cobb supérieur à 25° et un signe de Risser inférieur ou égale à 2, ou une augmentation de 5° de l'angle de Cobb ou de la rotation axiale des vertèbres en 6 mois (Negrini et al. 2018), ainsi qu'une évaluation du profil clinique (figure 5). La société de recherche pour la scoliose (SRS : Scoliosis Research Society - https://www.srs.org), définis le succès d'un traitement orthopédique si l'aggravation angulaire est inférieure ou égale à 5° à maturité osseuse. Le taux de succès d'un traitement bien conduit est d'environ 75% (Nachemson et Peterson 1995; Weinstein et al. 2013).

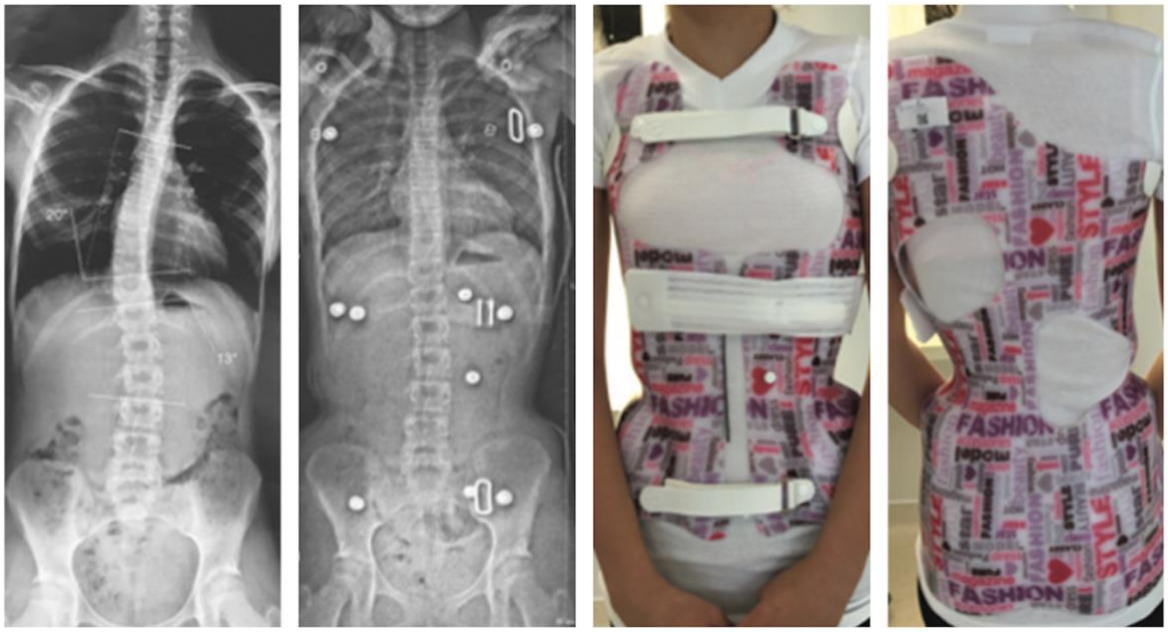

Figure 5: Scoliose thoracique droite traitée par corset de Cheneau-Toulouse-Münster (Langlais et Sales de Gauzy 2019).

- Le traitement chirurgical

L'objectif du traitement chirurgical est d'arrêter la progression de la courbure, d'obtenir une correction équilibrée et harmonieuse dans les trois plans de l'espace et d'aboutir à une arthrodèse de bonne qualité et pérenne dans le temps (figure 6). L'indication chirurgicale repose essentiellement sur trois critères : le déséquilibre, le type et la sévérité de la courbure. Une étude multicentrique française rétrospective de 258 scolioses opérées avec 20 ans de suivi (Pesenti et al. 2015) a permis de retenir les indications chirurgicales suivantes: une scoliose thoracique de plus de 45° d'angle de Cobb ou une scoliose thoraco-lombaire et lombaire de plus de 35° d'angle de Cobb.

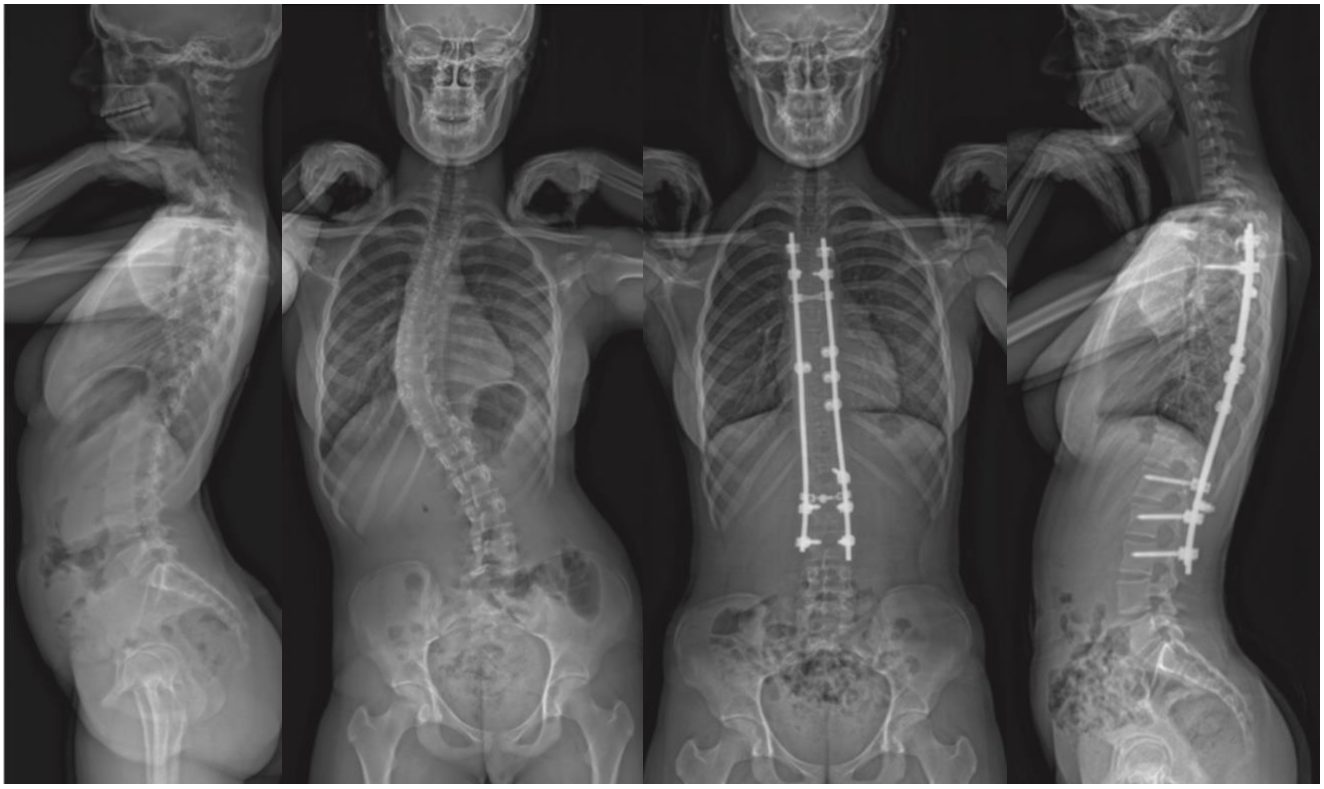

Figure 6: Correction et fusion postérieure T4-L3 d'une scoliose thoracique droite (Langlais, Vialle, et Sales de Gauzy 2020).

II.6 Résumé

La scoliose idiopathique de l'adolescent est une déformation tridimensionnelle dont son aggravation est liée à la croissance rachidienne. La stratégie thérapeutique dépend de la progression ou non de la déformation. Pour l'adolescent(e), le traitement par corset est difficile à accepter dans une société où l'image de soi est devenue incontournable. D'autant plus dans des régions où les conditions métrologiques sont un frein à l'observance du port du corset. Dans ce sens, il est important de ne pas surtraiter mais d'être conscient que le traitement par corset à un taux succès d'environ 75% s'il a été mis en place précocement et avec une bonne observance (Nachemson et Peterson 1995; Weinstein et al. 2013). L'enjeu est double : 1) pouvoir prédire une possible évolution afin d'adapter sa stratégie thérapeutique à un stade précoce ; 2) évaluer la stratégie thérapeutique afin de l'adapter à l'évolution de(s) la courbure(s). Le suivi de la croissance résiduelle, le bilan clinique et radiographique permet d'apporter au clinicien une aide précieuse à la prédiction de cette évolution et à l'évaluation thérapeutique. L'exemple de la scoliose thoracique droite de la figure 6 nous interpelle sur les caractéristiques géométriques des vertèbres, l'asymétrie des parties molles ou encore les contraintes exercées sur les disques intervertébraux lombaires en rapport avec l'inclinaison et la rotation axiale des vertèbres sus-jacents. Ces différentes réflexions nous interrogent sur l'existence de potentiel facteur ou paramètre de progression ou d'évaluation thérapeutique.

III - Revue de la littérature des facteurs et paramètres contribuant à aider au diagnostic d'une scoliose idiopathique progressive et à son évaluation thérapeutique

III.1 Les facteurs liés à la croissance

Les lois évolutives de Madame Duval-Beaupère regroupent plusieurs facteurs (tels que la croissance du rachis, la maturation pubertaire et le test de Risser) et ont été établies pour des scolioses idiopathiques juvéniles et de l'adolescent de moins de 30° (Duval-Beaupère et Lamireau 1985). Le diagramme de Duval-Beaupère comporte une courbe représentant l'aggravation angulaire d'une scoliose (en rouge) et une autre décrivant l'accroissement annuel du segment rachidien en cm (en bleu) (figure 7).

L'aggravation angulaire annuelle d'une courbure comporte trois pentes :

- Pente 1 (P1) : allant de l'âge de 4 ans au début de la puberté ;
- Pente 2 (P2) : débutante au point P finissant à la fin de la croissance du rachis soit le point R. Le point P correspond aux premiers poils pubiens ou saillie du mamelon. Le point R correspond à la fusion du noyau d'ossification de l'apophyse iliaque (test de Risser positif ou Risser = 4) (figure 8) (Risser 1958)
- Pente 3 (P3) : l'aggravation à l'âge adulte est progressive.

Ces pentes montrent que le risque de progression est maximal au moment de la croissance pubertaire. Ces diagrammes sont d'une grande aide clinique et permettent en consultation de situer un enfant sur la courbe afin de prédire son évolution et d'adapter son attitude thérapeutique.

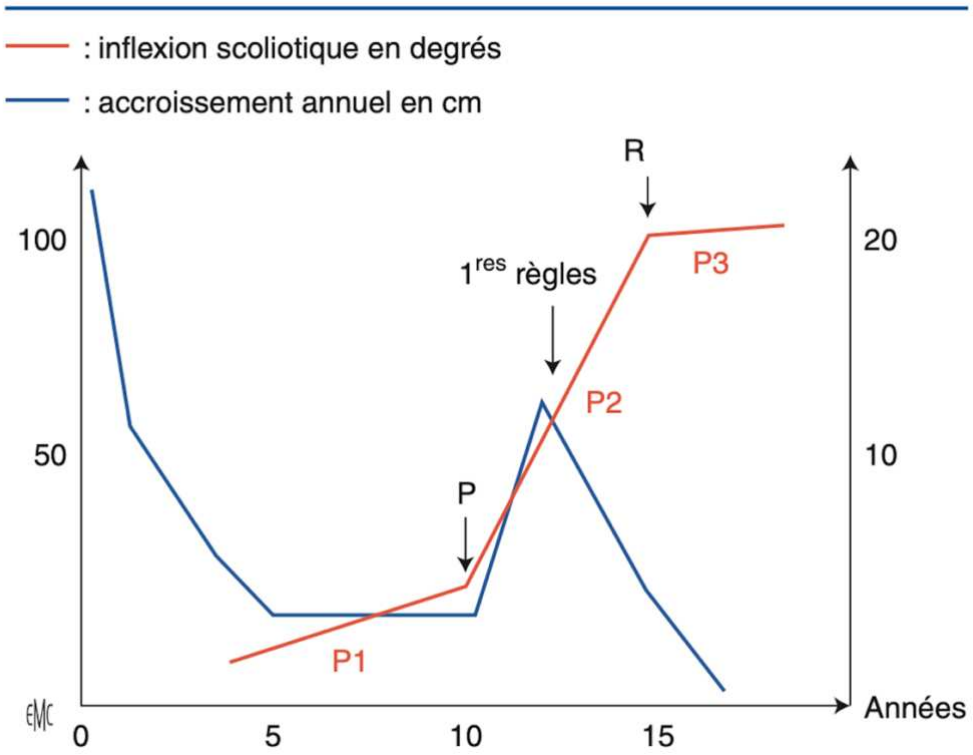

Figure 7: Courbes évolutives de Duval-Beaupère (Duval-Beaupère et Lamireau 1985)

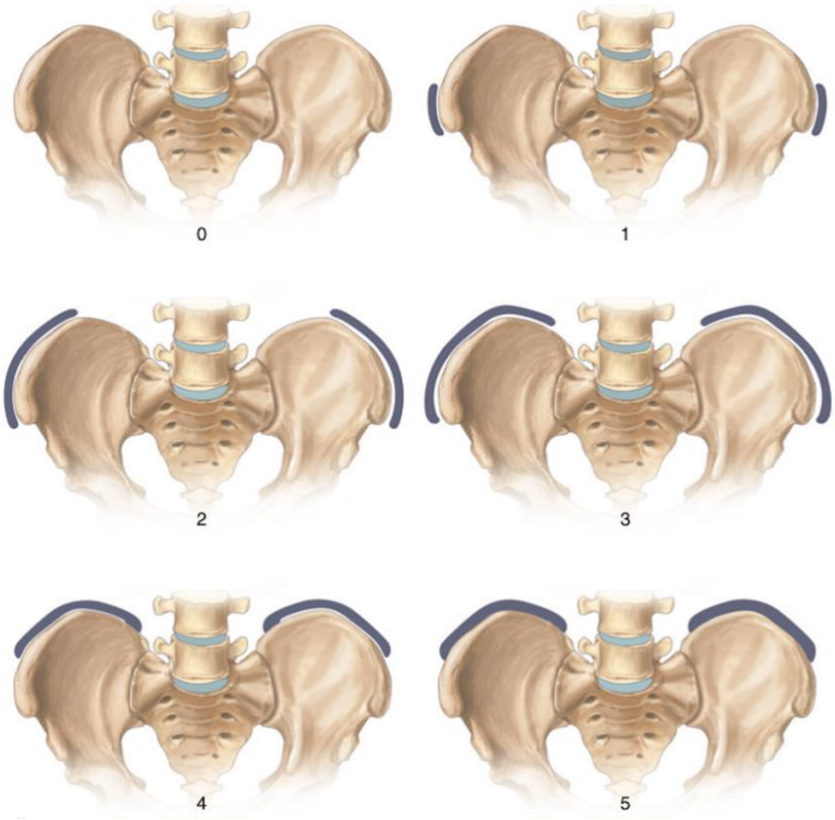

Figure 8: Détermination du stade de Risser (A). Risser 1 (B). Risser 3 (C). Le Risser 0 signifie qu'il n'y a aucune ossification. L'aile iliaque est ensuite divisée en trois, définissant les trois premiers stades d'ossification de l'apophyse. Le Risser 4 correspond au début de la fusion postérieure alors que le Risser 5 est défini comme une fusion complète (Risser 1958).

En résumé ces facteurs informent sur la situation d'une scoliose sur la courbe évolutive en fonction de la maturation squelettique mais ne peuvent prédire le caractère stable ou progressif d'une courbure.

III.2 Les paramètres radiographiques 2D du rachis

L'angle de Cobb coronal de la courbure (décrit en 1948 par J.R Cobb), à la consultation initiale, est un facteur prédictif bien décrit de l'évolution d'une courbure scoliotique idiopathique (Lonstein et Carlson 1984). D'après Tan et al., pour un angle de Cobb initial supérieur à 25°, la valeur prédictive positive était de 68,4 % (soit la probabilité d'avoir une

scoliose évolutive au-delà de 30° à la fin de la maturation squelettique) alors que pour un angle inférieur à 25°, la valeur prédictive négative était de 91,9 % (soit la probabilité de ne pas avoir une scoliose au-delà de 30° à la fin de la maturation squelettique) (Tan et al. 2009). La mesure de l'angle de Cobb sur une radiographie plane présente certains inconvénients. D'une part, le positionnement du patient influence la valeur de l'angle Cobb. Selon Schmid et al., une rotation vers la vertèbre apicale (soit une rotation droite pour une scoliose droite) de 15° diminue l'angle de Cobb de 11% et une rotation de 30° diminue l'angle de 23% (Schmid et al. 2016). D'autre part, il faut considérer la reproductibilité interopérateur qui est estimée entre 2.3 et 9° pour une mesure plane à l'aide d'un goniomètre (Labelle et al. 1995). Le développement des méthodes de reconstruction 3D a permis les mesures de l'angle de Cobb strictement de face (Pasha et al. 2016) ou dans le plan de la courbure maximale (Illés, Lavaste, et Dubousset 2019) et amélioré la reproductibilité interopérateur estimé entre 3.5 et 6.2° (Humbert et al. 2009; Ilharreborde et al. 2011). Cependant, l'angle de Cobb ne représente qu'une projection de la déformation (la théorie de l'ombre chinoise selon Jean Dubousset) et n'apporte pas d'information sur la déformation du plan axial et sagittal (Illés, Lavaste, et Dubousset 2019).

III.3 Les paramètres issus de la reconstruction 3D de la colonne osseuse

Depuis dix ans, le développement des radiographies numériques et des méthodes de reconstruction 3D ont permis de décrire plusieurs paramètres influençant l'évolution d'une courbure scoliotique. Les différents travaux ont abouti à la création de deux modèles prédictifs, dont l'objectif est de prédire la progression d'une courbure à la première consultation, que nous exposerons dans un second temps.

III.3.1 Les paramètres liés à la déformation du plan axial et sagittal

Ces paramètres ont été définis dans les travaux de thèse de X. Drevelle, N. Champain et A. Courvoisier à l'institut de biomécanique humaine Georges Charpak.

- *La rotation axiale de la vertèbre sommet*

La méthode de mesure, issue de la reconstruction 3D de radiographie biplanaire, a montré une très bonne fiabilité intra et interopérateur (Gille et al. 2007; Boyer et al. 2018). La mesure de la rotation axiale de la vertèbre sommet permettrait de distinguer différents types de courbure (Lee et al. 2020) et jouerait un rôle dans la prédiction d'une scoliose progressive. De plus, l'analyse de la correction de cette rotation est un paramètre objectif permettant d'évaluer l'efficacité d'une technique de correction (Dalal et al. 2011; Courvoisier et al. 2015).

- *La rotation intervertébrale axiale*

La rotation intervertébrale axiale est définie comme la rotation entre deux vertèbres adjacentes dans le plan axial avec comme référentiel l'une des deux vertèbres (Perdriolle 1979). La mesure de cette rotation au niveau jonctionnel supérieur et inférieur a montré son importance dans la prédiction d'une courbure progressive (Nault et al. 2013; Courvoisier et al. 2015).

- *L'indice de torsion*

Il représente la moyenne de la somme des rotations axiales intervertébrales de la jonction inférieure au sommet et du sommet à la jonction supérieure (Steib et al. 2004). Cet indice de torsion semble lié à la progression d'une courbure (Nault et al. 2013) et permet une évaluation dans le plan axial d'une technique de correction (Steib et al. 2004).

- *L'indice d'hypocyphose*

L'indice hypocyphose est défini comme la différence entre la cyphose (ou lordose) locale du sujet donné à l'apex de la courbure thoracique et la valeur moyenne au niveau équivalent pour les sujets non scoliotiques (Skalli et al. 2017). Ce paramètre semble également être lié à la progression d'une scoliose (Skalli et al. 2017).

III.3.2 Les paramètres morphologiques de la vertèbre

- *La cunéiformisation des vertèbres*

La cunéiformisation est un processus dérivant de la combinaison d'une rotation et d'une torsion des vertèbres. Elle peut être mesurée comme l'angle maximal entre le plateau supérieur et le plateau inférieur d'une vertèbre d'intérêt (Nault et al. 2013). Cet angle augmente proportionnellement avec l'angle de Cobb coronal dans les scolioses thoraciques (Villemure et al. 2001) mais il ne semble pas permettre de distinguer une scoliose progressive dès la première radiographie (Nault et al. 2013).

- *La hauteur et la largeur des vertèbres*

Nault et al. ont défini le ratio hauteur/largeur d'une vertèbre (Nault et al. 2013). Ce ratio de la colonne vertébrale dans son ensemble semble être plus élevé pour les scolioses stables (Nault et al. 2013).

- *La slenderness*

Vergari et al. ont défini la slenderness comme le rapport entre la hauteur vertébrale et la taille transversale de la vertèbre, en tenant compte de la forme de la section transversale (Vergari et al. 2020). Récemment, le résultat de l'évaluation de ce paramètre a montré qu'il n'était pas un signe de détection précoce d'une scoliose progressive (Claudio Vergari et al. 2022).

III.3.3 Les modèles prédictifs de progression

Les travaux fondamentaux sur les différents paramètres d'aggravation d'une scoliose ont débuté en 2001 et ont abouti, avec le soutien financier de la fondation Cotrel (https://www.fondationcotrel.org), à la validation d'un marqueur biomécanique défini comme un indice de sévérité renseignant sur le caractère progressif d'une scoliose (Skalli et al. 2017; Vergari et al. 2021). Par analogie à la définition d'un marqueur biologique, nous définissons un marqueur biomécanique comme un indicateur des processus biomécaniques normaux, pathogènes, ou liés à une(des) intervention(s) thérapeutique(s). Chaque marqueur

répond à un besoin, est mesuré de manière objective, peut être qualitatif ou quantitatif et doit être pertinent, utile et accessible en pratique clinique.

Cet indice repose sur des paramètres 3D issus d'une analyse factorielle discriminante. La progression d'une courbure est définie par la mise en place d'un corset par le clinicien selon les critères définis par la SOSORT (décrit dans la partie du traitement orthopédique). Une scoliose était définie stable si le test de Risser était supérieur à 3, l'angle de Cobb inférieur à 25° et aucun traitement par corset n'avaient été commencés. Le modèle a été validé chez 205 adolescents présentant une scoliose idiopathique, d'âge supérieur à 10 ans, un test de Risser de 0, 1 ou 2, un angle de Cobb coronal compris entre 10 et 25° et sans traitement préalable. Les paramètres incluent dans le modèle étaient : le signe de Risser, l'angle de Cobb coronal de la courbure sur la radiographie de face, la rotation axiale de la vertèbre sommet, la rotation intervertébrale de la zone jonctionnelle supérieure et inférieure, l'indice de torsion et l'indice d'hypocyphose. L'indice de sévérité a permis de classer correctement 82 % des patients comme étant progressifs ou stables, avec un taux de 8 % de patients qui ne pouvait être classé avec certitude dans aucune des deux catégories. Le modèle a montré dans cette cohorte, une sensibilité de 87% et une spécificité de 78%, conduisant à une valeur prédictive positive de 78% et une valeur prédictive négative de 85%.

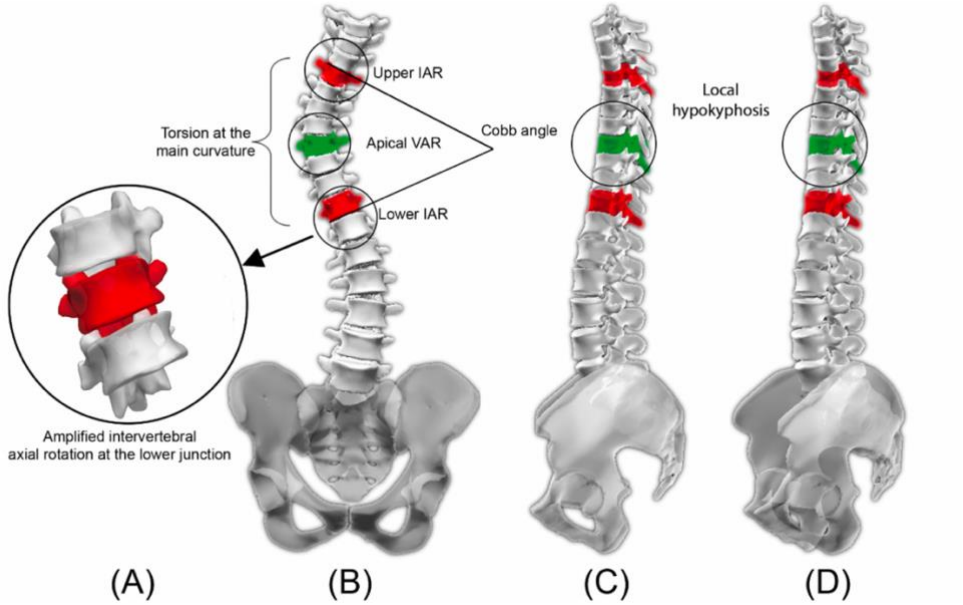

Figure 9: Représentation schématique du calcul de l'indice de sévérité de Skalli et al. (Skalli et al. 2017). On visualise sur la reconstruction de face (B) la mesure de l'angle de Cobb frontal, de la rotation axiale de la vertèbre sommet (en vert), de la rotation intervertébrale des jonctions supérieure et inférieure (en rouge) (A) et la représentation de l'indice de torsion. Sur la vue sagittale (C) et dans le plan élection (D) est représenté l'indice d'hypocyphose.

Parallèlement, un autre modèle prédictif a été élaboré et basé également sur l'analyse discriminante de paramètre biomécanique issu de la reconstruction 3D (Nault et al. 2013; 2020). Ce modèle a été validé sur 195 patients présentant une scoliose idiopathique de l'adolescent, d'âge supérieur à 10 ans, un test de Risser de 0 ou 1, un angle de Cobb coronal compris entre 11 et 40° et sans traitement préalable. Les paramètres incluent dans le modèle étaient : l'angle de Cobb coronal de la courbure sur la radiographie de face et dans le plan maximal de la déformation, l'angle de Cobb sagittal T4-T12 et L1-S1, la cunéiformisation de la vertèbre sommet et des disques intervertébraux T1-T2 et L4-L5, le ratio hauteur sur largeur (et profondeur) de la vertèbre T6, T12 et L4, le ratio de la longueur de la colonne T1-L5 sur la largeur (et profondeur) moyenne des vertèbres de T6 à T12 et L4, la rotation intervertébrale de la zone limite supérieur, inférieur, du sommet et de l'étage T12-L1 et l'indice de torsion. En

utilisant uniquement les informations disponibles lors de la première visite, le modèle de prédiction a pu expliquer 64,3 % de la variance de l'angle de Cobb final à maturité squelettique avec un R^2 = 0,618. Le modèle a montré dans cette cohorte, une sensibilité de 75% et une spécificité de 94%, conduisant à une valeur prédictive positive de 79% et une valeur prédictive négative de 94%, pour une concordance globale de 91%.

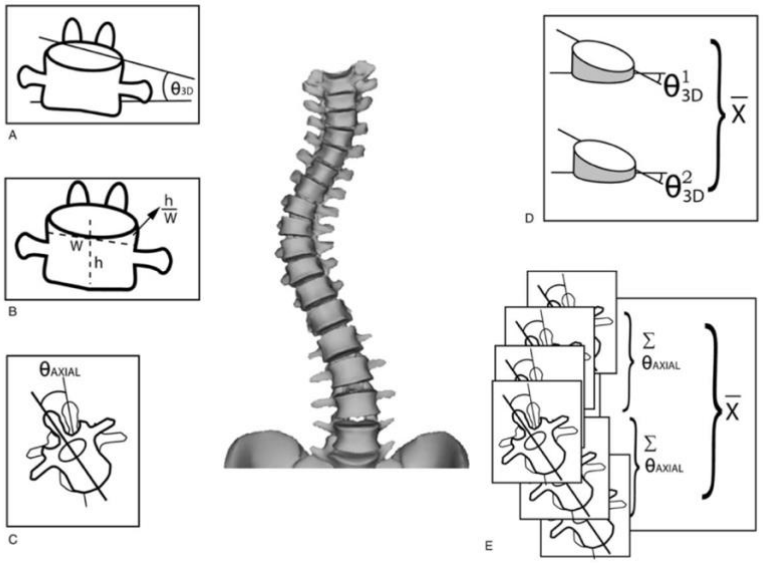

Figure 10: Représentation schématique du modèle prédictif de Nault et al. (Nault et al. 2020). On visualise la méthode de mesure de la cunéiformisation d'une vertèbre (A), de la somme de la cunéiformisation deux disques intervertébraux (D), du ratio hauteur sur largeur d'une vertèbre (B), de la rotation intervertébrale d'une vertèbre (C) et de l'indice de torsion (E).

Ce modèle prédictif se limite la prédiction de l'évolution de l'angle de Cobb à maturité squelettique. En d'autres termes, il s'intéresse uniquement à l'évolution de la courbure dans le plan frontal. Or, il est bien établi que la décision de traitement ne dépend pas uniquement de la mesure de l'angle de Cobb mais également de l'importance du déséquilibre coronal, de la rotation axiale ou encore de l'hypocyphose thoracique. Ainsi, nous nous intéresserons plutôt à l'indice de sévérité, la force de cet indice étant d'avoir validé et calculé ses performances sur un critère clinique (c'est-à-dire la décision de traiter). Néanmoins, d'autres paramètres tels que l'évaluation de l'alignement global, l'asymétrie du pli de taille ou la

barycentremétrie pourraient permettre d'affiner la pertinence et les performances de l'indice de sévérité.

III.3.4 Un paramètre lié à l'alignement

L'OD-HA est un paramètre quasi-invariant coronal et sagittal décrivant la position du processus odontoïde de C2 (approximativement le centre de la tête) par rapport au bassin et aux membres inférieurs, c'est un indicateur de l'alignement global du sujet (Amabile et al. 2016a). La mesure de l'OD-HA est un angle entre la position de l'odontoïde C2 (OD), et le point médian sur la ligne horizontale rejoignant les centres acétabulaires pelviens (HA). Cet angle est calculé à partir des reconstructions 3D issus des radiographies biplanaires. L'avantage de cette mesure, par rapport à des mesures comme la gîte de T9 ou C7 est de pouvoir apprécier l'alignement de la tête, de la colonne vertébrale entière, du pelvis et de l'axe du centre des têtes fémorales. La position de l'OD-HA est largement utilisée et a été mesurée de manière fiable chez des patients sains (Amabile et al. 2016a). Kim et al. ont montré la pertinence clinique de l'évaluation de l'angle OD-HA chez 199 adultes subissant une chirurgie de déformation du rachis. Les auteurs ont conclu que la mesure de l'angle OD-HA était corrélée au score de qualité de vie et aux complications mécaniques (Kim et al. 2021) alors que Ferrero et al. ont retrouvé des valeurs extrêmes d'ODHA chez des patients significativement âgés avec une déficience fonctionnelle importante. Ces sujets présentant une perturbation de l'alignement sagittal et une perte de lordose lombaire recrutaient des mécanismes compensatoires tels que la rétroversion pelvienne, l'hyperlordose cervicale pour maintenir la tête au-dessus du bassin (Ferrero et al. 2021). Hu et al. ont montré qu'il existait une corrélation positive (ou négative) entre la valeur de l'OD-HA sagittal (ou coronal) et l'âge (Hu et al. 2022) et qu'il existait des variations physiologiques de l'ordre de 1 à 3°. Ces variations physiologiques sont cohérentes avec le fait que l'angle OD-HA est quasi-invariant (Amabile et al. 2016a) et que la tête a tendance à rester au-dessus du bassin dans un petit cône de stabilité. Une étude de reproductibilité a été menée dans une population scoliotique sévère en pré et postopératoire sans différence significative entre les deux mesures et l'incertitude de mesure était d'environ 0,2° ou moins (Langlais et al. 2022).

Des études préliminaires mettent l'accent sur un possible déséquilibre sensoriel à un stade précoce (Guo et al. 2006; Assaiante et al. 2012) et les travaux précédents ont montré que

certains patients atteints de scoliose sévère pouvaient présenter un déséquilibre, quantifié par un OD-HA anormal (Langlais et al. 2022; Karam et al. 2022). Cependant, il n'est pas encore clair si une perturbation de l'alignement précoce peut être détectée dans la scoliose idiopathique de l'adolescent et renforcer l'indice de sévérité.

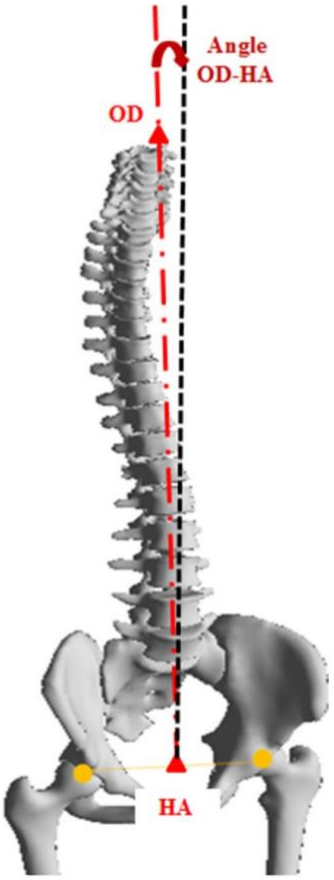

Figure 11: Représentation de l'angle OD-HA (Amabile et al. 2016a)

Ces différents paramètres sont issus de la reconstruction 3D de la colonne vertébrale et plus précisément des structures anatomiques osseuses. Les dernières avancées technologiques ont permis l'analyse des structures non osseuses et plus précisément de l'enveloppe externe. Les différents outils d'analyses de l'enveloppe externe se focalisent sur la caractérisation de son asymétrie.

III.4 Les paramètres issus de l'analyse de l'enveloppe externe

III.4.1 La topographie de surface

La topographie de surface est un outil non invasif, n'exposant pas l'adolescent aux rayons ionisants et qui permet de quantifier l'asymétrie de l'enveloppe externe du tronc. La topographie de surface du tronc a été validée dans le suivi (Bolzinger et al. 2021) et dans l'évaluation thérapeutique de patients (Gorton, Young, et Masso 2012; Gardner, Berryman, et Pynsent 2021) atteints de scoliose idiopathique. Cette technique utilise différents algorithmes selon les équipes et l'outil utilisé : il peut évaluer la proéminence des côtes pour Bolzinger et al., différents points anatomiques selon Mínquez et al. permettant de quantifier la déformation frontale et axiale (Bolzinger et al. 2021; Mínguez et al. 2007). La corrélation de cet outil d'évaluation avec les caractéristiques de la déformation osseuse (l'angle de Cobb ou la rotation vertébrale) reste controversée (Mínguez et al. 2007; Gorton, Young, et Masso 2012). En revanche, il semble être un bon indicateur des résultats de scores de qualité de vie et des mesures liées à l'apparence physique externe du tronc (Gorton, Young, et Masso 2012). Récemment, un nouvel outil, permettant la reconstruction 3D et à 360° du torse a été évalué et validé dans une population saine (Michalik et al. 2019).

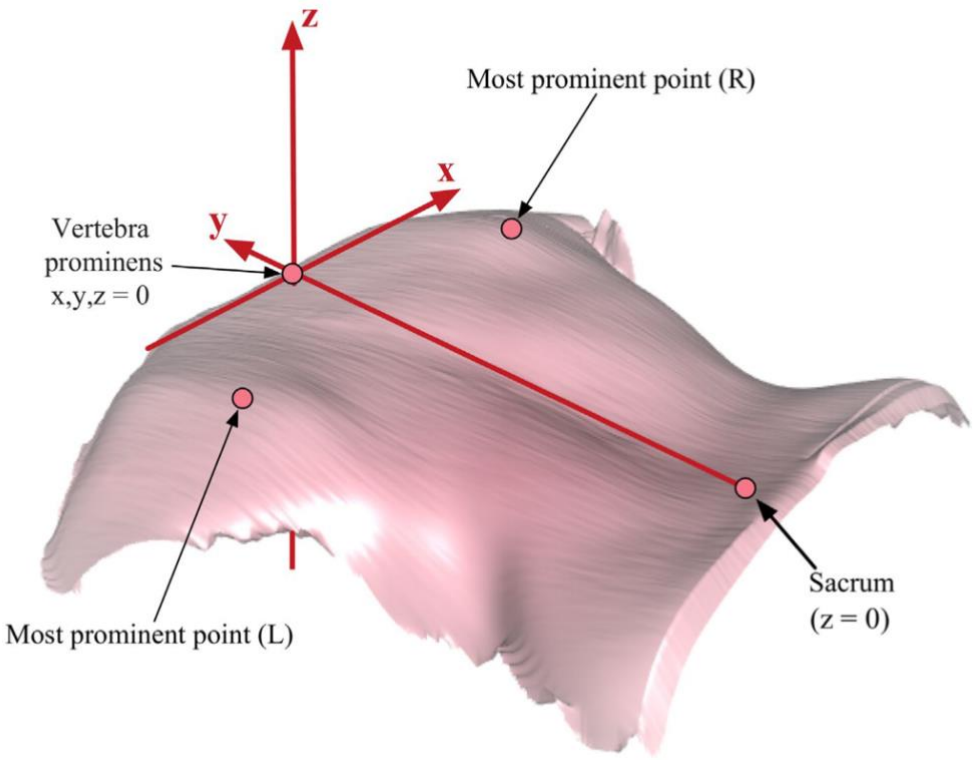

Figure 12: Représentation de la mesure de l'asymétrie de l'enveloppe du tronc postérieur selon Gardner et al. (Gardner, Berryman, et Pynsent 2021). On visualise les points les plus proéminents ainsi que les définitions des coordonnées x, y et z à partir de l'origine à la vertèbre proéminente.

La technique de la topographie de surface est prometteuse. Néanmoins, la réalisation de cette analyse nécessite un équipement spécifique et difficile accès en routine clinique. Récemment, l'acquisition de radiographies biplanaires basse ou micro dose permet la reconstruction et l'analyse 3D de l'enveloppe externe (Nérot et al. 2015).

III.4.2 Les paramètres issus de la reconstruction 3D de l'enveloppe externe

Une méthode de reconstruction 3D manuelle de l'enveloppe externe du patient en position libre, standardisée et debout (Nérot et al. 2015) issus des radiographies biplanaires a été développée. La procédure dure 15 minutes et se déroule en 2 étapes : 1) Un premier ensemble de multiples points de contrôle comprend l'emplacement de l'entrejambe, le point médian des disques intervertébraux C2-C3, L4-L5 et 8 centres

articulaires afin de mettre à l'échelle le motif de l'enveloppe corporelle sur les radiographies coronale et sagittale des sujets. Ces points ont été utilisés pour déformer un modèle générique afin de l'adapter à la morphologie spécifique du patient, et la forme externe a été projetée sur les deux radiographies (figure 13A).

2) Le deuxième ensemble comprend 77 points pour un ajustement fin du modèle. Ces points ont été disposés sur les parties du corps dont la forme varie fortement d'un individu à l'autre. En déplaçant manuellement chacun de ces points de contrôle, le modèle pouvait être ajusté pour correspondre au contour des radiographies coronal et sagittal (figure 13B).

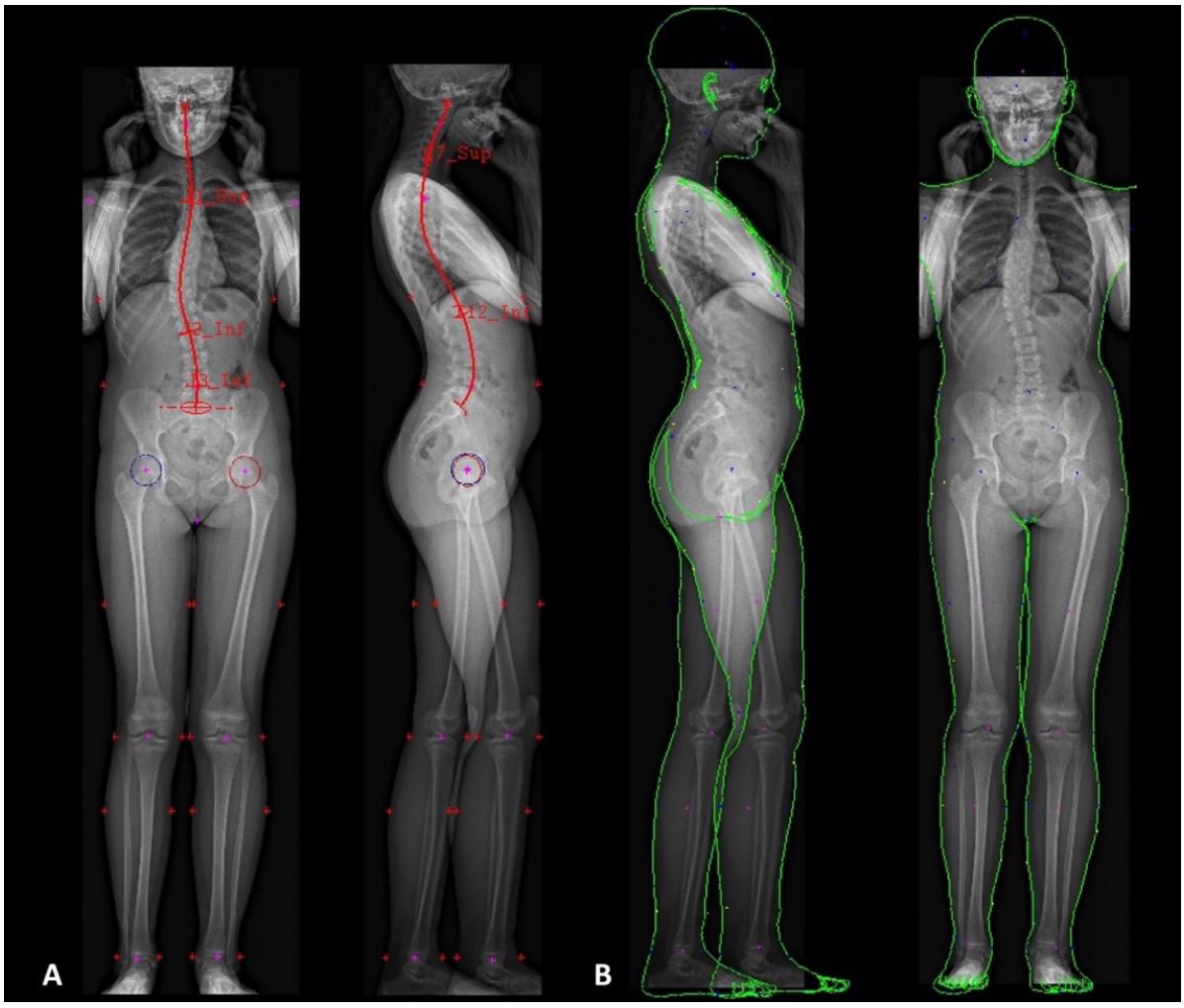

Figure 13 : Exemple de reconstruction quasi-automatique de la colonne vertébrale (A) d'une scoliose thoracique droite. Sur l'image A est représenté la première étape de la reconstruction de l'enveloppe externe soit le placement des points de contrôle. L'image B est générée automatiquement et représente l'étape de l'ajustement avec les multiples points à régler manuellement.

La reconstruction de l'analyse de l'enveloppe externe permet la caractérisation et la quantification de l'asymétrie du pli de taille chez les patients scoliotiques (figure 14) (Langlais et al. 2021). Cette asymétrie du pli de taille se traduit cliniquement par le signe de la lucarne (décrit dans la première partie). Cependant, il est physiquement non quantifiable. De plus, cette mesure n'a pas été évaluée comme prédicteur de la progression d'une courbure ou après une correction et fusion chirurgicale.

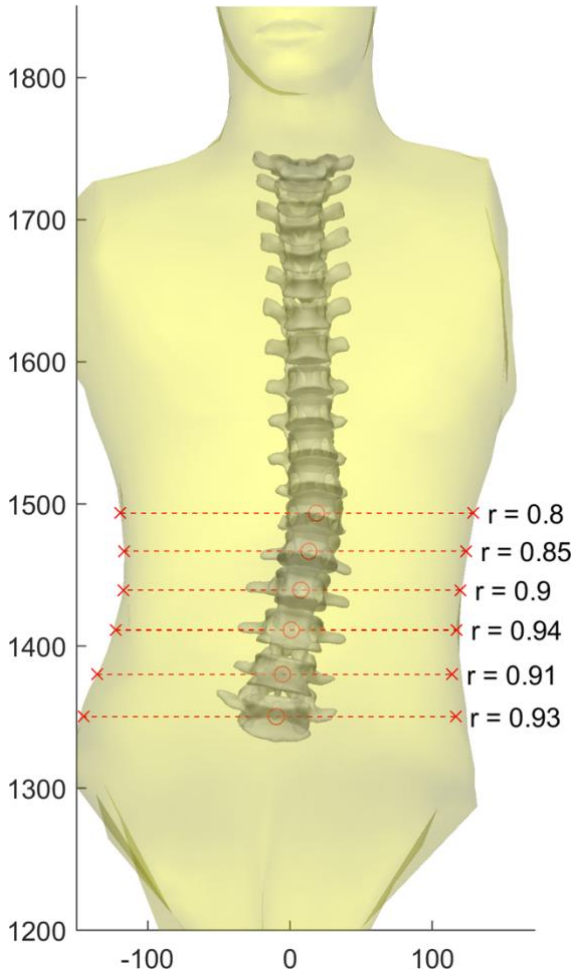

Figure 14: Illustration de la méthode de mesure de l'asymétrie de taille pour une vertèbre donnée (ordonnée et abscisse en millimètres)

Les travaux pionniers de Duval-Beaupère et al. se sont intéressés aux potentielles évolutives d'une courbure, à l'équilibre de la colonne vertébrale mais également de la barycentremétrie

(soit de l'analyse du(des) centre(s) de masse) pour caractériser une scoliose (Duval-Beaupère et Robain 1987). Mme Duval-beaupère utilisait une méthode d'analyse combinant le scanner à rayon gamma et la radiographie pour mesurer la masse corporelle à chaque niveau vertébral et son centre de masse, et pour représenter la position du centre de cette masse sur la radiographie sagittale de la colonne vertébrale.

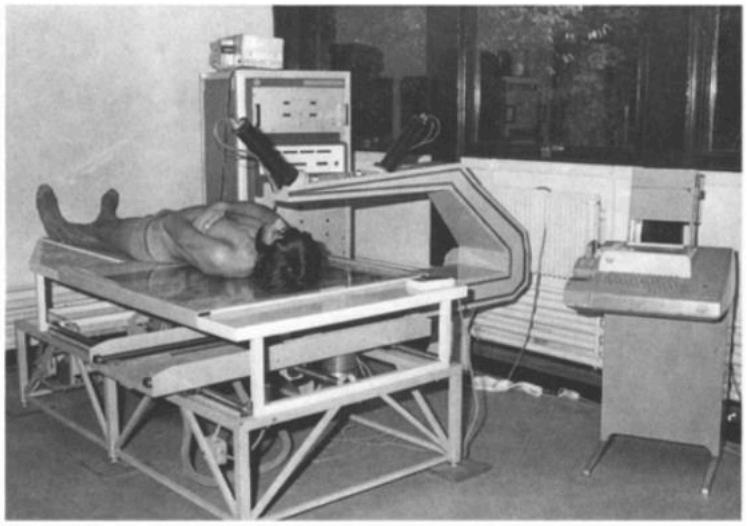

Figure 15: Exemple acquisition du barycentre issu du scanner à rayons gamma (Duval-Beaupère et Robain 1987)

Figure 16: Exemple pour un sujet du centre de la masse (39,1% du poids du corps) supporté par L1. Il est exprimé comme l'intersection de deux axes, l'axe vertical correspondant à la coordonnée sagittale et l'axe horizontal correspondant à la coordonnée de hauteur de ce centre de masse (Duval-Beaupère et Robain 1987).

Cependant, l'évaluation de la barycentremétrie par le scanner à rayons gamma est difficilement accessible en routine clinique et est réalisée en position couchée. Les dernières avancées et travaux fondamentaux sur la reconstruction 3D de l'enveloppe externe issus des radiographies biplanaires ont permis l'analyse de la barycentremétrie d'un sujet (Nérot et al. 2015). L'analyse des paramètres gravitationnels tels que la ligne de gravité (figure 17) ou le centre de masse (figure 18) ont pu être obtenus à partir de radiographies biplanaires en estimant la distribution de la masse dans différentes régions du corps pour évaluer son

équilibre segmentaire (Amabile et al. 2016b). Ces estimations ont été obtenues en utilisant une plate-forme de force en position debout (Schwab et al. 2006; Steffen et al. 2010). Il a été démontré qu'avec de telles méthodes, il est possible d'estimer avec précision la position du centre de masse tant chez les patients sains que chez les patients scoliotiques en estimant la densité de chaque segment du corps (Nérot et al. 2015; Hernandez et al. 2018). Deux paramètres issus de l'analyse de la barycentremétrie ont été analysés et calculés chez les patients scoliotiques.

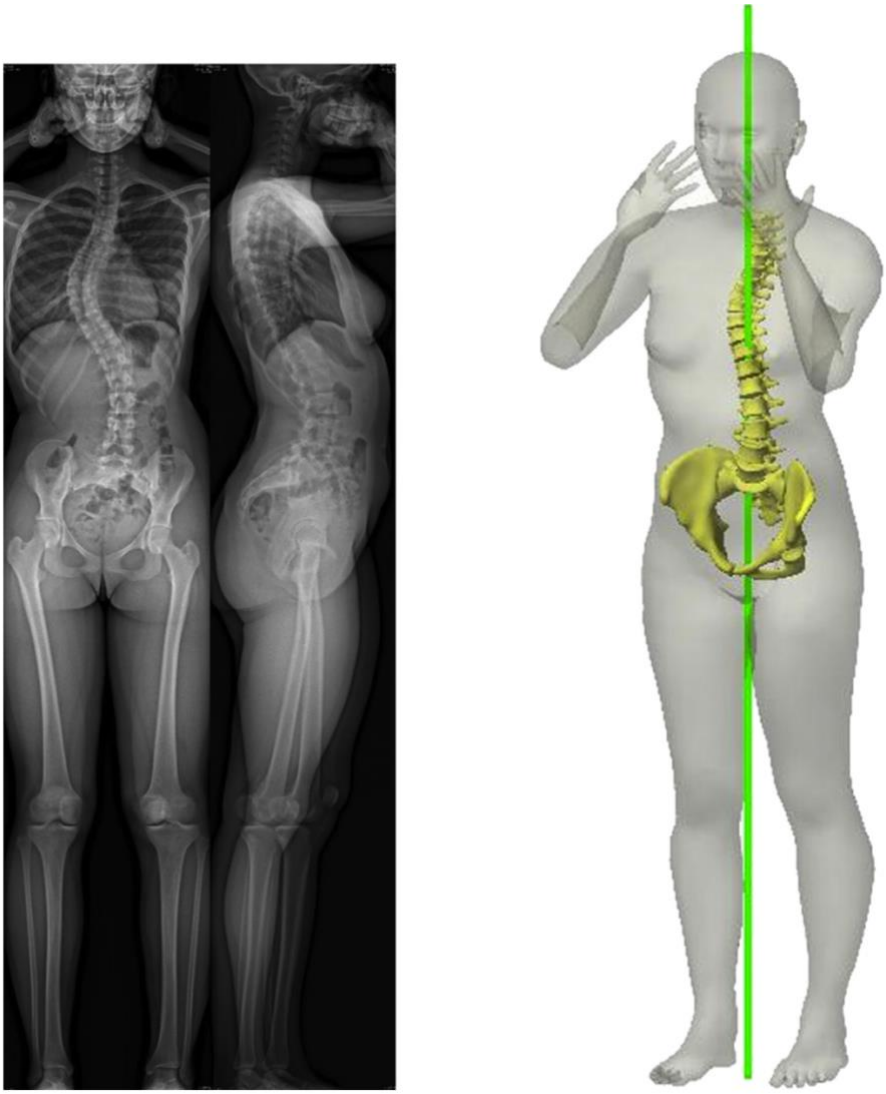

Figure 17: Exemple d'une scoliose thoracique droite avec la radiographie biplanaire de face et profil (à gauche) et la reconstruction 3D (à droite) de l'enveloppe externe et de la colonne vertébrale. La ligne de gravité passant par le centre de masse est représentée en vert (Thenard et al. 2019).

- Le centre de masse

Des tranches horizontales de l'enveloppe externe ont été virtuellement coupées à chaque niveau vertébral (incluant la vertèbre, la moitié inférieure du disque supérieur et la moitié supérieure du disque inférieur). Pour chaque vertèbre, le segment de corps situé au-dessus d'elle (c'est-à-dire la somme des tranches situées au-dessus d'elle) a été caractérisé en calculant son volume. En utilisant l'estimation des valeurs de densité proposée par Dempster (Dempster 1955) et par Amabile et al. pour le torse (Amabile et al. 2016b), le centre de masse est calculé (Thenard et al. 2019).

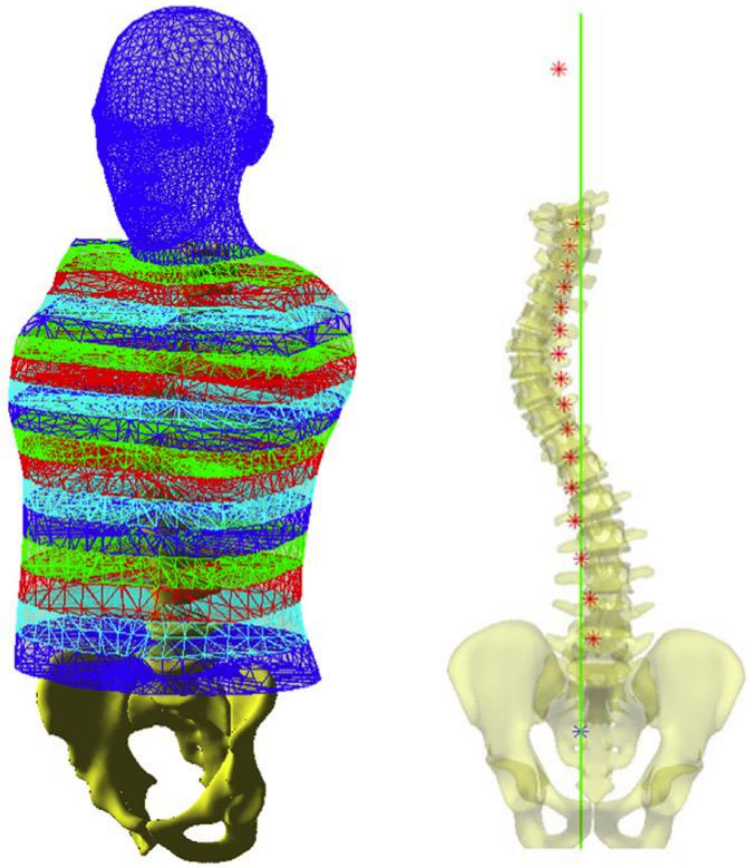

Figure 18: L'image de gauche représente la segmentation corporelle du tronc et les différentes tranches du tronc par niveau vertébral. La position du centre de masse chaque tranche est représentée par l'étoile rouge. La ligne de gravité passant par le centre de masse est représentée en vert (Thenard et al. 2019).

- *Le moment intersegmentaire*

Le moment intersegmentaire est défini comme le moment de torsion, par rapport à l'axe vertical, appliqué à chaque vertèbre résultant du déplacement latéral et de l'inclinaison sagittale de cette vertèbre, en raison de la masse du corps au-dessus de la vertèbre analysée et de la position du centre de masse de cette vertèbre. Par conséquent le moment intersegmentaire dépend de trois paramètres : l'orientation de la vertèbre (axiale, sagittale et latérale), le poids du segment corporel au-dessus de la vertèbre et la distance (c'est-à-dire le bras de levier) entre le centre de masse de cette vertèbre et le canal rachidien. En d'autres termes, un moment de torsion axiale est appliqué à une vertèbre uniquement si cette vertèbre est : 1) déplacée latéralement par rapport au centre de masse et 2) inclinés dans le plan sagittal (Thenard et al. 2019).

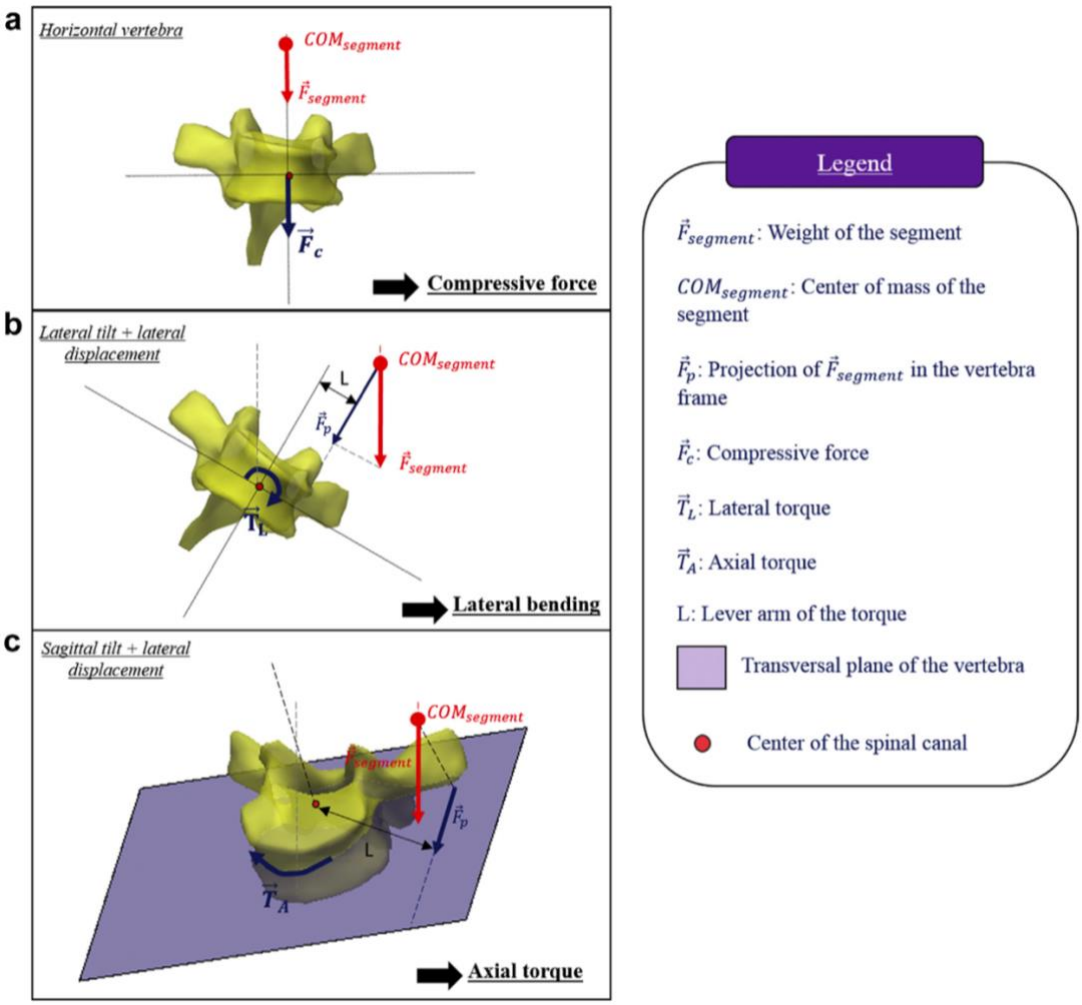

Figure 19: Représentation de la méthode de mesure du moment intersegmentaire d'une vertèbre (Thenard et al. 2019). Sur l'image A, on visualise une vertèbre horizontale qui est chargée par une force verticale alignée avec le canal rachidien. Le poids du segment qui la surmonte va créer une simple force de compression sur la vertèbre et aucun moment intersegmentaire axial. Sur l'image de B, on observe une inclinaison et un déplacement latéral de la vertèbre par rapport au segment du centre de masse (COM ; en rouge). Le bras de levier L créé par le déplacement latéral de la vertèbre et la projection du poids Fp créent une flexion latérale de la vertèbre. Sur l'image C, on observe une inclinaison sagittale et un déplacement latéral de la vertèbre. Le bras de levier L et la projection de la masse Fp tangente à la vertèbre créent un moment intersegmentaire axial appliqué à la vertèbre, produisant la torsion.

Ces différents paramètres sont issus de la reconstruction 3D de l'enveloppe externe et traduisent le déplacement des masses et de l'équilibre corporel. Les études antérieures ont montré leur faisabilité dans une population saine et de patients scoliotiques (Thenard et al. 2019). Cependant, il n'a pas été évalué l'intérêt de l'utilisation de ces paramètres dans la prédiction de l'aggravation d'une courbure ni du comportement de ces paramètres après une chirurgie correctrice.

Après avoir passé en revue, les paramètres issus de la reconstruction 3D de la colonne vertébrale et de l'enveloppe externe. Nous nous interrogeons sur la responsabilité du disque intervertébral dans la progression d'une courbure. Certains auteurs suggèrent que la scoliose soit liée à une décompensation mécanique et rotatoire de la colonne vertébrale débutant dans le plan transversal, ou horizontal (Skalli et al. 2017 ; Castelein et al. 2020). Ainsi, le disque intervertébral jouerait un rôle essentiel au déclenchement précoce de la cascade biomécanique menant à une torsion tridimensionnelle.

III.5 Les paramètres issus de l'analyse du disque intervertébral

Le disque intervertébral est composé de trois structures : l'*annulus fibrosus*, la zone de transition et le *nucleus pulposus* (caractérisé par une forte teneur en eau). L'*annulus fibrosus* est composé de collagène et d'élastine et est organisé en réseau concentrique de lamelles parallèles (Yu et al. 2002). Cette structure en réseau de fibres élastiques procure au disque intervertébral des propriétés biomécaniques et se modifie avec le temps. Les études *in vitro*, chez des patients scoliotiques, ont montré qu'il y avait une perte d'intégrité de ce réseau : diminution du nombre de fibres de collagènes et d'élastine, réseau interrompu et clairsemé (Yu et al. 2005; Kobielarz et al. 2016). Les études *in vivo* ont permis de montrer que la configuration géométrique du disque intervertébrale changeait lorsqu'un stress extérieur (compression, angulation, réduction de la mobilité) était appliqué (Stokes et al. 1996) et que sa déformation 3D était plus importante que la déformation des corps vertébraux chez les patients scoliotiques (Schlösser et al. 2014).

III.5.1 Les paramètres 3D issus de la reconstruction du rachis

- *La cunéiformisation du disque intervertébral*

La cunéiformisation du disque intervertébral est définie de la même manière que la cunéiformisation vertébrale (Nault et al. 2013). Contrairement à l'analyse vertébrale, la cunéiformisation des disques T1-T2 et L4-L5 est significativement corrélée avec le caractère progressif d'une scoliose idiopathique de l'adolescent (Nault et al. 2013; 2020). Ceci renforce l'idée selon laquelle la progression d'une scoliose idiopathique de l'adolescent provient en premier d'une cunéiformisation des disques avant d'engendrer une angulation des vertèbres (Will et al. 2009).

- *La hauteur, la largeur et la profondeur des disques intervertébraux*

Vergari et al. retrouvaient dans une étude comparative que les disques intervertébraux présentaient les mêmes caractéristiques que les vertèbres en matière de largeur et de profondeur (Vergari et al. 2020). En revanche, la hauteur des disques chez les adolescents scoliotiques était significativement plus élevée uniquement aux niveaux L2-L3 et L3-L4 par rapport une population asymptomatique de référence.

- *La slenderness des disques intervertébraux*

Elle est calculée selon la même méthode, décrite précédemment, que pour les vertèbres. Vergari et al. n'ont pas retrouvé de différence de cette mesure chez des patients scoliotiques comparés à une population asymptomatique de référence (Vergari et al. 2020).

L'analyse du disque intervertébral selon la méthode de reconstruction 3D des radiographies biplanaires est une analyse géométrique. Les propriétés biomécaniques du disque ont ainsi pu être mieux comprises avec les techniques d'acquisitions d'imagerie par résonance magnétique.

III.5.2 Les paramètres issus de l'imagerie par résonance magnétique

L'étude par résonance magnétique repose sur l'analyse quantitative du volume et de l'hydratation du disque intervertébral (Violas et al. 2007). Huber et al. ont constaté chez des patients scoliotiques que la dégénérescence (soit une diminution du taux hydratation du *nucleus pulposus* et une perturbation des propriétés mécaniques de l'*annulus fibrosus*) des disques intervertébraux était plus importante pour les disques compris dans la courbure que ceux en dehors de la courbure (Huber et al. 2016). En revanche, le degré de dégénérescence ne semblait pas lié à la mesure de l'angle de Cobb de la courbure. Ces paramètres biomécaniques ont également été évalués comme outil d'analyse thérapeutique. Violas et al. ont montré qu'à la suite d'une correction chirurgicale d'une courbure, le volume et l'hydratation des disques intervertébraux des segments libres sous l'arthrodèse sembleraient retrouver leur valeur initiale (et donc leurs propriétés biomécaniques) (Violas et al. 2007). Dans une autre étude Abelin-Genevois et al. ont rapporté également une amélioration de l'hydratation des disques lombaires sous l'arthrodèse d'une scoliose idiopathique (Abelin-Genevois et al. 2015). De plus, les mêmes auteurs ont montré que ces changements étaient influencés par l'alignement sagittal du complexe lombo pelvien (Abelin-Genevois et al. 2015).

L'IRM reste un examen onéreux et peu accessible en routine clinique avec un délai d'attente important. Ces dernières années, une alternative à l'IRM s'est développée : l'élastographie ultrasonore. Cet outil d'analyse rapide, non invasive et accessible au clinicien a permis une analyse quantitative des propriétés biomécaniques de l'*annulus fibrosus* lombaire.

III.5.3 Les paramètres issus de l'analyse par élastographie

L'élastographie mesure la vitesse de propagation des ondes de cisaillement d'un tissu qui est un paramètre relié au module élasticité de ce tissu (Gennisson et al. 2013). Les études in vitro (Vergari et al. 2014a) et in vivo (Vergari et al. 2014b) ont montré que cette mesure de la vitesse d'onde de cisaillement était liée aux propriétés biomécaniques de l'*annulus fibrosus*. La mesure de cette vitesse est altérée dans une cohorte d'adolescents scoliotiques et confirme que cet outil de mesure est sensible à l'altération biomécanique de l'*annulus fibrosus* (Langlais

et al. 2018). Les mêmes auteurs ont rapporté qu'une vitesse d'onde de cisaillement élevé (c'est-à-dire en dehors des valeurs établies dans une cohorte de référence) au niveau d'une zone jonctionnelle présentait un risque accru de progression d'une courbure scoliotique (Langlais et al. 2018). Cette analyse par élastographie ultrasonore des propriétés biomécaniques de l'*annulus fibrosus* semble pouvoir aider le clinicien dans la prédiction d'une courbure sous réserve d'une validation par une étude prospective de plus large effectif. En revanche, aucune analyse n'a été réalisée après une chirurgie de correction et fusion d'une scoliose.

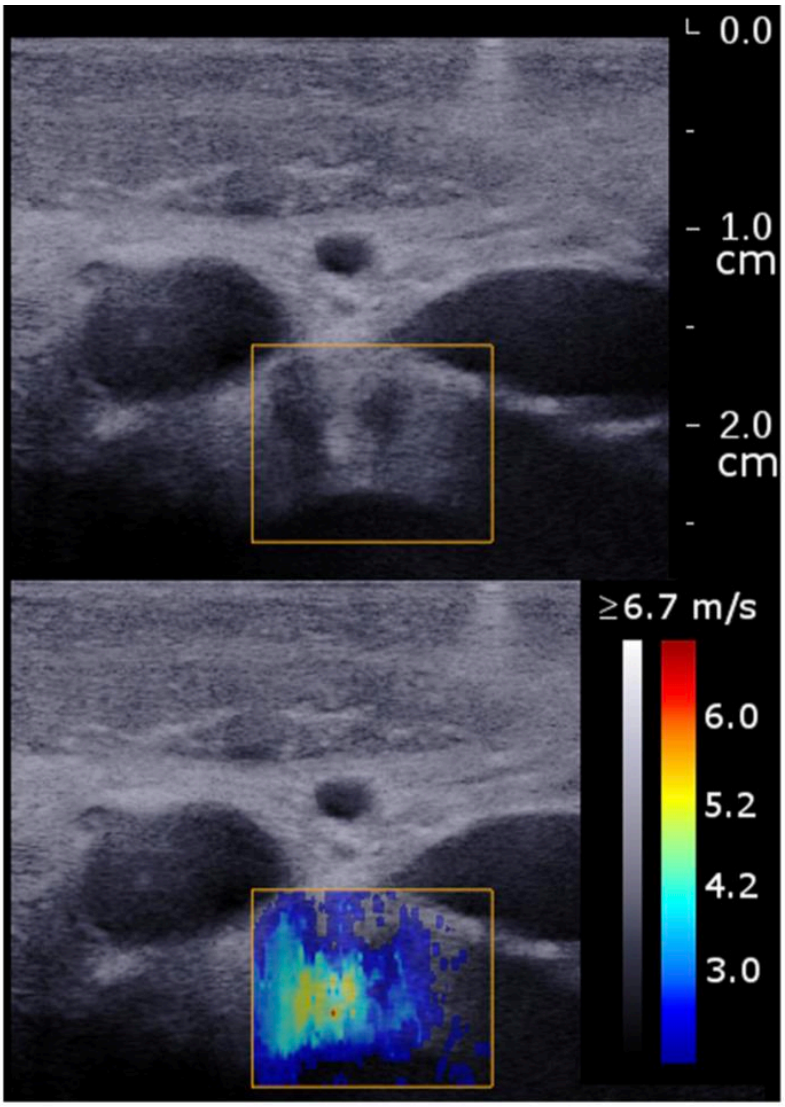

Figure 20: Exemple d'image échographique (cadre supérieur) et élastographique (cadre inférieur) de l'*annulus fibrosus* L3-L4. On visualise les fibres concentriques de l'*annulus fibrosus* (Langlais et al. 2018).

III.6 Résumé et perspective

Le développement des reconstructions 3D issues des radiographies biplanaires a permis de développer de nombreux paramètres biomécaniques objectifs, quantitatifs et fiables aidant le clinicien au diagnostic, au suivi et à l'évaluation thérapeutique. Pour l'aide au diagnostic, l'indice de sévérité a été développé et se compose uniquement de paramètres issus de l'analyse des structures osseuses. Cependant, des questions subsistent : L'analyse de l'équilibre global (évalué par l'OD-HA) pourrait-elle aider au diagnostic d'une scoliose progressive ? Le diagnostic d'une scoliose progressive pourrait-il être amélioré par l'analyse des paramètres issus de la reconstruction 3D de l'enveloppe externe ? En d'autres termes, nous nous demandons si l'analyse de l'alignement global, de l'asymétrie du pli de taille, de la barycentremétrie (soit de la distribution asymétrique des masses) d'un patient atteint d'une scoliose idiopathique pourrait aider le clinicien au diagnostic précoce d'une scoliose progressive. Quant à l'évaluation thérapeutique, de nombreux travaux se sont intéressés sur la correction chirurgicale des paramètres osseux. Mais nous nous demandons comment se comporte la répartition des masses après une correction chirurgicale ? Enfin, l'analyse par élastographie du comportement biomécanique de l'*annulus fibrosus* reste à évaluer.

Afin de répondre à un certain nombre de ces questions, notre démarche scientifique a été d'évaluer l'alignement global des sujets incluent dans les travaux de validation de l'indice de sévérité et étudier l'intérêt de l'ajout de ce paramètre (soit OD-HA) comme complément de l'indice de sévérité. Dans un second temps, nous avons mené une étude préliminaire où nous avons évalué la faisabilité et la pertinence de l'utilisation clinique des paramètres issus de la reconstruction de l'enveloppe externe (soit l'asymétrie du pli de taille, la position du centre de masse et le moment intersegmentaire) dans une population de sujet asymptomatique et scoliotique. Une seconde recherche a été réalisée avec la reconstruction de l'enveloppe externe des sujets de la cohorte de l'indice de sévérité et analysé l'asymétrie du pli de taille et la barycentremétrie comme complément de l'indice de sévérité. Enfin, nous avons analysé des paramètres issus de la reconstruction de l'enveloppe externe et évalué par élastographie des disques intervertébraux lombaires après une chirurgie correctrice.

IV - Évaluation de l'alignement global dans la prédiction précoce d'aggravation d'une scoliose idiopathique

Cet article va faire l'objet d'une soumission dans les prochaines semaines, comme 1er auteur.

Assessment of malalignment at early stage in adolescent idiopathic scoliosis

IV.1 Introduction

Idiopathic scoliosis is a three-dimensional (3D) spinal deformity of uncertain etiology, which can be defined in the coronal plane by a Cobb angle of at least 10◦ and axial vertebral rotation (Coonrad et al. 1998). Its aetiopathogeny is multifactorial and the causal factors poorly understood (Kouwenhoven et Castelein 2008) but several preliminary studies focus on a possible sensory imbalance at early stage (Guo et al. 2006; Assaiante et al. 2012).

Recently, a validated predictive model based on 3D biplanar reconstruction (i.e., the severity index described by Skalli et al.) were developed to distinguish between progressive and stable scoliosis at the first visit (Skalli et al. 2017). However, this predictive model still needs to be improved and is based solely on the 3D reconstruction of the spine and not on the overall head-spine-pelvis alignment. J. Dubousset introduced the concept of the "cone of economy" to describe the ideal position of the body's centre of gravity (Hasegawa et Dubousset 2022). In a static or dynamic balanced posture, the human head is located above the pelvis in all three planes. When the centre of gravity is outside of the stability area, several musculoskeletal compensation mechanisms are activated to bring it back in. In the literature, several studies used the centre of the body of C7 as a reference point in relation to the posterosuperior edge of the sacral plateau to assess the global balance of a subject in a static position (Berthonnaud et al. 2005).

Recently, Amabile et al. described a new quasi-invariant parameter (i.e OD-HA parameter) describing the position of the head (or, more precisely, of the odontoid process of C2) relative to the pelvis, which is a proxy for the global alignment of the subject (Amabile et al. 2016a).

Our previous work showed that some severe scoliosis patients could present an imbalance, as quantified by an abnormal OD-HA (Karam et al. 2022). However, it is not yet clear whether

early malalignment can be detected in adolescent idiopathic scoliosis (AIS) using this new parameter from the 3D reconstruction of low dose biplanar radiography.

Our objective was to assess abnormalities of OD-HA angle in a mild scoliotic population, relative to a control cohort, in order to determine whether screening for spine malalignment would help predict the distinction between progressive and stable scoliosis at an early stage. Furthermore, the effect of including OD-HA parameter extracted from 3D reconstruction to the severity index was studied.

IV.2 Materials and methods

Subjects

Data from scoliotic patients were obtained from 6 centres in 4 countries (with a minimal of 10% inclusions per centre) within a follow-up clinical survey. This cohort of scoliotic patients has been previously reported in studies using a severity index to predict scoliosis progression (i.e., the severity index and its six parameters) (Skalli et al. 2017; Vergari et al. 2019; 2021), which did not include assessment of 3D malalignment (i.e., OD-HA assessment). Data from asymptomatic subjects were collected at a single centre and within a research protocol. Parents, children, and adults were informed about the protocol and consented to participate before inclusion. This study was approved by the ethics committee (C.P.P. Ile de France VI 6001) and by the local ethical committees.

Data were collected prospectively, between 2013 and 2020, and divided in 2 groups: asymptomatic (A) and AIS (S). Asymptomatic adolescents were included in group A if they had no history of spinal disease. A physical examination was performed by a spine physician to rule out any spinal disorder. In the S group, inclusion criteria were: (1) confirmed diagnosis of AIS; (2) Cobb angle between 10° and 25°; (3) European Risser sign lower than 3 (Duval-Beaupère 1970); (4) age higher than 10 years; and (5) no previous treatment (such as brace or spine surgery). Patients with non-idiopathic scoliosis, transitional anomalies or supernumerary vertebrae were excluded from this study.

Protocol

All subjects underwent a low dose biplanar X-ray (EOS system, EOS Imaging), in the free-standing position (Faro et al. 2004), at the onset of inclusion. Patients were classified by location of the main curve (Stagnara et Queneau 1953; Perdriolle 1979; Lenke et al. 2002), i.e. according to the location of the apex: thoracic (apex between the T2 vertebra and the T11-T12 intervertebral disc), thoracolumbar (apex between the T12 and L1 vertebrae), and lumbar (apex between the L1-L2 intervertebral disc and the L4 vertebra).

Patients were then followed until one of these two events occurred: 1) the patient reached skeletal maturity of the trunk (with a Risser sign greater than or equal to 3), without progression of the curvature (i.e., a Cobb angle of the main curvature less than 25°) and without treatment. These patients were classified as "stable"; 2) a corrective brace was prescribed, in which case patients were classified as "progressive". Quantitative and objective criteria were used to decide on brace treatment according to the International Society on Scoliosis Orthopaedic and Rehabilitation Treatment guidelines, i.e. a Cobb angle of the main curvature greater than 25° and a Risser sign less than or equal to 2, or an increase of 5° in Cobb angle or vertebral axial rotation within 6 months (Negrini et al. 2018), as well as an assessment of the clinical profile.

Imaging data and 3D reconstruction processing

A quasi-automatic 3D spine reconstruction was performed, from the biplanar radiography acquired at inclusion, using a previously validated method (Gajny et al. 2019; Vergari et al. 2019). OD corresponded to the position of the C2 odontoid, as an estimate of the head centre of mass, and HA was the midpoint of pelvic acetabula (figure 21 and 22). The 3D OD-HA angle was computed automatically, and then projected on the coronal and sagittal patient's planes (Amabile et al. 2016a). A positive sagittal OD-HA corresponds to a frontal lean, while a positive coronal OD-HA corresponded to a lean towards the right side. The end vertebrae of the scoliotic curve were manually selected by an experienced operator, and the Cobb angle was computed automatically from the 3D reconstruction.

For each patient, the calculation of the severity index (ranging from 0 to 1) was automatic (Skalli et al. 2017) and considered the stage of the European Risser sign, as previously described (Vergari et al. 2021). The index was weighted according to the OD-HA value. When

the OD-HA was greater than two standard deviations from the reference cohort value, a multiplication factor of 1.5 was applied. In cases where the OD-HA was less than one standard deviation from the normal cohort value, the multiplication factor 0.8 was applied, thus lowering the severity index. An index lower than 0.4 is indicative for a stable curve, while an index higher than 0.6 is indicative for a progressive one. No prediction was issued for values in-between, and patient was unclassified.

Statistics

Descriptive results were presented according to their mean, one standard deviation (SD) and range. After checking that values did not follow a normal distribution (Lilliefors normality test), the Mann-Whitney test's was applied. Significance was set a 0.05. A reference corridor for OD-HA values in asymptomatic subjects was calculated as the range [5^{th}-95^{th} percentiles]. The number of AIS having their OD-HA values higher than the corridor's limits was reported and their values were defined as abnormal. Odds ratios were calculated to evaluate the relationship between abnormal OD-HA and risk of progression. Its confidence interval [5%-95%] was calculated according to the Wolff method, and an interval including the value one was considered non-significant. To analyze the weighting of the severity index with the OD-HA, we reported the sensitivity, specificity, positive and negative predictive value of the test according to the locations of the curvature.

IV.3 Results

Description of population

Eighty-three asymptomatic subjects (50 females; 33 males; 12 years old, SD=2) and two hundred and five scoliosis (12 years old, SD=1.5; 171 females and 34 males; 88 thoracic, 52 thoraco-lumbar and 65 lumbar) were included. These two cohorts were not statistically different for the age criterion ($p>0.8$). Mean Cobb angle of scoliotic patients was (16.1°, SD=3.7°; range from 10° to 24.8°). After the clinical and biplanar radiographic follow-up, 109 AIS (53%) was classified as stable and 96 (47%) as progressive. In the stable patients, the European Risser sign was evenly distributed (0 in 42/109, 1 in 32/109, 2 in 35/109 patients).

In the progressive group, a European Risser sign was 0 in 78/96 patients while it was only 1 and 2 in 18/96 patients. The demographic characteristics are resumed in table 1.

Table 1: Demographics characteristics of population

	Asymptomatic (n=83)	**AIS population**		
		Total (n=205)	**Stable (n=109)**	**Progressive (n=96)**
Age: yo, SD (range)	12, 4 (7-18)	12, 1 (10-15)	12, 1 (10-15)	11, 1 (10-14.5)
Gender: n (%)				
- Girls	58 (70%)	171 (83%)	90 (83%)	81 (84%)
- Boys	25 (30%)	34 (17%)	19 (17%)	15 (16%)
Curve topography: n (%)				
- Thoracic		88 (43%)	46 (42%)	42 (44%)
- Thoraco-lumbar		52 (25%)	27 (25%)	25 (26%)
- Lumbar		65 (32%)	36 (33%)	29 (30%)
Cobb angle (°): mean, SD (range)		16.1, 4.4 (8.8-24.8)	14.7, 4.6 (8.8-22.8)	17.4, 3.8 (10.3-24.8)

OD-HA parameters

Coronal and sagittal OD-HA in the asymptomatic group was 0.2°, SD=1° with a range between 5th and 95th percentile of [-1°;2°] and -2.5°, SD=2.4° [-6°;1°], respectively. In AIS, mean coronal OD-HA was 0.3°, SD=1.4°; range from -4.6° to 4.3° and the mean sagittal OD-HA was -0.8°, SD=2.5°; range from -9° to 5.6°. Nine asymptomatic subjects (N=83, 10.8%) and 56 AIS (N=205, 27.5%) were outside the reference corridor for coronal OD-HA (OR=3.1; CI=1.4-6.6).

For sagittal OD-HA, nine asymptomatic subjects (N=83, 10.8%) and 55 AIS (N=205, 26.8%) were outside the reference corridor (OR=3; CI=1.4-6.4). The 3D position of OD relative to the inter-hip axis suggests that AIS patients are almost two times more likely to have an abnormal OD-HA value (OR=2.3; CI=1.1-4.9). The number of AIS with abnormal OD-HA position values did not differ by curvature location (p=0.2) (table 2).

Table 2: Number of AIS with OD-HA position values outside the reference corridor based on the topography of the main curvature. n is the number of patients included

	Thoracic (n=88)	**Thoraco-Lumbar (n=52)**	**Lumbar (n=65)**
Coronal OD-HA : n (%)	25 (28%)	16 (31%)	15 (23%)
Sagittal OD-HA : n (%)	19 (21%)	14 (27%)	22 (34%)
3D OD-HA : n (%)	14 (16%)	9 (17%)	13 (20%)

OD-HA analysis by patient outcome

The mean coronal and sagittal OD-HA were 0.3° (SD=1.2°; range -4.6° to 4°) and -0.8° (SD=2.5°; range -9.1° to 5.3°) in stable scoliosis while the means were, respectively, 0.4° (SD=1.5°; range -3.6° to 4.5°) and -0.8° (SD=2.6°; range -7° to 5.6°) in progressive scoliosis. For coronal OD-HA, 20 stable scoliosis (N=109) and 36 progressive patients (N=96) were outside the reference corridor (OR=2.7; CI=1.4-5). For sagittal OD-HA, 25 stable AIS (N=109) and 30 progressive patients (N=96) were outside the reference corridor (OR=1.5; CI=0.8-2.8). For the 3D OD-HA (i.e, position of OD relative to the inter-hip axis), the odds ratio was of 2.2 (CI=1-4.5). Focusing on the topography of the curvature, the odds ratios were not significant (i.e., the confident interval include the value of one).

OD-HA and the severity index

Following the previous results, only the odds ratio of coronal OD-HA between stable and progressive scoliosis was significant. Therefore, the weighting of the S-index was

performed only with the coronal OD-HA values. All results are summarized in table 3. Adding to the s-index a weighting factor based on coronal OD-HA improved the positive predictive value by 6% and the specificity by 7%. For thoracic scoliosis, the specificity increases by 13% and the positive predictive value by 9%.

Table 3: Classification, performance of index with coronal OD-HA weighting according to curve location. n is the number of patients; S-index * corresponds at the S-Index with OD-HA weighting. Values in italics and bold are values for which the weighting of the S-index increased the performance of the test by 5%.

	Total Cohort		**Thoracic scoliosis**		**Thoraco-lumbar scoliosis**		**Lumbar scoliosis**	
Sample size : n	205		88		52		65	
Stable scoliosis : n	108		46		28		34	
Progressive scoliosis : n	97		42		24		31	
	S-index	**S-Index ***	**S-index**	**S-Index ***	**S-index**	**S-Index ***	**S-index**	**S-Index ***
Correctly classified : n (%)	154 (75%)	149 (73%)	66 (75%)	63 (72%)	39 (75%)	38 (73%)	49 (75%)	48 (74%)
Misclassified : n (%)	35 (17%)	25 (12%)	15 (17%)	8 (9%)	9 (17%)	7 (13%)	11 (17%)	10 (15%)
Unclassified : n (%)	16 (8%)	31 (15%)	7 (8%)	17 (19%)	4 (8%)	7 (13%)	5 (8%)	7 (11%)
Sensitivity (%)	87%	87%	90%	91%	73%	76%	89%	89%
Specificity (%)	78%	***85%***	73%	***86%***	88%	92%	75%	77%
Positive predictive value (%)	78%	***84%***	77%	***86%***	84%	89%	76%	77%
Negative predictive value (%)	85%	88%	88%	91%	79%	81%	89%	89%

IV.4 Discussion

In this study, the measurement of the OD-HA position could be determined in a healthy adolescent population and in AIS. This 3D measurement is based on a quasi-automatic reconstruction method (Gajny et al. 2019) which can be compatible with daily clinical practice since it takes less than 5 minutes.

Previously, several angles and distances have been described to assess the overall balance of the spine. For instance, the sagittal T9 plumbline described by Beauval-Beaupère who considered T9 to approximate the trunk's centre of gravity. The coronal and sagittal C7 plumblines are commonly used to assess the balance of the thoracic and lumbar spine (Clement et al. 2020). The disadvantage of these parameters is that it does not consider the alignment of the superior cervical spine-hip axis. As an example, Kim et al. showed the clinical relevance of OD-HA angle assessment in 199 adults undergoing spinal deformity surgery. As a result, the OD-HA angle measurement was correlated with the quality-of-life score and mechanical complications while the T1-pelvis angle was associated with the spino-pelvic parameter (Kim et al. 2021). Gangnet et al. described the 3D position of the line connecting the middle of the external acoustic meatus to the middle of the bi-coxo-femoral axis (Gangnet et al. 2003). The measurement of the OD-HA position is a natural extension of this, since it approximates the position of the head's centre of mass, like the centre of the acoustic meati, but it is more clearly visible in radiographs. The OD-HA parameter can therefore complement other 3D radiographic analyses of alignment, including the upper and lower cervical spine, the pelvic vertebrae, and the lower limb. Previous studies have shown that OD-HA can be reliably measured in healthy patients (Amabile et al. 2016a) and in pre- and postoperative AIS patients with a measurement uncertainty of around 0.2° or less (Langlais et al. 2022). In our study, we found values for coronal and sagittal OD-HA in the asymptomatic group around 0.2° (SD=1°) and -2.5° (SD=2.4°). In a population of 516 subjects of Chinese origin and asymptomatic, Hu et al. found values around 0.2° (SD=1.1°) for the coronal and −0.2° (SD=2.5°) for the sagittal angle. The same authors also showed that there was a positive (or negative) correlation between the sagittal (or coronal) OD-HA value and age (Hu et al. 2022). In other words, the OD-HA values varied with age (and more precisely between from 20s to 80s) by 2.45° for the sagittal measure and by 1.06° for the coronal angle (Hu et al. 2022). These small physiological variations are

consistent with the fact that the OD-HA angle is quasi-invariant (Amabile et al. 2016a) and that the head tends to remain above the pelvis in a small cone of stability.

The main finding of this work suggests that AIS patients can show almost three times the odds to have a coronal and sagittal OD-HA malalignment, and this at an early stage. Different strategies can be deployed to maintain postural alignment and a constant position of the OD-HA, which has been demonstrated to be invariant even during breathing (Clavel et al. 2020). These strategies can involve the whole body from head to toe, and they depend on the functional capacities of each subject. For example, elderly people prefer to recruit compensation mechanisms in the pelvis, cervical spine and ultimately lower limbs (Barrey et al. 2012; Diebo et al. 2015; Amabile et al. 2016a). For example, Ferrero et al. found extreme ODHA values in significantly elderly patients with significant functional impairment (Ferrero et al. 2021). These subjects with sagittal malalignment and loss of lumbar lordosis recruited compensatory mechanisms such as pelvic retroversion, cervical hyper-lordosis to maintain the head above the pelvis. On the other hand, young subjects can adjust their spinal-pelvic alignment by adjusting the curvature of their spine and the orientation of their pelvis, or even the shape of their pelvis by a modification of the incidence (W et al. 2006; Vidal, Mazda, et Ilharreborde 2016; Alzakri et al. 2019). Indeed, with an approximate head weight of 4 to 5 kg (Vital et Senegas 1986; Sandoz et al. 2010), it appears that a strict alignment of the head upon the pelvis is a requirement for an economic posture. Failing to maintain the head upon the pelvis could indicate abnormal balance but the mechanism is still to investigate.

The other interesting finding is that progressive scoliosis is almost three times more likely to have coronal OD-HA malalignment than stable thoracic scoliosis without difference between topography of curvature. It is still difficult to understand the origin of this global malalignment of the scoliotic patient and especially in progressive scoliosis. Numerous studies have shown that global alignment is closely linked to neurological sensory inputs (Gómez Cristancho et al. 2022) such as oculomotor (Lion et al. 2013), vestibular (Pialasse et al. 2015) or proprioceptive (Pialasse et al. 2017) systems. The position of the OD-HA is a quasi-invariant factor and the results of this study show that it could be a biomarker of progression in thoracic scoliosis. However, it is probably not the only marker involved in the progression of the biomechanical

cascade. Disturbances in the mechanical properties of the intervertebral discs probably play a role in the progression of curvature and torsion of the axial plane (Karam et al. 2022), especially at the junctional levels (Langlais et al. 2018). These biomechanical mechanisms seem to be interrelated.

Finally, we assessed the influence of the coronal OD-HA measurement on the previously published severity index (Skalli et al. 2017). For thoracic scoliosis, the specificity and predictive positive value is improved by 13% and 9%, respectively and thus increases the probability of being a stable scoliosis when the index is less than 0.4 and of being a progressive scoliosis when the index is greater than 0.6. In clinical practice, this means that we decrease the number of false positives, so we treat less stable scoliosis, but we do not significantly decrease the risk of mistaking progressive scoliosis as stable scoliosis. Indeed, this weighting decreases the number of misclassified patients by 8% and therefore the risk of over- or under-treatment, However, it also decreases the number of correctly classified patients by 3%. This apparently contradictory result is explained by the increased number of unclassified patients by 11% and therefore challenges the clinician to insist on close monitoring of this scoliosis whose index is between 0.4 and 0.6 (as illustrated in figure 21). A factorial discriminant analysis could in the future allow the addition of coronal OD-HA to the severity index, under the defined conditions. Meanwhile, the coronal OD-HA is a factor that the clinician could consider at the first visit, particularly for the thoracic curves (as illustrated in figure 22).

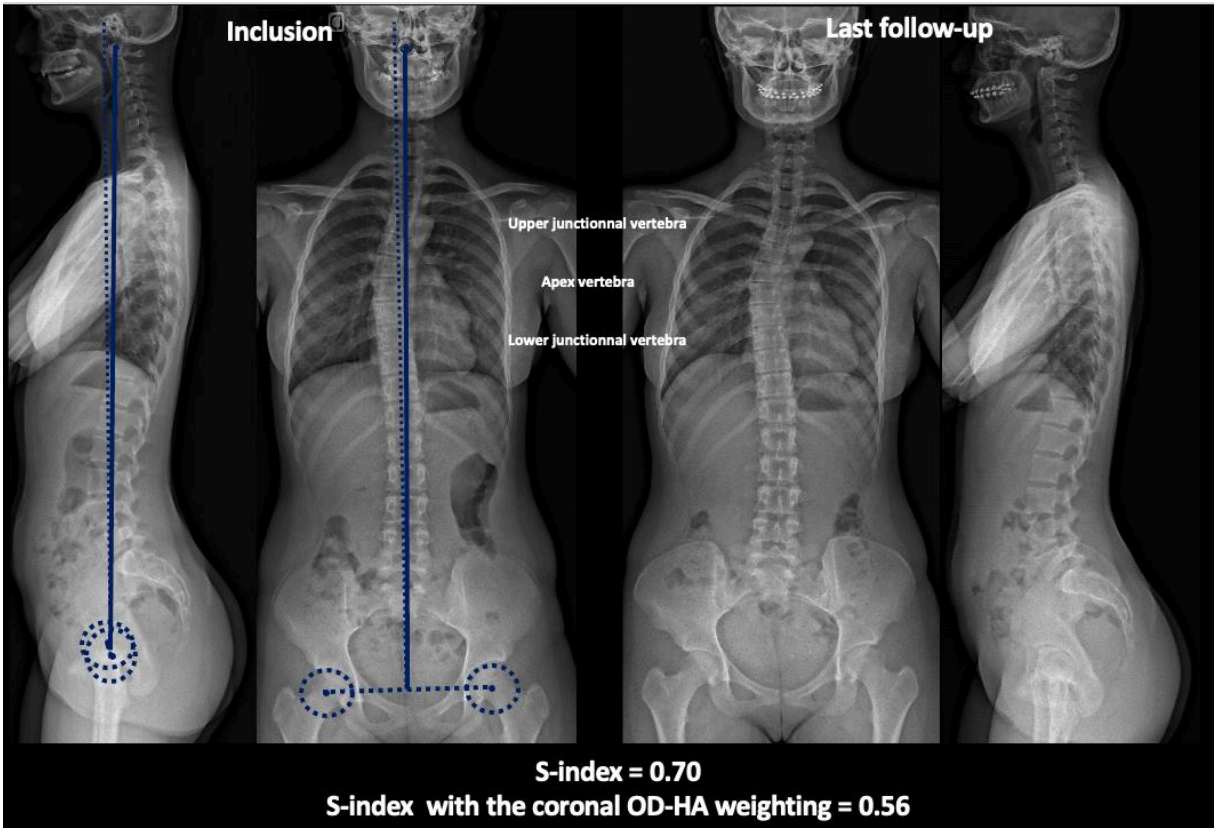

Figure 21: Illustration of sagittal and coronal OD-HA measurement on the biplanar inclusion radiograph of a thoracic scoliosis. The S-index was 0.70 and classified the scoliosis as "progressive" whereas the radiograph 3 years later (illustrated by the image on the right) shows that the scoliosis is stable. Weighting by coronal OD-HA brings the S-index down to 0.56 (<0.6) and thus into the unclassified group.

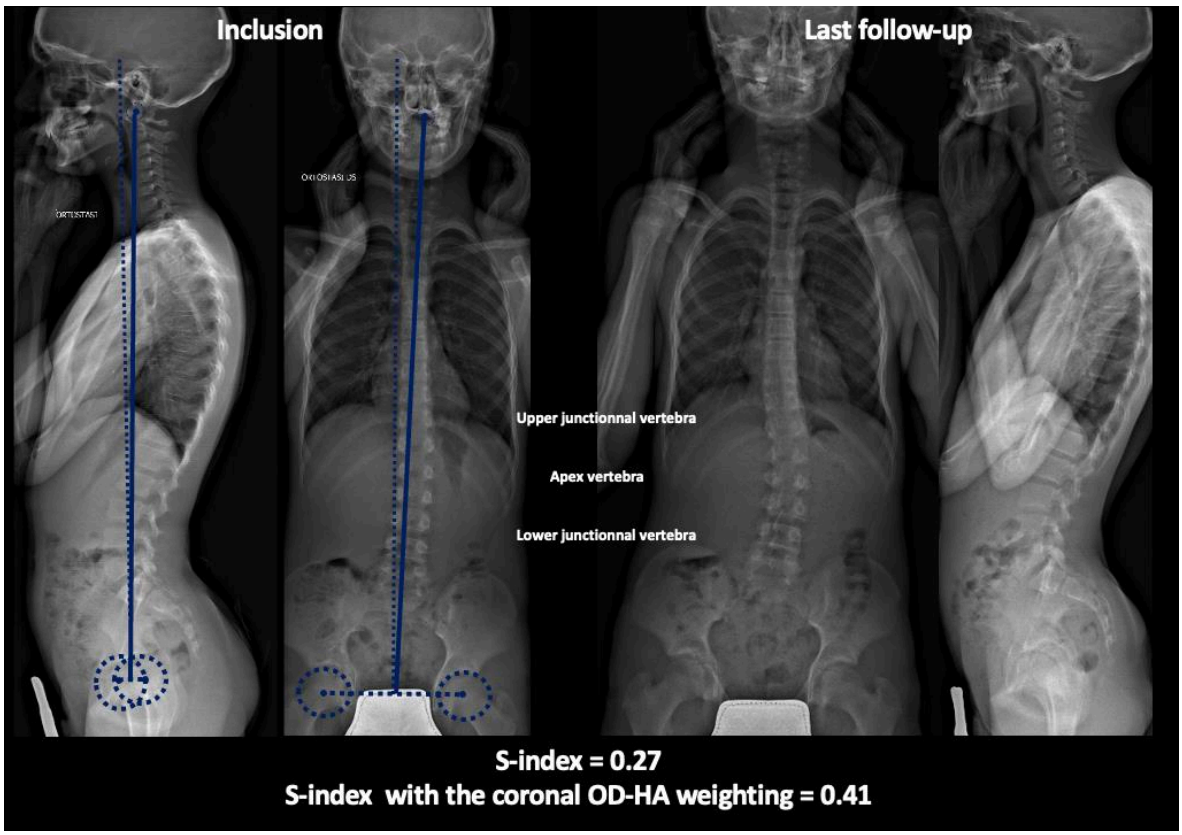

Figure 22: Illustration of sagittal and coronal OD-HA measurement on the biplanar inclusion radiograph of a lumbar scoliosis. The S-index was 0.27 and classified the scoliosis as "stable" whereas the radiograph 2 years later (illustrated by the image on the right) shows that the scoliosis is progressive. Weighting by coronal OD-HA brings the S-index down to 0.41 (<0.4) and thus into the unclassified group.

The main limitation of this work is that this study focuses on a static approach and therefore focus on alignment. However, it has been established that the dynamic proprioceptive system is affected in patients with idiopathic scoliosis (Assaiante et al. 2012). Rebeyrat et al. investigated changes in dynamic OD-HA on adult spinal deformities and found that dynamically unbalanced spinal patients had postural malalignments that persisted during walking, associated with kinematic alterations of the trunk, pelvis and lower limbs, making them more prone to falls (Rebeyrat et al. 2022). For thoracic AIS with abnormal radiological OD-HA, further investigations could concern how dynamic OD-HA is affected, providing a better understanding of the relationship between malalignment and imbalance.

The second limitation is that the Cobb angle of the main curvature of progressive scoliosis was larger than that of stable scoliosis. This difference could indirectly increase the ratio of patients with abnormal and normal 3D OH-HA position. Finally, although high odds ratios have been estimated in this study, the confidence intervals suggest that their significance could be low (confidence interval close to one). A study on a larger cohort could give a more robust answer to the question of malalignment in early scoliosis.

In conclusion, the analysis of OD-HA malalignment, using biplanar radiographs, suggests that AIS patients are almost three times more likely to have a malalignment, and at an early stage, weighting the severity index by considering the coronal OD-HA was improved, particularly for thoracic scoliosis. Therefore, the coronal OD-HA parameter may be useful to the clinician as a complement in thoracic scoliosis. Further investigation on a larger cohort could allow integration of this parameter for future improvement of the severity index.

IV.5 Conclusion

Cette analyse de l'alignement global suggère que les patients porteurs d'une scoliose idiopathique sont presque trois fois plus susceptibles d'avoir un trouble de l'alignement, et à un stade précoce. L'analyse de la pondération de l'indice de sévérité par la mesure de l'OD-HA coronale a montré que les performances de l'indice étaient améliorées, en particulier pour les scolioses thoraciques. Dans le prochain chapitre, nous allons évaluer les paramètres issus de la reconstruction de l'enveloppe externe. Dans un premier temps, nous avons réalisé une étude préliminaire visant à évaluer l'utilité et la pertinence de ces paramètres tels que l'asymétrie du pli de taille et la barycentremétrie dans une population de sujets sains et scoliotiques qui a fait l'objet d'une publication puis nous avons analysé la pondération de l'indice de sévérité par ces paramètres dans un second article prêt pour une soumission dans une revue à comité de lecture.

V - Évaluation des paramètres issus de la reconstruction 3D de l'enveloppe externe dans la prédiction précoce d'aggravation d'une scoliose idiopathique

V.1 Évaluation préliminaire dans une cohorte de sujets asymptomatiques et porteurs d'une scoliose idiopathique

Cet article a fait l'objet d'une publication dans la revue Medical Engineering and Physics, comme 1er auteur : https://doi.org/10.1016/j.medengphy.2021.06.004

Balance, barycentremetry and external shape analysis in idiopathic scoliosis: What can the physician expect from it?

V.1.1 Introduction

Idiopathic scoliosis is a 3-dimensional (3D) spinal deformity of uncertain etiology defined in the coronal plane by a Cobb angle of at least 10° and axial vertebral rotation (Coonrad et al. 1998). 3D reconstruction of the spine from low-dose biplanar X-rays has made it possible to quantify the deformation in a standing posture using new objective biomechanical markers (e.g. intervertebral axial rotation, torsion index) (Skalli et al. 2017). These markers can help in the characterization of scoliosis and its potential progression, as well as in the planning of treatment and analysis of outcomes (Skalli et al. 2017; Vergari et al. 2019).

Concurrent with localized bone deformity, progressive idiopathic scoliosis can lead to postural imbalance and thus disturb the overall balance of the trunk and waist (Hong et al. 2017). Recently, preliminary studies have investigated biomechanical factors resulting from external shape reconstruction such as the center of mass or the intersegmental moment (Hernandez et al. 2018; Thenard et al. 2019). Furthermore, the feasibility of assessing center of mass using 3D reconstruction of the external envelope from biplanar x-rays was demonstrated, reporting an uncertainty within 6 mm (in terms of twice the standard deviation) when compared to a force plate (Hernandez et al. 2018). Differences have been found in scoliotic patients and more

precisely at the junctional level (Thenard et al. 2019), but the clinical relevance of external shape analysis, and on the many parameters that it can provide, has not been evaluated yet. How do these parameters adjust depending on the severity and/or location of the curvature? Can they guide the physician in the diagnosis or therapeutic assessment? In particular, this analysis might help corroborate the hypothesis that scoliosis is a decompensation of the spine that starts in the transverse plane. The hypothesis of this work was that barycentremetry and external shape analysis is relevant in characterizing the 3D deformity of adolescent idiopathic scoliosis (AIS). Our objective was to establish a corridor of normality for the 3D parameters and then to assess these variables in a scoliotic population according to curve severity and location.

V.1.2 Materials and methods

Subjects

Data were collected prospectively from orthopedic department within follow-up clinical investigation for the scoliosis group (group S) and as part of the research protocol for the asymptomatic group (group A). Parents, children and adults were informed about the protocol and consented to participating before inclusion. Parents or adults signed informed consent, which was approved by the ethics committee (C.P.P. Ile de France VI 6001). Asymptomatic young adults were included in group A if they had no history of spinal disease. A systematic clinical examination was per- formed by a spine surgeon to rule out any diagnosis of scoliosis for these subjects. A pathognomonic scoliosis sign, a rib hump and other clinical signs like dorsal pain, asymmetry of the shoulders or pelvic asymmetry were criteria for exclusions.

Adolescent with idiopathic scoliosis Lenke (Lenke et al. 2002) 1, 3 and 5, aged less than 18 years (y), with a main Cobb angle between 10 and 25° (mild scoliosis) and superior than 35° (severe scoliosis) were included. Patient with congenital, syndromic or neuro-muscular scoliosis, early onset scoliosis (less than 10 years), supernumerary vertebrae, a transitional anomaly, or history of spine surgery were excluded. Weight, height and body mass index were measured for each subject. All patients underwent a low dose biplanar X-ray (EOS system, EOS Imaging, Paris, France) at inclusion, in the standardized free-standing position (Faro et al. 2004). Patients who did not respect this position were excluded (arms held too high, too low

or asymmetrically, obvious leaning forwards or backwards, etc.). Group Scoliosis (S) was divided for analysis into two groups according to curve severity: “mild” scoliosis defined by a Cobb angle between 10° et 25°, European Risser sign (Nault et al. 2010) from 0 to 2 and no previous treatment, whereas “severe” scoliosis was defined by a Cobb angle higher than 35°. Patients were also grouped by main curve location: main thoracic curve scoliosis grouped together Lenke 1 and 3 (T) whereas thoraco-lumbar or lumbar scoliosis corresponded to Lenke 5 (TLL).

3D spinal reconstruction

A quasi-automatic 3D reconstruction of the spine was performed with a previously validated technique (Gajny et al. 2019; Vergari et al. 2019). Briefly, the operator selected a few anatomical landmarks on the frontal and lateral radio- graphs: sacral plate, left and right acetabula, the spinal midline through the center of all vertebral bodies from the odontoid apophysis of C2 to L5 lower endplate. The upper endplate of C7 and lower endplate of T12 were also selected in the lateral view, while the two endplates delimiting the main scoliotic curve were selected in the frontal view. The junctional levels of the main curve were defined to obtain the maximization of Cobb angle, and they were often characterized by a local discontinuity of vertebral axial rotation (i.e., a sudden change of vertebral axial orientation). An automatic algorithm provided an initial solution of 3D reconstruction, on which the operator could perform fast manual adjustment of some key vertebrae (the apex, junctions and the adjacent to the junctions) to improve accuracy (figure 21A). The 3D reconstruction allowed for the automatic computation of classical spinopelvic parameters, such as Cobb angle, OD-HA, T1-T12 and T4-T12 kyphosis, L1-S1 lordosis, pelvic incidence (PI), pelvic tilt (PT) and sacral slope (SS).

3D external shape reconstruction

External shape (head, thorax, abdomen, arms, legs, and feet) was reconstructed using a validated manual technique (Nérot et al. 2015). The procedure takes 15 minutes and consists in 2 steps:

1) A first set of 49 control points included the location of the crotch, the midpoint of the L4-L5 intervertebral disc, and 8 joint centers in order to scale the body envelope

pattern on the coronal and sagittal radiographs of the subjects. These points were used to deform a generic template to fit the patient-specific morphology, and the external shape was projected onto both radiographs (figure 23A).

2) The second set included 77 skin points for a fine deformation of the template. These points were disposed on the body parts of high shape variation between individuals, such as the waist, which depends on subjects' weight and muscle structures. By manually moving each of these skin control points, the template could be adjusted to match the contour from the frontal and lateral radiographs (Fig. 23B). Finally, a second well-trained operator performed a quality control procedure, and errors were adjusted if necessary (figure 23C).

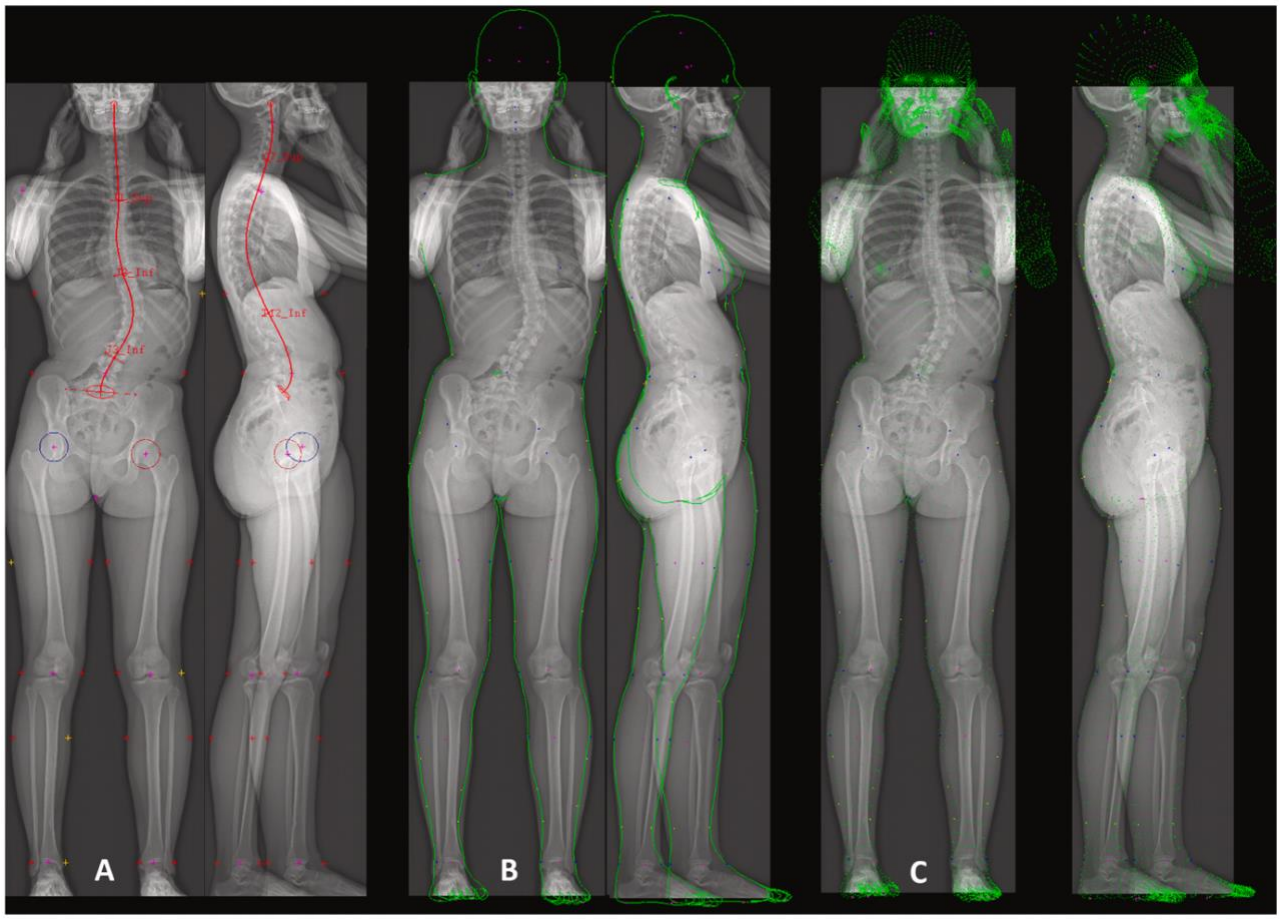

Figure 23: Example of spinal and external shape reconstruction

External shape parameters

Body segments weights were calculated according to a recent estimation of segmental mass density (Amabile et al. 2016b). Then, three parameters resulting from the reconstruction were automatically computed:

1) The center of mass (CoM) position

Horizontal slices of the external envelope were virtually cut at each vertebral level. The lateral CoM of each slice was computed to calculate its distance from the vertical line passing through the middle of the interacetabular axis in the coronal plane. This distance was calculated at all vertebral levels in asymptomatic controls, in order to define a normality corridor, and at specific vertebral levels in scoliotic patients: apical, upper junctional and lower junctional (Thenard et al. 2019). This parameter represents the lateral mass displacement at specific regions (figure 24B). Furthermore, the position of the global trunk CoM relatively to the pelvic acetabula was computed.

2) Intersegmental moment

Intersegmental moment was the torsional moment applied to each vertebra (apical, upper and lower junction) as a result of its lateral displacement and inclination in the sagittal plane, due to the mass of the body above the vertebra and the position of this segment's center of mass (Thenard et al. 2019) (figure 24C).

3) Coronal trunk balance

Coronal trunk balance was quantified using the lateral offset of the envelope. This parameter was computed at each vertebral level below T10 as follows: a series of horizontal lines were defined in the coronal plane, passing through the center of each vertebral body. The intersections between these lines and the externals envelope were marked. Finally, the ratio of the distances between the vertebral body and the left and right intersection were computed automatically. Furthermore, this ratio was defined at apical and lower junctional if these vertebral levels were below T10 (figure 22D). This parameter represents the local lateral asymmetry of the external envelope in the lumbar region.

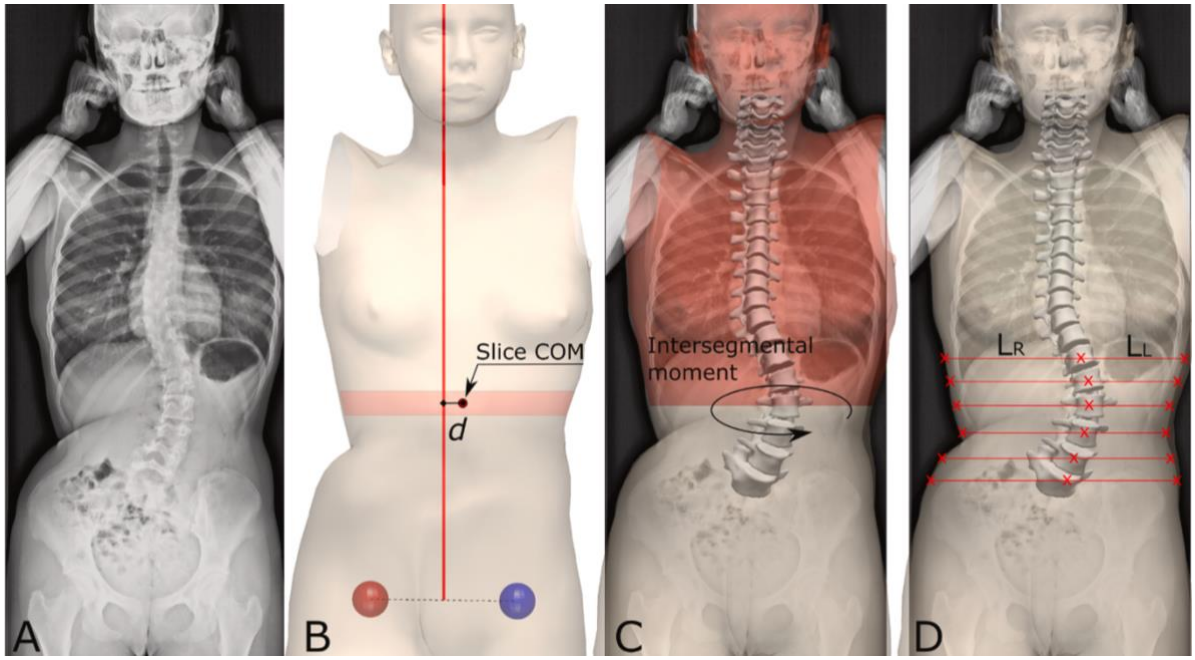

Figure 24: (A) frontal radiograph of a scoliotic patient. (B) Lateral position of the center of mass (CoM) of a horizontal body slice corresponding to a vertebral level. (C) Intersegmental moment applied to a vertebra by the above body regions. (D) Coronal trunk balance quantified at each vertebral level as the ratio of the distance between the vertebra and the left and right sides of the body.

Statistical analysis

Reliability of the novel parameters (lateral center of mass position, spinal intersegmental moment and lateral offset of the envelope) was estimated with a Monte Carlo procedure: the 3D reconstruction of each patient was virtually modified by adding uncertainty to the vertebral orientations and positions, as well as on the position of the CoM. The uncertainty was randomly picked from a normal distribution of errors based on previous evaluations of local uncertainty (Hernandez et al. 2018; Gajny et al. 2019). This was repeated 50 times for each patient, for a total of 5050 simulations, which allowed to estimate a standard deviation of uncertainty for each parameter. Non-parametric statistical tests were used because not all variables were normally distributed (Lilliefors normality test). In order to compare spinal and external shape parameters according groups, the Mann-Whitney's test was applied. In order to compare the relationship between spinal and external shape parameters, Spearman's correlation was applied. A normality corridor of asymptomatic

subjects was calculated as the range [5^{th}-95^{th} percentiles] for external shape parameters at each vertebrae level. The number of scoliotic children having their external shape parameters higher than the corridor's limits was reported and their values were defined as abnormal. Statistical analysis was performed using R software (v3.6.3). Significance was set at 0.05.

V.1.3 Results

Subjects

Forty-one asymptomatic subjects (19 females; 22 males) were included with a mean age of 21y (SD=4; from 10 to 31 y) and a mean BMI of 21.7 $kg.m^{-1}$ (SD=2; from 16.7 to 26.4 $kg.m^{-1}$). Sixty adolescent idiopathic scoliosis (56 females; 4 males) were included with mean age of 13y (SD=1.9; from 10 to 18 y). The mean BMI was 18.5 $kg.m^{-1}$ (SD=0.1; from 13.3 to 27.3 $kg.m^{-1}$).

Thirty AIS (27 females and 3 males; 12y with SD=1.8; 17.8 $kg.m^{-1}$ with SD=3; 13 Lenke 1, 4 Lenke 3 and 13 Lenke 5) were classified as mild scoliosis while 30 AIS were severe (28 females and 2 males; 15y with SD=1.4; 19.1 $kg.m^{-1}$ with SD=3; 13 Lenke 1, 4 Lenke 3 and 13 Lenke 5). Thirty-four AIS (33 females and 1 male; 13.4y with SD=6; 18.8 $kg.\ m^{-1}$ with SD=3; mean main Cobb angle = 37.7° with SD=17.7) had a thoracic main curve while 26 AIS were thoracolumbar or lumbar (22 female and 4 male; 13.7y with SD=1.9; 18.4 $kg.m^{-1}$ with SD=2.4; mean main Cobb angle = 35.7° with SD=20.3).

Spinopelvic parameters

In asymptomatic controls, the average OD-HA was 0.8° (SD=0.6) T1- T12 kyphosis of 48° (SD=10.7), T4-T12 kyphosis of 34.2° (SD=10), L1- S1 lordosis of 44.7° (SD=11.5), pelvic incidence of 49.2° (SD=9.5), pelvic tilt of 8.4° (SD=5.7) and sacral slope of 39.8° (SD=8.5). Spino- pelvic parameters in scoliosis group were described in table 4.

Table 4: Spinal parameters for scoliosis group and following the severity and topography; Results are presented as mean ± standard deviation; Significant p-values were marked in bold. *p-value* 1 and 2 represents respectively the significance of the difference between severity groups and scoliosis localization groups.

	Scoliosis (N=60)	Mild scoliosis (N=30)	Severe scoliosis (N=30)	*p-value* $_1$	T curve (N=34)	TLL curve (N=26)	*p-value* $_2$
Main Cobb angle (°)	36 ± 18	20 ± 6	53 ± 9	<0.0001	37 ± 17	36 ± 20	0.7
OD-HA (°)	1.6 ± 1	1.2 ± 0.7	1.9 ± 1.2	0.2	1.4 ± 0.9	1.8 ± 1.2	0.4
T1-T12 (°)	32 ± 16	32 ± 19	33 ± 11	0.7	30 ± 17	37 ± 13	0.2
T4-T12 (°)	22 ± 16	24 ± 17	20 ± 15	0.2	18 ± 14	27 ± 16	0.05
L1-L5 (°)	41 ± 20	39 ± 24	43 ± 13	0.9	39 ± 24	44 ± 11	0.7
PI (°)	43 ± 11	40 ± 7	46 ± 13	0.07	44 ± 11	42 ± 11	0.7
PT (°)	4 ± 7	3 ± 7	5 ± 7	0.5	4 ± 7	4.6 ± 8	0.6
SS (°)	39 ± 9	36 ± 8	41 ± 9	0.06	40 ± 9	38 ± 9	0.3

Reliability

The uncertainty did not exceed 0.8 mm for the lateral position of CoM at all vertebral levels, 0.5 N/m for the intersegmental moment and 0.1 for the coronal trunk balance.

External body shape parameters

The normality corridors for the parameters related to external body shape were reported in table 5 and values for scoliotic patients in table 6.

Table 5: Normality corridors for parameters of external shape analysis. Results are pre- sented such as median [5th-95th percentile]; na = not applicable; CoM: center of mass of body slices at each vertebral level.

Vertebrae level	Intersegmental moment [N/m]	Lateral CoM position [mm]	Coronal trunk balance
T1	0.07 [0-0.29]	6.82 [0.34-17.27]	na
T2	0.07 [0-0.33]	7.62 [0.72-24.15]	na
T3	0.23 [0-0.87]	8.96 [0.40-20.83]	na
T4	0.34 [0.06-1.58]	8.67 [0.98-20.57]	na
T5	0.34 [0-1.31]	5.86 [0.04-14.56]	na
T6	0.44 [0.05-1.51]	5.96 [0.44-12.72]	na
T7	0.42 [0.08-1.98]	5.72 [0.37-14.08]	na
T8	0.49 [0.03-2]	6.13 [0.70-12.30]	na
T9	0.45 [0.01-1.65]	6.36 [0.87-12]	na
T10	0.45 [0-1.23]	6.31 [0.25-13.06]	na
T11	0.48 [0.01-1.32]	6.26 [0.41-13.09]	0.92 [0.80-0.98]
T12	0.48 [0.01-1.28]	6.10 [0.04-12.98]	0.92 [0.81-0.99]
L1	0.44 [0.06-0.9]	5.54 [0.53-11.14]	0.91 [0.81-0.99]
L2	0.48 [0.06-1.23]	4.75 [0.43-11.23]	0.93 [0.82-0.98]
L3	0.23 [0.02-1.09]	4.1 [0.31-12.1]	0.94 [0.83-1]
L4	0.29 [0-0.9]	3.17 [0.09-9.82]	0.95 [0.84-0.99]
L5	0.40 [0.03-1.45]	2.53 [0.14-10.12]	0.97 [0.86-0.99]

Table 6: Parameters related to the body external shape in scoliotic patients (mean ± standard deviation). CoM: center of mass.

		Vertebral level		
		Upper junctional	Apex	Lower junctional
Lateral CoM position [mm]	Mild	7.8 ± 4.5	7.3 ± 4.8	6.4 ± 4.5
	Severe	15.7 ± 10.2	17.3 ± 9.6	17.5 ± 9
	T curve	9.2 ± 6.5	10.8 ± 8.7	12.1 ± 10
	TLL curve	14.9 ± 10.2	14.2 ± 9.3	11.7 ± 6.5
Intersegmental moment	Mild	1.4 ± 0.7	0.6 ± 0.5	0.6 ± 0.5
	Severe	4.6 ± 1.9	1.6 ± 1	2.6 ± 1.5
	T curve	3.2 ± 2.2	1 ± 1	1.8 ± 1.6
	TLL curve	2.7 ± 1.9	1.2 ± 1	1.3 ± 1.2
Coronal trunk balance	Mild	0.9 ± 0.1	0.9 ± 0.1	0.9 ± 0.1
	Severe	0.8 ± 0.2	0.7 ± 0.1	0.8 ± 0.1
	T curve	0.9 ± 0.1	0.9 ± 0.1	0.8 ± 0.1
	TLL curve	0.8 ± 0.1	0.8 ± 0.1	0.8 ± 0.1

The lateral position of the CoM was abnormal in 32% (N=19/60) of upper junctional vertebrae, 42% (N=25/60) of apical and 43% (N=26/ 60) in lower junctional vertebrae, even though the average values were similar between AIS and asymptomatic controls (p=0.37). Upper junctional and apical lateral CoM position values are higher in TLL than in T group (p=0.01). When the global trunk CoM in asymptomatic subjects was analyzed in 3D, the 95^{th} percentile of normality corridor, as viewed from a top view, corresponded to a small ellipse of in the middle of the pelvic acetabula (figure 25). In this representation, the global trunk CoM of 60% (N=18/30) severe patients and 53% (N=16/30) mild patients fell outside this corridor.

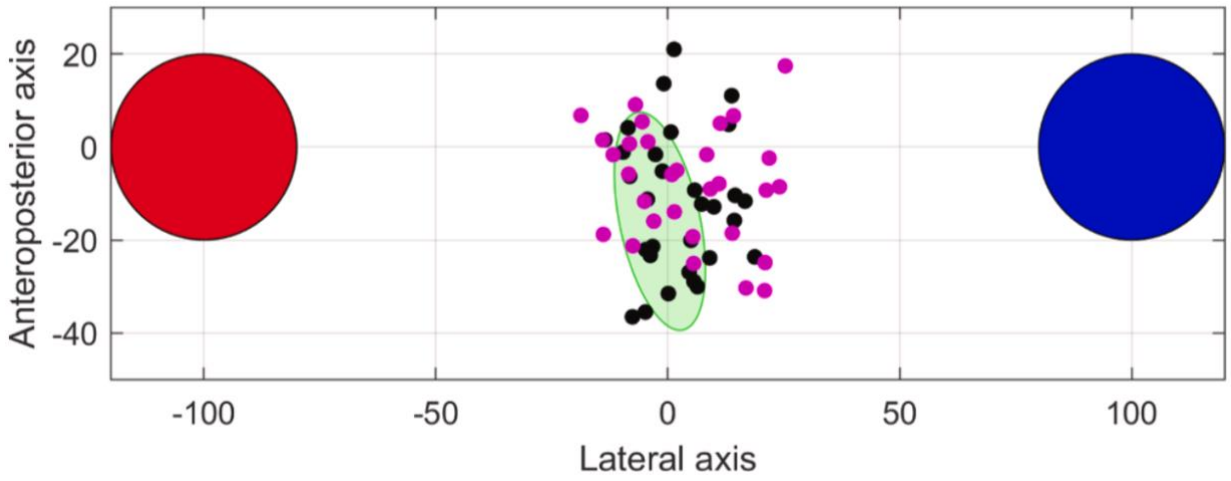

Figure 25: Top view of the position of the CoM in mild (black) and severe scoliosis (pink) relative to its position in asymptomatic controls (green area, represent- ing the 95th percentile). The red and blue circles represent the left and right pelvic acetabula, respectively. The distance between acetabula was normalized to 200, in order to place all patients in a common anatomical scale.

The intersegmental moment applied to the upper junctional vertebra was abnormal in 70% (N=48/60) of scoliosis patients, while less than 50% in apex and lower junctional vertebrae were above ($p<0.0001$). These results were confirmed by a subgroup analysis according to curve's severity (figure 26).

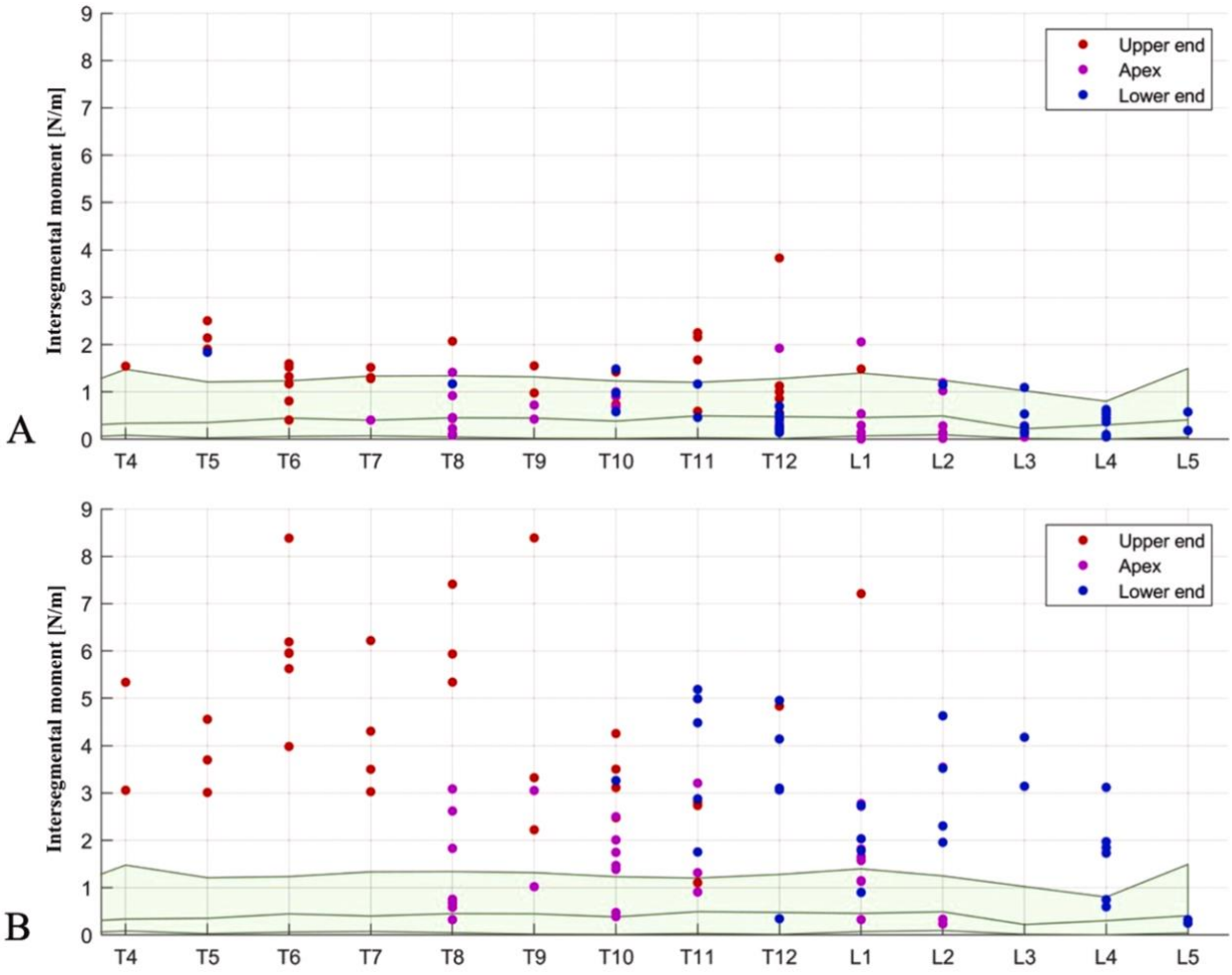

Figure 26: Intersegmental moment values at junctional and apical levels, according to the normality corridor [5th-95th percentiles] (green shaded area), in mild (A) and severe scoliosis (B).

Thirty-eight percent of scoliosis subjects (N=10/60) was abnormal for the apical coronal trunk balance and 45% (N=21/60) for lower junctional (p=0.41). Abnormal apical coronal trunk balance values were of 60% (N=6/10) in severe scoliosis (versus 25% in mild) and 43% (N=9/21) in TLL (versus 17% in T).

Lateral CoM position and intersegmental moment were correlated with main Cobb angle, and the lateral CoM position was also correlated to OD-HA (figure 27).

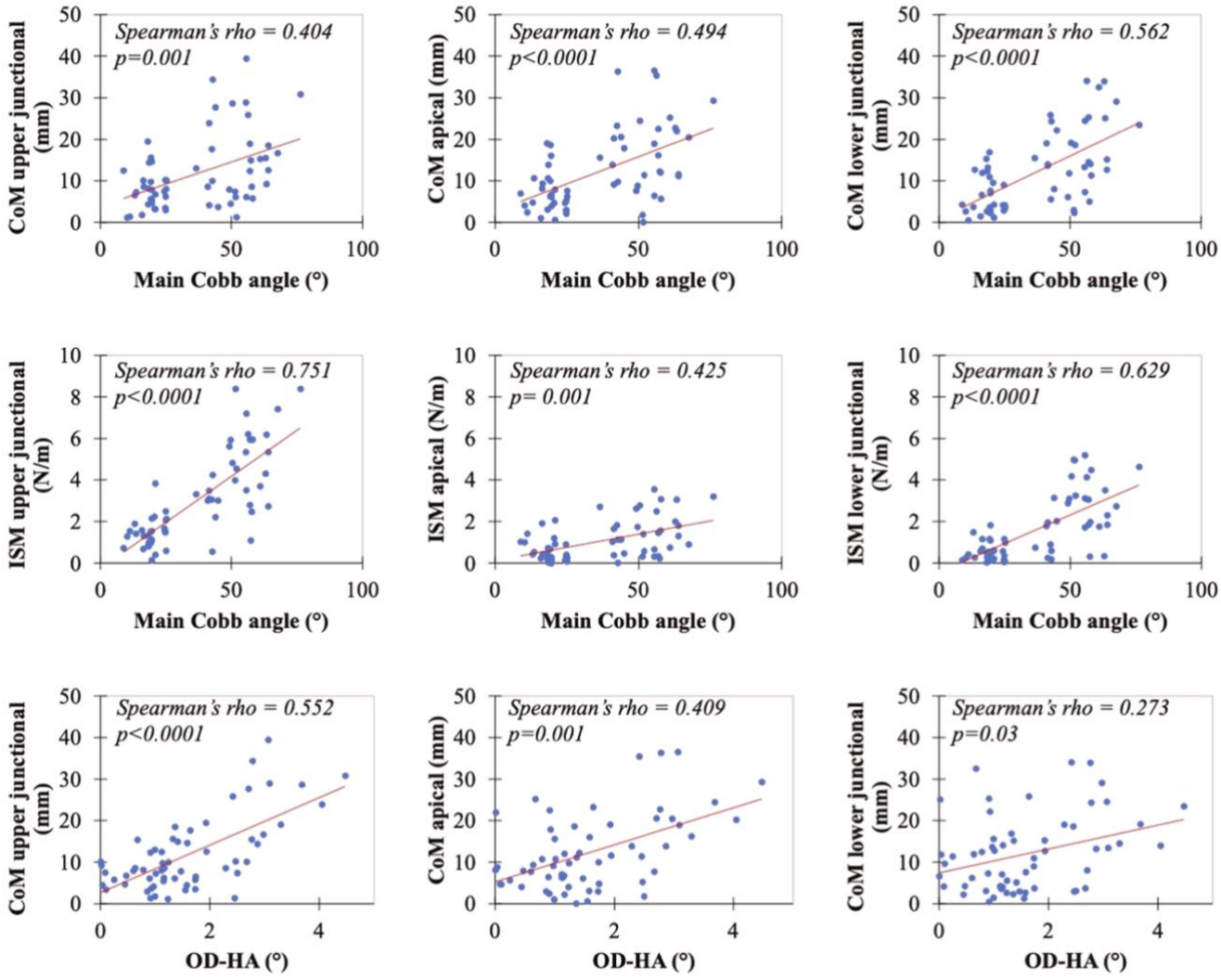

Figure 27: Scatter plot graph between main Cobb angle and the lateral CoM position, main Cobb angle and intersegmental moment (ISM) and OD-HA and the lateral CoM position parameters.

V.1.4 Discussion

In the monitoring of idiopathic scoliosis, the physician endeavors to use objective, reproducible, reliable and minimally invasive criteria to detect progressive scoliosis and in some cases to assess its treatment. In addition to the clinical and skeletal maturation criteria described initially by Duval Beaupère (Duval-Beaupère 1970; 1992), the clinician can use biomechanical parameters. The pioneering work of Duval Beaupère et al. showed that the 2D

centre of mass study is related to the sagittal curvatures and pelvic parameters of young healthy patients (Duval-Beaupère, Schmidt, et Cosson 1992). Recently, further work has shown that the determination of the anatomical connection of the individual gravity is thus of primary importance for the evaluation of sagittal balance (J. Legaye et Duval-Beaupere 2008). From our results, barycentremetry and external shape analysis seems to be relevant in characterizing the 3D deformity of adolescent idiopathic scoliosis for various reason. Longitudinal studies are under way to determine whether the proposed approach could lead to a reliable objective prediction of the curve's progression and enable clinical follow-up.

The first relevant finding is that the lateral center of mass position and the coronal trunk balance factors increase with the curve severity, independently of the curve location. This is not surprising that clinical postural imbalance is radiographically translated by alterations of these factors. In this sense, a preliminary study had demonstrated a correlation between imbalance and the distance between the plumb line and the gravity line in biplanar X-rays (Hernandez et al. 2018). In this study, a correlation between OD-HA and the center of mass position was found. The posture imbalance can thus be quantified and could help the physician to quantitatively monitor the curve progression, but also to assess the therapeutic outcomes obtained by brace or spinal fusion correction. Sagittal balance was not analyzed in the present work because while scoliotic subjects often present a characteristic flat back, the also maintain a good sagittal alignment, with minimal imbalance, thanks to their good compensating mechanisms.

It was interesting to notice that the upper junctional intersegmental moment is higher in scoliotic patients than in asymptomatic controls. We found that 68% of scoliosis patients had an upper junctional inter- segmental moment above 95th of normality corridor. This factor is also a good indicator of severity as 97% of severe patients was above the 95th of normality corridor. These results confirm the findings about the upper junctional intersegmental moment in the study of Thenard et al. (Thenard et al. 2019). Perdriolle (Perdriolle 1979) had reported, on his clinical experience, that the intervertebral torsion of the upper junction level was an important factor in the vicious cycle leading to progression. The present results are consistent with his findings but require further study to confirm them. Forty percent of mild scoliosis showed an abnormal upper junctional intersegmental moment. Future work may

focus on the relevance of this factor in helping to identify progressive scoliosis at an early stage.

Indeed, an important point is the potential link between the intersegmental moment and the biomechanical disturbance of the intervertebral disc and vertebrae. Larouche Guilbert et al. showed that intervertebral efforts (medio-lateral and antero-posterior) are larger in the adolescent with idiopathic scoliosis compared to the healthy adolescent, except for the axial intersegmental moment (Larouche Guilbert et al. 2019). Adam et al. had concluded in preliminary biomechanical analysis about eight idiopathic scoliosis that the gravity-induced intersegmental moment is a likely cause of intravertebral rotation in progressive idiopathic scoliosis (Adam, Askin, et Pearcy 2008). However, the intersegmental torque that was estimated in this work does not necessarily reflects the actual loading of the disc; as Pomero et al. (Pomero et al. 2004) suggested through musculoskeletal modelling, the intersegmental moment is related to musculo-tendon forces and translates into disc compression and shear. Thus, intersegmental moment in this work should be considered as a biomarker reflecting the position and orientation of the vertebra, as well as the position and asymmetry of the mass above it.

The third relevant finding is that the values of the lateral CoM position are higher for thoraco-lumbar and lumbar scoliosis. Once again, this objectively reflects the fact that these curvatures cause greater postural imbalance. In the future, these quantitative factors could be considered in the assessment of a treatment for thoraco-lumbar or lumbar scoliosis.

In our study, we also reported values for the studied parameters (i.e. intersegmental moments, CoM position and coronal trunk balance) in a cohort of 41 healthy individuals with a mean age of 21 years. Blondel et al. (Blondel et al. 2012) described a method of measuring intersegmental moments in a healthy 30-year-old patient. We found almost similar values in the upper thoracic and lower lumbar regions. However, our values were significantly lower in the thoracolumbar region. Larouche Guilbert et al. (Larouche Guilbert et al. 2019) found intersegmental moment values of the same order of magnitude and with the same distribution across levels as our study. For the CoM position and the external envelope analysis we did not find similar results.

The three-dimensional analysis method is accessible to the physician. Bone reconstruction is quasi automatic, taking less than 5 minutes and with good reliability of measurements (Vergari et al. 2019). On the other hand, the external envelope analysis is still a manual reconstruction method requiring about twenty minutes. Its automation is under development. Nevertheless, 3D assessment of barycentremetry and external shape may provide guidance to the physician in the diagnosis and monitoring of idiopathic scoliosis. First of all, it provides objective and reliable information on the severity of the bone curvature, but also on the imbalance and its disturbances in the axial plane. Other minimally invasive methods of analysis have focused on the external envelope analysis. Jaremko et al. showed that the 360° torso asymmetry indices developed show a strong relationship between the surface and the spine in scoliosis (the Cobb angle is estimated from the torso indices to within 5° in 65% of patients and to within 10° in 88%) with minimal radiological radiation (Jaremko et al. 2002). However, Patias et al. cautioned that the analysis of these different indices in the literature has divergent characteristics in terms of observer-induced error, accuracy, sensitivity and specificity (Patias et al. 2010). Recently, Bolzinger et al. (Bolzinger et al. 2021) proposed a new analysis method for monitoring curvature progression by analysis using surface topography. This analysis allows to differentiate patients with or without increased Cobb angle with a good reproducibility (ICC: 0.816) and has allowed to decrease the number of radiographs by 30%.

The findings of our study might help the question we can address is whether a good correction of the lower intersegmental moment will spare the underlying disc degeneration, or if the correction of the imbalance reflect the patient's satisfaction after a specific treatment, or even to assess the position of the axial center of mass in relation to various brace or instrumentation. This study has certain limitations. EOS biplanar X-ray system is limited to 34 cm in width for the radiographic acquisition. All patients whose contours on the front and lateral view were missing were excluded from the study. Nevertheless, this technical constraint is less frequently encountered in a pediatric population. Another limitation is the position of the arms, which was not standardized for each patient. This could disturb the contour marking of the external shape and has a known effect on the mass distribution (Legaye et Duval-Beaupere 2017). However, a standardized free-standing position was adopted in the study, and the radiographs were excluded if the position was not correct. Our

group of asymptomatic subjects mostly consisted of young adults with an average age of 21 years. A cohort of age-matched asymptomatic adolescent was difficult to recruit for this research study. Indeed, ethical standards will enable us to perform biplanar radiography in healthy children. The asymptomatic cohort could be continued with younger subjects in order to improve the corridor of normality. On the other hand, we have deliberately excluded scoliosis between 25 and 35° to limit potential measurement bias and to clearly differentiate between mild and severe scoliosis. Results of barycentremetry and external shape analysis in idiopathic scoliosis are promising. The intersegmental moment, the center of mass position and the coronal trunk balance parameters appear to be relevant in characterizing the 3D deformity of adolescent idiopathic scoliosis. The upper junctional intersegmental moment seems to be able to distinguish the different stages of curvature severity regardless of curve's location. These findings on biomarkers need to be further investigated, but they could be helpful to the physician in monitoring idiopathic scoliosis, in predicting progression and in assessing treatment outcomes.

V.1.5 Conclusion

Dans cet article, nous avons établi des valeurs de références pour la mesure de l'asymétrie du pli de taille, la position du centre de masse et le moment intersegmentaire à chaque étage issus de l'analyse de l'enveloppe externe dans une population jeune et sans déformation rachidienne. Nous avons évalué la pertinence de ces mesures dans une population d'adolescent porteur d'une scoliose idiopathique modérée et sévère. Les résultats sont prometteurs et les trois paramètres semblent être liés à la sévérité de la courbure. Nous allons dans la partie suivante évaluer leur rôle comme prédicteur d'une scoliose progressive.

V.2 Évaluation des paramètres issus de la reconstruction de l'enveloppe externe dans la cohorte de validation de l'indice de sévérité

Cet article va faire l'objet d'une soumission dans les prochaines semaines, comme 1er auteur.

3D external shape analysis and barycentremetry can provide early signs of progression in adolescent idiopathic scoliosis

V.2.1 Introduction

Idiopathic scoliosis is a three-dimensional (3D) spinal deformity of uncertain aetiology defined in the coronal plane by a Cobb angle of at least 10◦ and an axial vertebral rotation (Coonrad et al. 1998). Its aetiopathogeny is multifactorial and the causal factors poorly understood (Kouwenhoven et Castelein 2008) but several preliminary studies emphasize a possible sensory imbalance at an early stage (Guo et al. 2006; Assaiante et al. 2012). Early detection is a public health issue to implement early treatment. On the other hand, being able to distinguish a stable scoliosis from a progressive form at an early stage would make it possible to avoid over-treatment and save the costs associated with brace treatment and also reduce the risk of surgery (Nachemson et Peterson 1995).

Recently, a validated predictive models based on 3D biplanar reconstruction (i.e., the severity index described by Skalli et al. (Skalli et al. 2017) was developed to make this distinction at the first visit. However, this predictive model still needs to be improved and are based solely on the 3D reconstruction of the spine. It is acknowledged that scoliosis is a multifactorial 3D process and includes other anatomical abnormalities such as muscle balance (Jung et al. 2015) and disc mechanical properties (Langlais et al. 2018) among others. In a recent previous study (Langlais et al. 2021), we reported alterations in the distribution of masses resulting from the analysis of the external shape associated to density models in a population of scoliotic patients. The current work aims to ascertain whether barycentremetry could improve the early detection of progressive scoliosis and thus complement predictive models of bone parameters.

To this end, the balance and barycentremetry of a cohort of adolescent idiopathic scoliosis (AIS) was assessed at early stage and compared with their curve progression. Furthermore, the effect of including parameters extracted from external shape analysis and barycentremetry to the severity index was studied.

V.2.2 Materials and methods

Subjects

A cohort of 205 scoliotic patients was considered. Data were collected, between 2013 and 2020 from 6 centres in 4 countries (with a minimal of 10% inclusions per centre), and they were previously reported in studies using a severity index to predict scoliosis progression (Vergari et al. 2021), which did not include any assessment of barycentremetry. Parents, children, and adults were informed about the protocol and consented to participate before inclusion. This study was approved by the ethics committee (C.P.P. Ile de France VI 6001) and by the local ethical committees.

Inclusion criteria were: (1) confirmed diagnosis of AIS; (2) Cobb angle between 10° and 25°; (3) European Risser sign lower than 3 (Duval-Beaupère et Lamireau 1985); (4) age superior to 10 years; and (5) no previous treatment (such as brace or spine surgery). Patients with non-idiopathic scoliosis, transitional anomalies or supernumerary vertebrae were excluded from this study.

Protocol

All subjects underwent a low dose biplanar X-ray (EOS system, EOS Imaging), in the free-standing position (Faro et al. 2004), at the onset of inclusion. Patients were classified by location of the main curve following according to the location of the apex: thoracic (apex between the T2 vertebra and the T11-T12 intervertebral disc), thoracolumbar (apex between the T12 and L1 vertebrae), and lumbar (apex between the L1-L2 intervertebral disc and the L4 vertebra) (Stagnara et Queneau 1953; Perdriolle 1979; Lenke et al. 2002). The follow-up could be stopped at either of two points in time: 1) when the patient reached a Risser sign greater than or equal to 3, without treatment and without progression of the curvature (i.e., a Cobb angle of the main curvature less than 25°). These patients were classified as "stable"; 2) when

a corrective brace was prescribed, in which case patients were classified as "progressive". Quantitative and objective criteria were used to decide on brace treatment according to the International Society on Scoliosis Orthopaedic and Rehabilitation Treatment guidelines, i.e., a Cobb angle of the main curvature greater than 25° and a Risser sign less than or equal to 2, or an increase of 5° in Cobb angle or vertebral axial rotation within 6 months (Negrini et al. 2018), as well as an assessment of the clinical profile.

Imaging data and external shape analysis

A quasi-automatic 3D reconstruction of the spine was performed, from the biplanar radiography acquired at inclusion, using a previously validated method (Vergari et al. 2019; Gajny et al. 2019). An automatic algorithm provided an initial solution of 3D reconstruction, on which the operator could perform fast manual adjustment of some key vertebrae (the apex, junctions and the adjacent to the junctions) to improve accuracy. The 3D reconstruction allowed for the automatic computation of coronal and sagittal OD-HA (Amabile et al. 2016a) and the 6 parameters of the severity index, previously validated (Skalli et al. 2017), i.e., the Cobb angle, the apical vertebral axial rotation, the upper and lower intervertebral axial rotation, the torsion index, and the hypokyphosis index. External shape was reconstructed, retrospectively, using a validated technique (figure 28) (Nérot et al. 2015). The reconstruction takes about 15 minutes, and it allows automatic estimation of body segments weights, according to a recent estimation of segmental mass density (Amabile et al. 2016b), calculation the apical center of mass position (CoM), the apical, upper and lower junction intersegmental moment (Thenard et al. 2019; Langlais et al. 2021) and the apical coronal trunk balance ratio (which is computed for thoraco-lumbar and lumbar scoliosis) (figure 28 and 29).

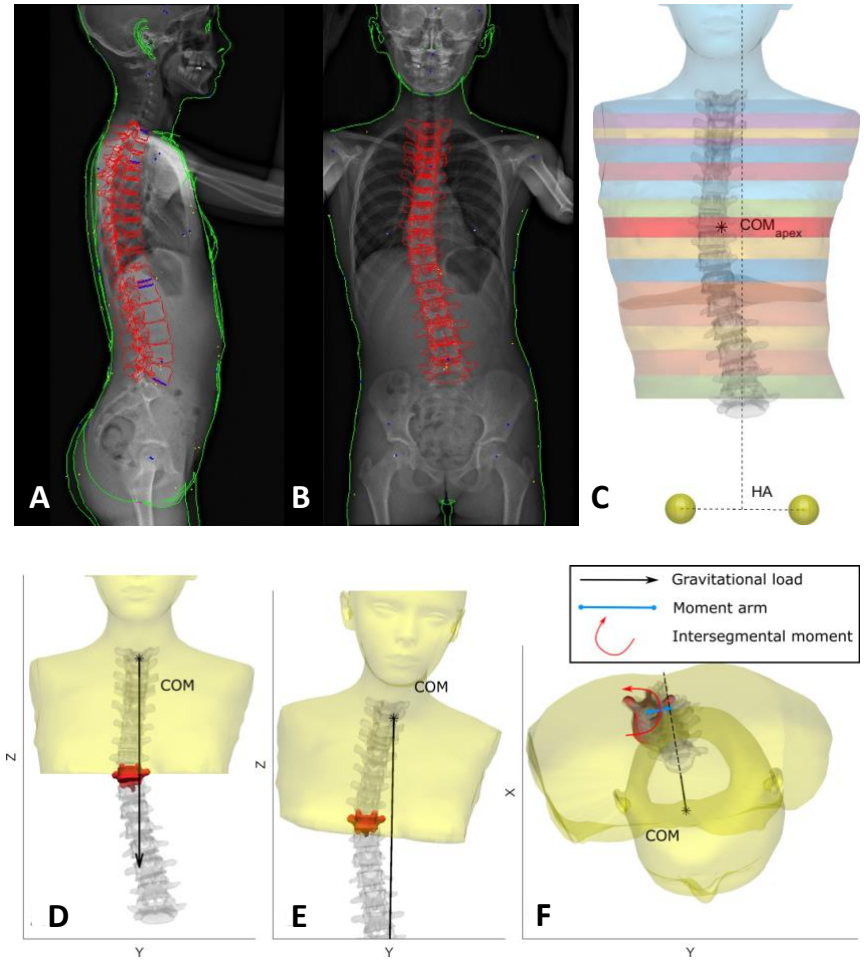

Figure 28: Example of external envelope reconstruction in sagittal (A) and frontal (B) from a biplanar radiograph of a right thoracic scoliosis. Image C illustrates the measurement of the apex centre of mass position. Horizontal slices of the outer shell were virtually cut at each vertebral level. The apex centre of mass slice was calculated to determine its distance from the vertical line passing through the middle of the HA axis in the coronal plane. Frame D, E, F is a visual representation of the apex intersegmental axial moment. Panel D show the 3D reconstruction of the spine, with the apex vertebra highlighted in red, as well as the part of the trunk above this vertebra and its centre of mass (COM). The gravitational load is indicated by the arrow. Panel E show the same 3D reconstruction, but the patient (and the gravitational load) has been virtually rotated so that the apex vertebra is now perfectly horizontal. Panel F shows the same configuration as E in top view, so that the apex vertebra is now horizontal and seen from above. The blue line represents the lever arm ans in red, the apex intersegmental moment was plotted.

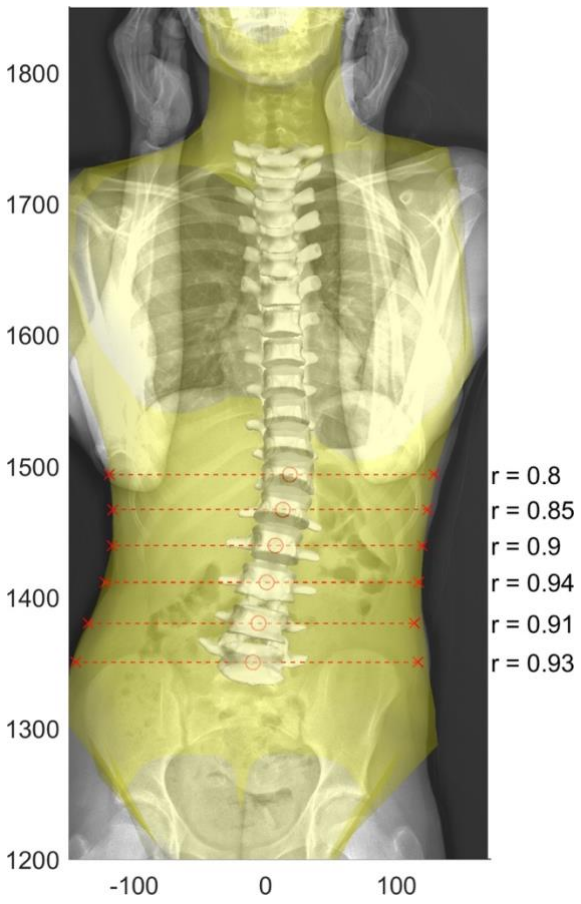

Figure 29: Example of the ratio coronal trunk balance measure. In this case, the apex vertebra is T12 and the ratio was 0.8 (y-axis and x-axis in millimetre)

S-index calculation and weighting protocol

For each patient, the severity index (ranging from 0 to 1) was automatically computed (Skalli et al. 2017; Vergari et al. 2019) and it included the stage of the European Risser sign as a weighing factor (Vergari et al. 2021). The index was further weighted according to the external shape parameters, and the weights were calculated as follows: first, the 5^{th} and 95^{th} percentiles of each parameter were determined in a cohort of asymptomatic subjects (Langlais et al. 2021). Then, if a patient showed a center of mass position or coronal trunk balance ratio greater than the 95^{th} percentile from the asymptomatic cohort, a multiplication factor of 1.5 was applied to the severity index. For the upper, apical, and lower intersegmental moment, a multiplication factor of 1.5 was applied when the parameter was greater than the

95th percentile, while if the scoliotic patient's value was lower than 5th percentile, a multiplication factor of 0.8 was applied. A severity index lower than 0.4 was considered indicative of a stable curve, while an index higher than 0.6 was indicative of a progressive one. No prediction was issued for values in-between, and patient corresponding was unclassified.

Statistics

Numeric variables were expressed as mean (SD) and discrete outcomes as absolute and relative (%) frequencies. Stable and progressive scoliosis was compared for external shape parameters. Normality and heteroskedasticity of continuous data were assessed with Shapiro-Wilk and Levene's test respectively. Continuous outcomes were compared with unpaired Student t-test, Welch t-test or, Mann-Whitney U test according to data distribution. Spearman's correlation was used to assess linear dependence between severity index and external shape parameters. Correlation was judged very strong from 1 to 0.9, strong from 0.9 to 0.7, moderate from 0.7 to 0.5, low from 0.5 to 0.3 and poor from 0.3 to 0. A multivariate linear regression was performed to assess the relation between the external shape parameters with the the severity index parameters and OD-HA. Data were checked for multicollinearity with the Belsley-Kuh-Welsch technique. Heteroskedasticity and normality of residuals were assessed respectively by the Breusch-Pagan test and the Shapiro-Wilk test. The alpha risk was set to 5% and two-tailed tests were used. To analyze the weighting of the severity index with the external shape parameters, we reported the sensitivity, specificity, positive and negative predictive value of the test according to the locations of the curvature. We reported the results of the weighting only when the performance of the test was to improve by at least 5%. Statistical analysis was performed with EasyMedStat (version 3.19; Neuilly-sur-Seine).

V.2.3 Results

Population

One hundred and sixty-two scoliosis (12 years old, SD=1; 139 females and 23 males; 73 thoracic, 40 thoraco-lumbar and 49 lumbar) were included in the external shape analysis. Forty-three patients were excluded because the external shape reconstruction was not

feasible (i.e., the patient's external envelope was outside the limits of the radiograph). Mean Cobb angle of scoliotic patients was 16.0°, SD=3.7°; range from 10.0° to 24.8°. After the clinical and biplanar radiographic follow-up, 87 AIS (53%) were classified as stable and 75 (47%) as progressive. The demographic characteristics are resumed in table 7. The values of the 6 severity index parameters and OD-HA are reported in table 8.

Table 7: Demographics characteristics of population. n represents the number of patients; SD = Standard deviation

	AIS population		
	Total (n=162)	**Stable (n=87)**	**Progressive (n=75)**
Age: yo, SD (range)	12, 1 (10;15)	12.5, 1 (10;15)	11.5, 1 (10;14.5)
Risser Sign: n (%)			
- 0	94 (58%)	33 (38%)	61 (81%)
- 1	35 (22%)	25 (29%)	10 (14%)
- 2	33 (20%)	29 (33%)	4 (5%)
Gender: n (%)			
- Girls	139 (85%)	74 (85%)	65 (87%)
- Boys	23 (14%)	13 (15%)	10 (13%)
Curve topography: n (%)			
- Thoracic	73 (45%)	40 (46%)	33 (44%)
- Thoraco-lumbar	40 (25%)	19 (22%)	21 (28%)
- Lumbar	49 (30%)	28 (32%)	21 (28%)

Table 8: Values of the 6 index severity parameters and OD-HA. Results are presented such as mean (SD). n represents the number of patients; SD = Standard deviation; VAR = Vertebral axial rotation; IAR = Intervertebral axial rotation

	AIS population		
	Total (n=162)	**Stable (n=87)**	**Progressive (n=75)**
Cobb angle (°)	16 (3.7)	15 (3.2)	17 (3.9)
Apical VAR (°)	5.9 (4.2)	4.7 (3.4)	7.3 (4.6)
Upper IAR (°)	-3 (3.2)	-1.8 (3.1)	-4.4 (2.8)
Lower IAR (°)	2 (3.1)	1.4 (3.2)	2.7 (2.9)
Torsion index (°)	4.2 (2.5)	3.3 (1.8)	5.1 (2.8)
Hypokyphosis index (°)	-1 (3.1)	-0.3 (3.1)	-2 (2.9)
Coronal OD-HA (°)	0.3 (1.2)	0.3 (1)	0.4 (1.4)
Sagittal OD-HA (°)	-0.9 (2.3)	-1.03 (2.3)	-0.9 (2.4)

External shape parameters

A correlation was found between severity index and the apical center of mass position (ρ=0.15; p=0.04) and the upper intersegmental moment (ρ=0.4; p<0.001). Only the apical center of mass position was statistically different between the stable and progressive AIS groups (6 mm, SD=4 mm for whole cohort; 5 mm, SD=4 mm for stable scoliosis versus 7 mm, SD=4 mm for progressive group; p=0.02) but this difference was not found in the analysis by curvature type (p>0.05 for all curve locations).

Correlation between external shape parameters, the severity index parameters and OD-HA

In multivariate analysis, apical vertebral axial rotation (β=0.3, [02;0.5], p<0.0001) and coronal OD-HA (β=1, [0.5;1.5], p<0.0001) were associated with higher values of the apical center of mass position. Torsion index (β=0.04, [0.01;0.08], p= 0.021) and Cobb angle (β=0.05, [0.03;0.08], p<0.0001) were associated with higher values of upper junctional intersegmental moment. Hypokyphosis index (β=0.03, [0.01;0.05], p= 0.01) and sagittal OD-HA (β=0.05,

[0.02;0.08], p= 0.003) were associated with higher values of lower junctional intersegmental moment.

External shape analysis and performance of S-index

The performance of the severity index predictive power with the addition of barycentremetry parameters are detailed in table 9 for the whole cohort and according to curve location. If we focus on thoracic scoliosis, the specificity and positive predictive value of S-index increased by 19% and 16% respectively by adding the apical vertebral intersegmental moment. In other words, it increases the likelihood that if the severity index is greater than 0.6, it means that the patient is truly progressive. This is reflected (table 9) by reducing the number of misclassified by 9% but increasing the number of unclassified by 15% (figure 30).

Table 9: Performance of S-index weighting external shape parameters according to the localization curve. w/ = means S-index weighting the external shape parameters; COM = Center of mass position; UJM = Upper junctional intersegmental moment; AM = Apical vertebra intersegmental moment; LJM = Lower junctional intersegmental moment; CTB= Coronal trunk balance ratio (thoraco-lumbar and lumbar scoliosis) ; Values in italics and bold are values for which the weighting of the S-index increased the performance of the test by 5% compared to the S-index without weighting.

	Total Cohort					**Thoracic scoliosis**					**Thoraco-lumbar scoliosis**						**Lumbar scoliosis**					
	S-index	w/ COM	w/ UJT	w/ AM	w/ LJT	S-index	w/ COM	w/ UJT	w/ AM	w/ LJT	S-index	w/ COM	w/ UJT	w/ AM	w/ LJT	w/ CTB	S-index	w/ COM	w/ UJT	w/ AM	w/ LJT	w/ CTB
Sample size: n	162					73					40						49					
Stable scoliosis: n	87					40					19						28					
Progressive scoliosis: n	75					33					21						21					
Correctly classified n (%)	120 (74)	119 (73)	119 (73)	113 (70)	113 (70)	54 (74)	52 (71)	52 (71)	49 (67)	48 (66)	28 (70)	28 (70)	29 (73)	27 (68)	28 (70)	29 (73)	38 (78)	39 (80)	38 (78)	37 (76)	37 (76)	39 (80)
Misclassified n (%)	26 (16)	25 (15)	28 (17)	18 (11)	27 (17)	12 (16)	12 (16)	12 (16)	5 (7)	11 (15)	8 (20)	7 (18)	9 (23)	7 (18)	9 (23)	7 (18)	6 (12)	6 (12)	7 (14)	6 (11)	7 (14)	7 (14)
Unclassified n (%)	16 (10)	18 (11)	15 (9)	31 (19)	22 (14)	7 (10)	9 (12)	9 (12)	19 (25)	14 (19)	4 (10)	5 (13)	2 (5)	6 (15)	3 (8)	4 (10)	5 (10)	4 (8)	4 (8)	6 (11)	5 (10)	3 (6)
Sensitivity (%)	86	87	86	82	82	91	90	90	88	89	74	78	75	72	70	79	89	89	89	88	84	89
Specificity (%)	79	79	77	***90***	80	74	73	74	***93***	75	82	82	78	88	82	82	85	85	81	88	84	81
Positive predictive value (%)	79	79	77	***88***	78	76	76	75	***92***	75	82	82	79	87	82	83	80	81	77	88	80	76
Negative predictive value (%)	86	87	86	85	83	89	89	89	90	89	74	78	74	74	70	78	92	92	91	88	88	92

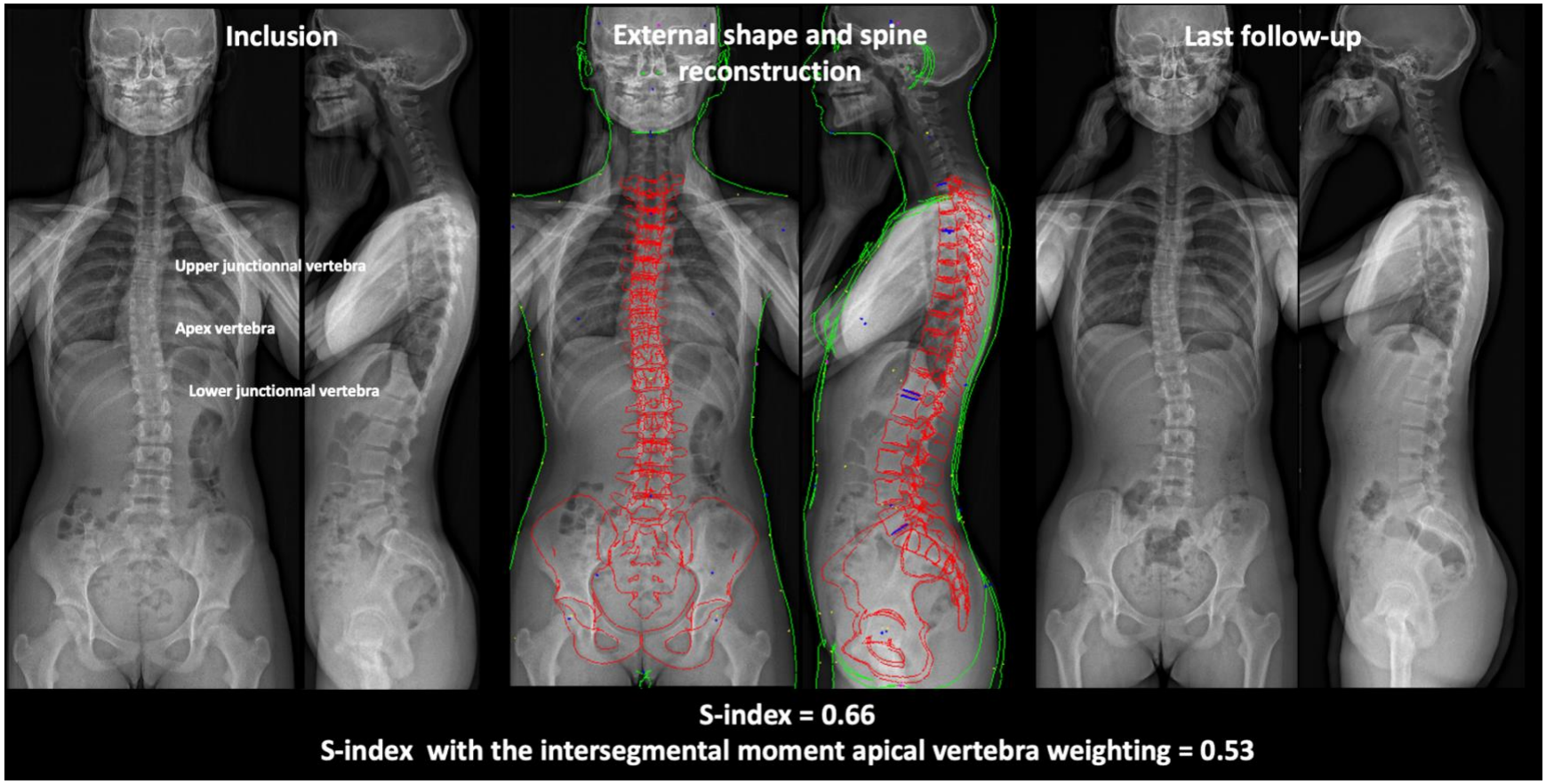

Figure 30: Example of stable thoracic scoliosis. The inclusion and the last follow-up radiographic were reported. The middle frame shows the external shape and spine reconstruction. The calculated severity index was 0.66, i.e. a so-called "progressive" scoliosis and therefore misclassified with the risk of unsuitable treatment. The weighting with the intersegmental moment of the apical vertebra decreases the severity index to 0.53, i.e. a so-called unclassified scoliosis and calls for particular attention by the clinician. The radiograph of the last follow-up (i.e., Risser 4) shows that this is a stable scoliosis which has not undergone brace treatment

V.2.4 Discussion

In this study, we assessed the biomechanical markers issued from the reconstruction of the external shape, which were previously validated in a population of healthy subjects and patients (Langlais et al. 2021). These biomarkers reflect the displacement and distribution of body masses and provide an original, modern approach to spinal deformation. Previous studies focused (Bolzinger et al. 2021; Groisser et al. 2022) on the analysis of external deformity using a surface topography device and focusing on torso asymmetry. The correlation of this tool with bone deformation characteristics (either Cobb angle or vertebral rotation) remains controversial (Mínguez et al. 2007; Gorton, Young, et Masso 2012). On the other hand, it appears to be a good indicator of outcomes for quality-of-life scores and measures related to the external physical appearance of the trunk (Gorton, Young, et Masso 2012). Recently, a new tool, allowing 3D and 360° reconstruction of the torso has been evaluated and validated in a healthy population (Michalik et al. 2019). However, to our knowledge, there are no studies on the external shape analysis from low dose biplanar radiographs used in daily clinical practice.

The main finding of the present work is that the apical CoM values was significantly different between progressive and stable scoliosis. The CoM represents the lateral mass displacement at apical regions (figure 28), and we found that it correlates with the severity index, the coronal OD-HA and the apical vertebral axial rotation. The hypothesis is that this displacement requires scoliotic patients to adjust their balance to maintain the CoM above the pelvis. In their assessment of CoM using a force plate, Dalleau et al. showed that in scoliotic patients there is a compensatory action due to the frontal deformation, resulting in a backward offset of the CoM to maintain postural balance (Dalleau et al. 2011). This backward trunk displacement was previously described in studies by Nault et al. (Nault et al. 2002) and Damavandi et al. (Damavandi et al. 2013). In our study, we could not demonstrate this backward displacement difference between progressive and stable scoliosis on the first visit biplanar radiograph, which suggests that this trunk shift could develop later in the progression of the deformity. The open question is to understand why the other barycenter parameters at this stage of deformation are not different between progressive and stable forms. According to previous studies (Thenard et al. 2019; Langlais et al. 2021), the upper junction

intersegmental moment correlates with the severity of scoliosis. In this study, we found a correlation of the upper intersegmental moment with the severity index (and more precisely the Cobb angle and the torsion index). One of the hypotheses that the differences between the markers are still small at this stage of the deformation. The uncertainty of these biomechanical markers had been evaluated and did not exceed 0.8 mm for the lateral position of CoM at all vertebral levels, 0.5 N/m for the intersegmental moment and 0.1 for the coronal trunk balance (Langlais et al. 2021). It is likely that there are no significant differences due to this uncertainty. One solution could be to improve the 3D reconstruction method to lower its uncertainty or increase the number of patients included. Nevertheless, early disruptions in the centre of mass of the apical vertebrae disrupt the distribution of body masses in AIS.

An important result of this study was the analysis of biomarkers resulting directly from the bone reconstruction and their relationship with the displacement of the CoM. The apical CoM displacement was explained by the increase of the apical vertebra axial rotation and the coronal OD-HA. Recently, Karam et al. showed that frontal malalignment was related to the apical vertebra axial rotation (Karam et al. 2022). The important information for the clinician is that the frontal Cobb angle, measured in daily clinical practice, does not influence the position of the CoM in scoliotic deformities at an early stage. Furthermore, we found that this lateral displacement of the trunk was positively correlated with the apical vertebra axial rotation. This result is supported by J. Dubousset's and W. Skalli's theory that it is important to evaluate the deformity in the axial plane, especially at an early stage (Castelein et al. 2020; Illés, Lavaste, et Dubousset 2019).

The last important finding of the study was the preliminary assessment of the impact of including barycentremetry to the S-index. For thoracic scoliosis, including the intersegmental moment of the apical vertebra improves the specificity and positive predictive value (by 19% and 17% respectively) without significantly altering the sensitivity and negative predictive value (by -3% and 1%, respectively). This result is promising as it decreases the number of misclassified patients by 9%, which means a decrease in the probability of "over-treating" a supposedly stable scoliosis (figure 30). On the other hand, it increases the number of unclassified patients by 15%, which leads in clinical practice to continued radiographic

monitoring. The other point to note is that the center of mass position, although the values were different between stable and progressive scoliosis, did not influence overall test performance. Future prospective studies should take this parameter into account to determine its clinical significance. Surprisingly, the coronal trunk balance did not improve the s-index's performance for lumbar scoliosis. The hypothesis is that this waist imbalance is more apparent at higher curvatures. On the other hand, it would be beneficial to improve the adjustment of the waist reconstruction method.

This study presents some limitations, but these results are promising and is the first study of its kind. This is a retrospective assessment, and the values of the weighting multipliers were chosen arbitrarily. This explains why 43 subjects were excluded for issues concerning the framing of the external envelope. Nevertheless, the cohort was included prospectively for validation of the severity index and this study showed how the assessment of intersegmental moment, centre of mass position and waist imbalance could improve the prediction of progressive scoliosis. Another limitation of this study is the time of the external shape reconstruction which is around 15 to 20 minutes of operator time per patient but a partial automated process should be available soon. Finally, the main limitation of this work is that this study focuses on a static approach to assess balance and barycentremetry. However, it has been established that the dynamic proprioceptive system is affected in patients with idiopathic scoliosis (Assaiante et al. 2012). The remaining question is how these external shape parameters would be affected under dynamic conditions.

Early assessment of the external envelope from biplanar X-ray reconstruction of idiopathic scoliosis showed promising results. The apical centre of mass position was significantly different between progressive and stable scoliosis. The inclusion of the intersegmental moment of the apical vertebra in the severity index seems to improve this performance in thoracic scoliosis and needs to be confirmed by a discriminant factorial study.

V.2.5 Conclusion

L'évaluation précoce des paramètres issus des reconstructions de l'enveloppe externe à partir de radiographie biplanaire d'une scoliose idiopathique a donné des résultats

prometteurs. La position du centre de masse de la vertèbre sommet était significativement différente entre les scolioses progressives et stables. L'inclusion du moment intersegmentaire de la vertèbre apicale dans l'indice de sévérité semble améliorer les performances de l'indice et particulièrement chez les scolioses thoraciques.

À la suite de ces résultats, nous nous demandons si la correction chirurgicale des scolioses sévères pouvait rétablir ces paramètres à des valeurs similaires à celles des patients asymptomatiques.

VI - Évaluation des paramètres issus de la reconstruction de l'enveloppe externe après correction et fusion chirurgicale

Cet article va faire l'objet d'une soumission dans les prochaines semaines, comme 1er auteur.

External shape and barycentremetry assessment after surgical correction in adolescent idiopathic scoliosis: a new approach to 3D mass distribution based on biplanar radiographs

VI.1 Introduction

Idiopathic scoliosis is a three-dimensional (3D) spinal deformity in which the goal of surgical treatment is to achieve a successful arthrodesis in a patient-satisfactory 3D balance position. Given the multiplicity of implants and industrial processes, an objective, reproducible and operator-independent therapeutic evaluation has become necessary. The objective of the evaluation is to assess the axial correction (i.e. the reduction of the rib hump), the frontal correction (i.e. a satisfactory balance of the shoulders and the height) and the sagittal balance (i.e. a thoracic kyphosis in adequacy with the lumbar lordosis and the pelvic parameters). The 3D reconstruction of the spine from low dose biplanar radiographs allows quantification of the bone correction in the standing position using geometrical parameters (e.g. intervertebral axial rotation, torsion index) (Courvoisier et al. 2013). However, this 3D analysis method only focuses on the alignment, and it does not inform us on balance related to the forces acting on the spine, and in particular on the asymmetrical displacement of mass and of the centre of gravity.

Recently, the barycentremetry analysis made possible by the 3D reconstruction of the external envelope from biplanar x-rays, has allowed the analysis of new biomechanical markers such as the intersegmental moment analysis (Thenard et al. 2019), the position of the centre of mass (Thenard et al. 2019) and the coronal trunk balance (Langlais et al. 2021). These studies showed that there were alteration of load and mass distribution in scoliosis patients compared to a cohort of subjects without spinal pathology (Langlais et al. 2021). However, it remained unclear if surgical correction of severe cases could restore these parameters to values similar to asymptomatic patients.

To this end, parameters from 3D reconstruction of the external envelope were studied in a cohort of patients who were undergoing surgery for idiopathic scoliosis.

VI.2 Materials and methods

Subjects

All adolescent with idiopathic scoliosis (Lenke 1 and 3) (Lenke et al. 2002) who underwent posterior spinal fusion surgery at our centre between January 2019 and December 2019 were included retrospectively. Spinal surgery was proposed if the frontal thoracic Cobb angle was greater than 40°, Risser's sign greater than 1 (Risser 1958), closed triradiate cartilage and at least one of clinical trunk malalignment and/or lower thoracic hypokyphosis of 20°. Exclusion criteria were transitional anomaly, previous spinal surgery, halo traction before fusion and incomplete follow-up. A single spine surgeon performed the surgical interventions, using an all-screw fixation (except a transverse hook at the top of construct) in all patients under somatosensory and motor evoked potentials monitoring. Correction was done by a posteromedial translation method (Lamerain et al. 2017). An institutional ethics committee (C.P.P. Ile de France IV: Records 14 409) approved this single-centre retrospective study.

Imaging data assessment

All patients underwent frontal and sagittal biplanar radiographs (EOS^{TM} system, EOS imaging, Paris, France) (J. Dubousset et al. 2007) in the free-standing position (Faro et al. 2004) before surgery, 4 months after surgery and at the last follow-up. Incorrect positioning on biplanar radiographs was an exclusion criterion. Quasi-automatic 3D reconstructions of the spine were performed using a previously validated technique (Gajny et al. 2019; Vergari et al. 2019). The upper and lower boundary vertebra of the main curve were defined to obtain the maximization of the Cobb angle. An automatic algorithm provided an initial 3D reconstruction solution, upon which the operator could perform rapid manual adjustment of the vertebrae to improve accuracy. The reconstruction took about 5 minutes on average. The 3D reconstruction allowed the automatic calculation of spinopelvic geometric parameters: Cobb angle of the main curve (°), kyphosis T4-T12 (°), L1-S1 lordosis (°), pelvic tilt (°), pelvic incidence (°), the OD-HA angle coronal and sagittal (°) (where OD was the position of the C2 odontoid,

as an estimate of the centre of mass of the head, and HA was the midpoint of the pelvic acetabulae) (Amabile et al. 2016a), the index torsion (Steib et al. 2004) the hypokyphosis index (Skalli et al. 2017), the intervertebral axial rotation at the upper and lower end vertebra, the vertebra axial rotation at the apex and the spinal length T1-T12 and T1-S1 (Langlais et al. 2022) (Langlais et al. 2021).

3D external shape and barycentremetry assessment

Preoperative, postoperative and last follow-up external shape was reconstructed (3 reconstructions per patient = 3 x 29 patient = 87 reconstructions), retrospectively, using a validated technique (Gajny et al. 2020) (figure 31). The reconstruction takes about 15 minutes, and it allows automatic estimation of body segments masses, according to a recent estimation of segmental mass density (Amabile et al. 2016b), calculation the apex and the upper and lower end vertebra intersegmental moment (Thenard et al. 2019; Langlais et al. 2021), the lateral center of mass position at the apex, the upper and the lower end vertebra, and the ratio of the coronal trunk balance at each level between T12 and L5 vertebra. The intersegmental moment was the torsional moment applied to each vertebra (apical, upper and lower boundary) as a result of its lateral displacement and inclination in the sagittal plane, due to the mass of the body above the vertebra and the position of this segment's center of mass (Thenard et al. 2019) (figure 32). Horizontal slices of the body envelope were virtually cut at each vertebral level. For each slice, the lateral position of the centre of mass was calculated to determine its distance from the vertical line passing through the middle of the inter-acetabular axis in the coronal plane. This distance was calculated at the apical, upper and lower end vertebrae. This parameter represents the lateral displacement of the mass in these three specific regions (Thenard et al. 2019). The coronal balance of the trunk was quantified using the lateral envelope shift. This parameter was calculated at each vertebral level below T12 as follows: a series of horizontal lines were defined in the coronal plane, passing through the centre of each vertebral body. The intersections between these lines and the outer shell were marked. Finally, the ratio of the distances between the vertebral body and the left and right intersection was automatically calculated (Langlais et al. 2021). This parameter represents the local lateral asymmetry of the outer shell in the lumbar region (figure 33). The pre-, postoperative and last follow-up values of these parameters were analyzed, as well as their correlation with the spinal parameters. Finally, the pre- and

postoperative values were compared to a previously published reference corridor for asymptomatic subjects (Langlais et al. 2021). The percentage of scoliotic patients outside this reference corridor (i.e., outside the values between the 5th and 95th percentiles) for the pre- and postoperative values were calculated.

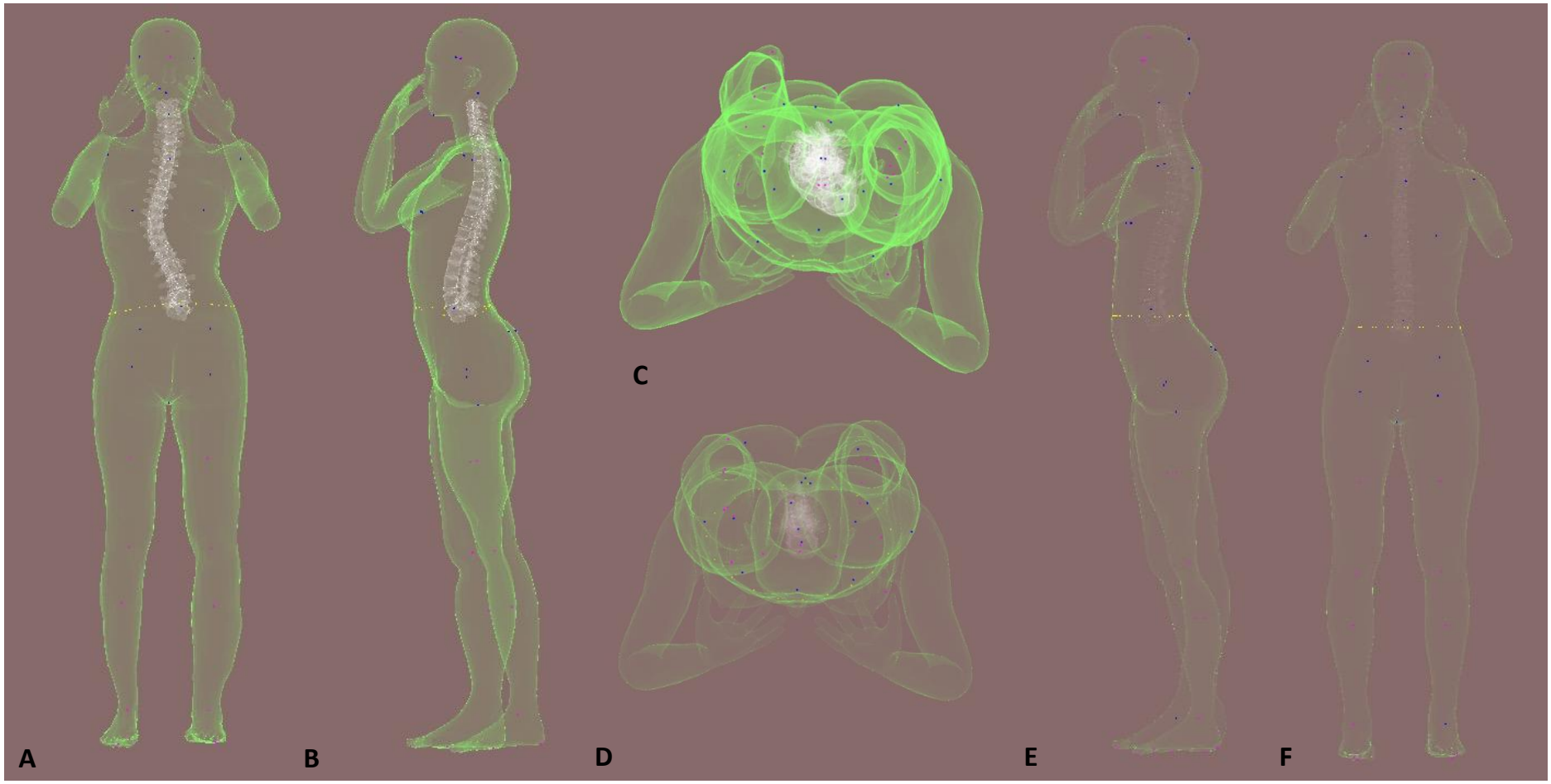

Figure 31: Example of the preoperative (A: frontal, B: sagittal, C: top of view) external envelope reconstruction and the postoperative (D,E,F).

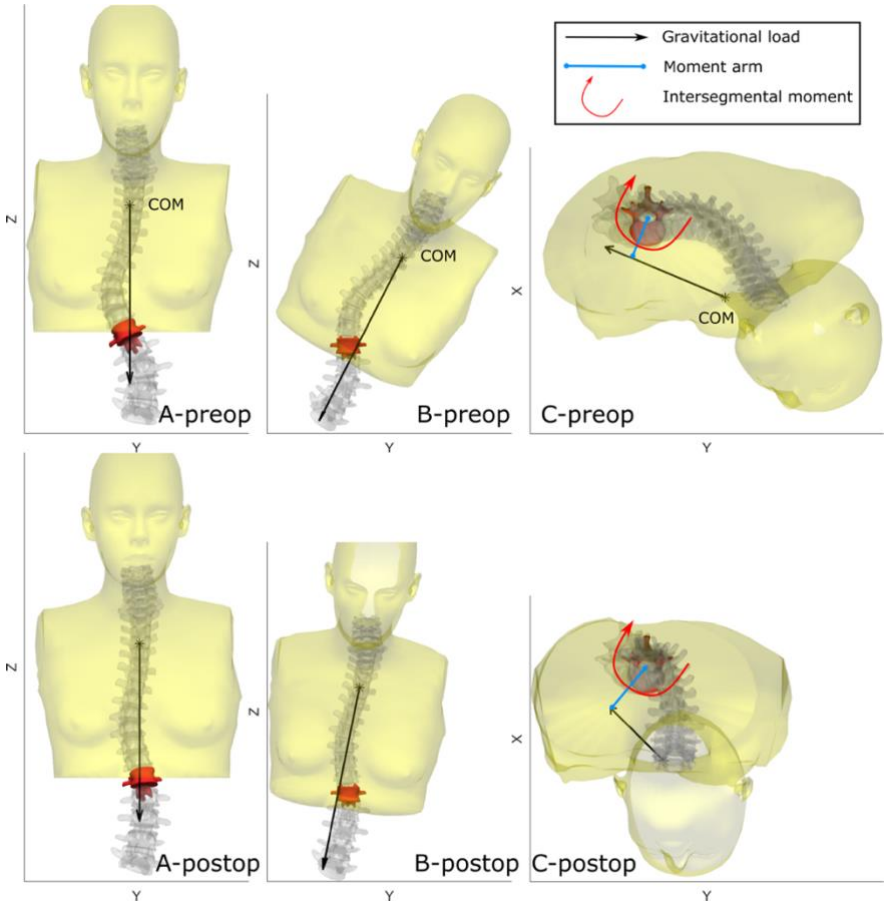

Figure 32: Visual representation of the intersegmental axial moment at the lower junctional vertebra in a patient, preop and postop. Panels A show the 3D reconstruction of the spine, with the junctional vertebra highlighted in red, as well as the portion of the trunk above this vertebra and its center of mass (COM). The gravitational load is shown by the arrow. Panels B show the same 3D reconstruction, but the patient (and gravitational load) was virtually rotated so that the lower end vertebra is now perfectly horizontal. Panels C show the same configuration as B from a top view, so now the end vertebra is horizontal and viewed from above. It can be noticed that the lever arm in preop and postop is similar, and the load is identical (as it depends on the weight of the trunk above the vertebra); however, in C-postop the load arrow appears much shorter than in B-preop. This is due to the different orientation of the vertebra in the two cases, which affects the component of the load vector in the XY plane. Hence, even if the load and the lever arm are similar preop ad postop, the postop intersegmental torque is lower because the axial component of the load vector is much smaller.

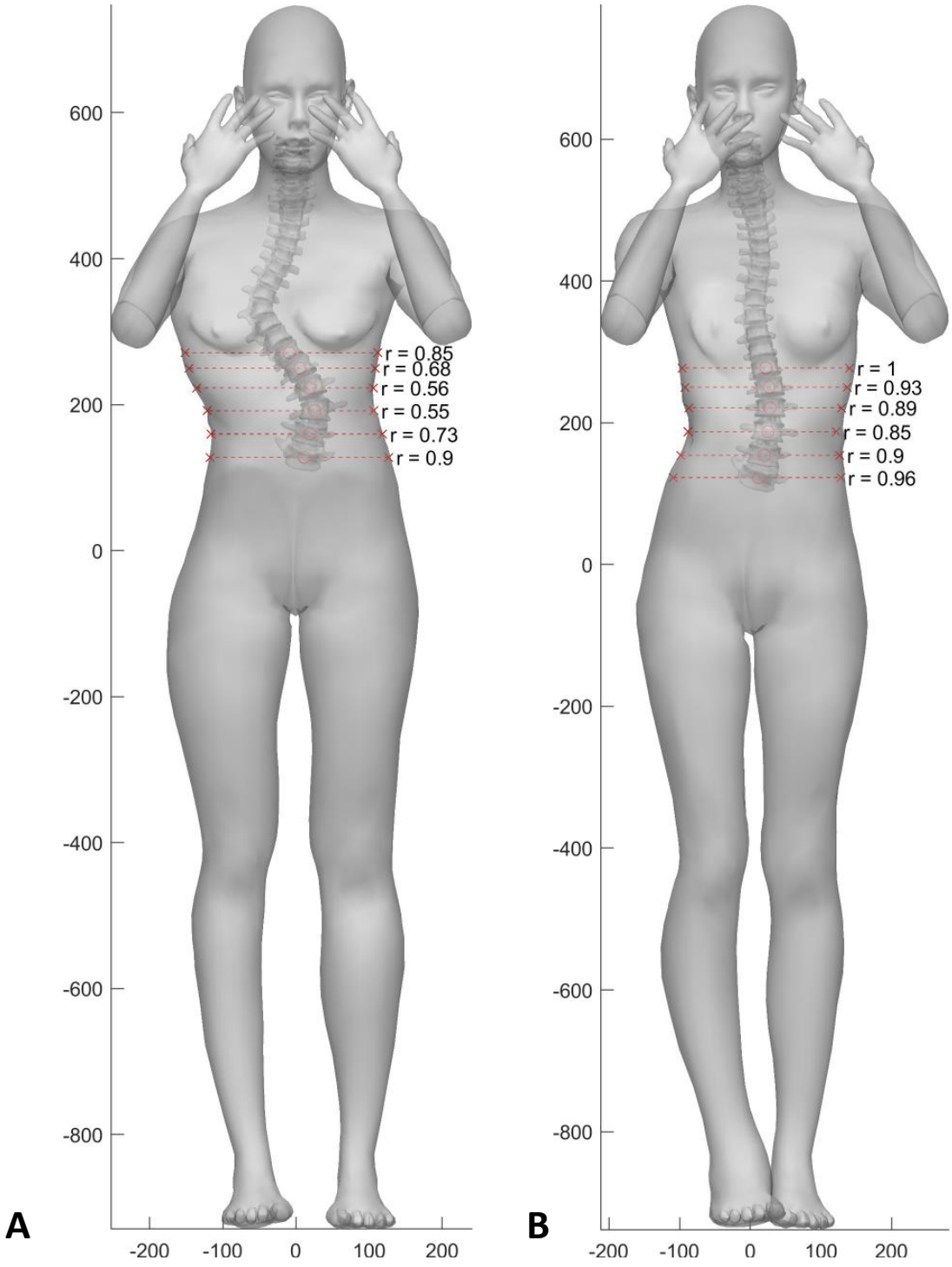

Figure 33: Example of the preoperative (A) and postoperative (B) ratio coronal trunk balance measure

Statistical analysis

Results are presented by mean (SD; range). The normality was verified with the Shapiro-Wilk test. The difference between pre, postoperative and the last follow-up was assessed with the Student's paired t-test or the Wilcoxon signed-rank test, depending on the normality condition. For correlation assessment between spinal and 3D barycentremetry parameters, the Spearman's or Pearson's coefficient was used, depending on the normality condition. Correlation was considered very strong from 1 to 0.9, strong from 0.9 to 0.7, moderate from 0.7 to 0.5, low from 0.5 to 0.3 and poor from 0.3 to 0. For the comparative analysis of pre- and postoperative values outside the reference corridor, a Fisher exact test was used. Alpha risk was set to 5% ($\alpha = 0.05$). Statistical analysis was performed with EasyMedStat (version 3.20.2; Neuilly-sur-seine, France).

VI.3 Results

Cohort description

Twenty-nine patients were included (23 with type 1 and 6 with Lenke type 5 curves or 23 thoracic, 3 thoracolumbar and 3 lumbar scoliosis) after removal of one patient was excluded because his external envelope was outside the frame of the frontal X-ray acquisition. The mean age at surgery was 14.8 years (SD = 1.6; range 11-17) and the mean body mass index was 19 $kg.m^{-2}$ (SD = 3.3; range 7.8-27). The mean Risser's sign was 3 (SD = 1; range 2-5). The mean follow-up was 20 months (range from 10 to 48 months).

Spinal radiographic assessment

The pre, postoperative and last follow-up spinal parameters are reported in table 10. The surgical procedure decreased the Cobb angle by 35.8° (CI95% = [32.6;39] ; p<0.001), the torsion index by 7.3° (CI95% = [5.8;8.9] ; p<0.001), the hypokyphosis index by 2.9° (CI95% = [0.9;4.5] ; p=0.003), the intervertebral axial rotation at the lower end vertebra by 3.6° (CI95% = [2.5;4.4] ; p<0.001), and the vertebral axial rotation at the apex by 10.7° (CI95% = [9.4;15] ; p<0.001) ; increase the T4-T12 kyphosis by 6.9° (CI95% = [2.3;11.5] ; p=0.005); and achieved a mean gain in T1-T12 length of 6.4 mm (CI95% = [4.1;8.7] ; p<0.001 and T1-L5 of 7.8 mm (CI95% = [5.5;10.1]; p<0.001).

Table 10: Pre, postoperative and last follow-up spine radiographic parameters. Results are presented by mean (SD) *[range]*. p-value[1] refers to the analysis of pre- and postoperative data while p-value[2] refers to postoperative and final follow-up data. Significant p-values are shown by an asterisk*.

	Preoperative	Postoperative	Last follow-up	p-value[1]	p-value[2]
Cobb angle (°)	53 (10) *[40;77]*	17 (8) *[1;32]*	17 (9) *[1;37]*	<0.001*	0.4
T4-T12 Kyphosis (°)	23 (14) *[-3;46]*	30 (9) *[13;45]*	28 (9) *[5;42]*	0.005*	0.2
L1-S1 Lordosis (°)	56 (12) *[35;74]*	53 (10) *[34;70]*	52 (10) *[30;73]*	0.2	0.9
Pelvis Tilt (°)	6 (9.3) *[-12;31]*	8 (10) *[-13;31.8]*	8 (7) *[-12;31]*	0.08*	0.2
Pelvic Incidence (°)	47 (15) *[23;75]*	48 (13) *[27;75]*	47 (11) *[28;74]*	0.2	0.7
OD-HA sagittal (°)	3 (3) *[-5;8]*	2 (4) *[-7;8]*	3 (3) *[-2;9]*	0.2	0.2
OD-HA coronal (°)	-1±2.7 *[-7;4]*	-0.5±2.1 *[-6;5]*	-1.2±1.5 *[-5;2]*	0.6	0.1
Torsion index (°)	11 (5) *[3.;20]*	3 (2) *[0.6;9]*	3 (3) *[0.3;12]*	<0.001*	0.8
Hypokyphosis index (°)	-2 (5) *[-16;14]*	1 (3) *[-6;7]*	1 (3) *[-6;10]*	0.003*	0.7
Intervertebral axial rotation at the upper end vertebra (°)	3 (1) *[0.6;6]*	2 (2) *[0.1;5]*	2 (2) *[0.7;9]*	0.07	0.8
Intervertebral axial rotation at the lower end vertebra (°)	5 (3) *[0.6;12]*	2 (1) *[0.6;6]*	2 (1) *[0.8;4]*	<0.001*	0.5
Vertebral axial rotation at the apex (°)	16 (8) *[0.5;30]*	5 (4) *[0.01;11]*	5 (3) *[0.09;16]*	<0.001*	0.8
Spinal length T1-T12 (mm)	237 (13) *[212;271]*	244 (15) *[214;285]*	245 (16) *[218;286]*	<0.001*	0.7
Spinal length T1-L5 (mm)	398 (21) *[361;454]*	406 (22) *[366;468]*	406 (25) *[369;470]*	<0.001*	0.7

3D barycentremetry assessment

The 3D barycentremetry outcomes are reported in table 11. The surgical procedure decreased the intersegmental moment at the upper end vertebra by 2.5 N/m (CI95% = [1.9;3] ; p<0.001), at the apex by 0.6 N/m (CI95% = [0.4;1] ; p=0.004), at the lower end vertebra by 2 N/m (CI95% = [1.5;2.8] ; p<0.001), the center of mass at the apex by 6.1 mm (CI95% = [0.6;11.5] ; p=0.023) and at the lower end vertebra by 10.6 mm (CI95% = [5.4;15.4] ; p<0.001). The coronal trunk balance ratio is also improved (i.e., approaches 1) for levels from T12 (p=0.002)

to L4 (p<0.001 from L1 to L4). There was no statistical difference for spinal and barycentremetry parameters between the postoperative radiographic and the last follow-up (p>0.05).

Table 11: Pre, postoperative and last follow-up spine barycentremerty parameters.

Results are presented by means (SD) *[range]*. p-value[1] refers to the analysis of pre- and postoperative data while p-value[2] refers to postoperative and final follow-up data. Significant p-values are shown by an asterisk*.

	Preoperative	Postoperative	Last follow-up	p-value[1]	p-value[2]
Intersegmental moment at the upper end vertebra (N/m)	4 (2) *[1;9]*	2 (1) *[0.1;4]*	2 (1) *[0.3;3]*	<0.001*	0.2
Intersegmental moment at the apex (N/m)	1 (1) *[0.1;6]*	1 (1) *[0.03;4]*	1±1 *[0.02;4]*	0.004*	0.6
Intersegmental moment at the lower end vertebra (N/m)	3 (1) *[0.3;7]*	1 (1) *[0.01;2]*	1 (1) *[0.04;2]*	<0.001*	0.1
Center of mass position at the upper end vertebra (mm)	13 (10) *[0.4;36]*	9 (6) *[0.16;22]*	9 (5) *[0.9;23]*	0.1	0.7
Center of mass position at the apex (mm)	16 (9) *[0.9;33.7]*	10 (7) *[1.3;26.7]*	8 (6) *[0.4;25]*	0.02*	0.2
Center of mass position at the lower end vertebra (mm)	18 (9) *[1.5;34]*	8 (6) *[0.2;22]*	7 (6) *[1.7;26]*	<0.001*	0.8
Coronal trunk balance ratio at T12 level	0.8 (0.1) *[0.5;0.9]*	0.9 (0.07) *[0.8;1]*	0.9 (0.07) *[0.7;1]*	0.002*	0.1
Coronal trunk balance ratio at L1 Level	0.8 (0.1) *[0.6;0.9]*	0.9 (0.07) *[0.8;1]*	0.9 (0.06) *[0.8;1]*	<0.001*	0.09
Coronal trunk balance ratio at L2 Level	0.7 (0.1) *[0.6;1]*	0.9 (0.06) *[0.8;1]*	0.9 (0.06) *[0.8;1]*	<0.001*	0.3
Coronal trunk balance ratio at L3 Level	0.8 (0.1) *[0.5;1]*	0.9 (0.0.06) *[0.8;1]*	0.9 (0.0.06) *[0.8;1]*	<0.001*	0.6
Coronal trunk balance ratio at L4 Level	0.9 (0.07) *[0.7;1]*	0.9 (0.07) *[0.7;1]*	0. (0.07) *[0.7;1]*	<0.001*	0.5
Coronal trunk balance ratio at L5 Level	0.9 (0.05) *[0.8;1]*	0.9 (0.04) *[0.8;1]*	0.9 (0.05) *[0.8;1]*	0.07	0.8

Correlation between spinal and 3D barycentremetry parameters

A correlation was found between the correction of intersegmental moment at the upper end vertebra and the correction of Cobb angle (ρ=0.4; p=0.03), the variation of kyphosis T4-T12 (ρ=0.6; p<0.001), the correction of hypokyphosis index (ρ=0.5; p=0.04) and the correction of the vertebra axial rotation at the apex (ρ=0.5; p=0.006). Another correlation was found between the correction of intersegmental moment at the lower end vertebra and the variation of kyphosis T4-T12 (ρ=0.4; p=0.03), the decrease in the torsion index (ρ=0.5; p=0.003) and the intervertebral axial rotation in the lower end vertebra (ρ=0.4; p=0.03). Lastly, a correlation was found the correction of the coronal trunk balance ratio at the T12, L1, L2 level with the correction of torsion index (ρ=0.5, 0.6 and 0.4; p=0.002, 0.001 and 0.03, respectively) and at the L1 and L2 level with the correction of the lower intervertebral axial rotation (ρ=0.4 and 0.5; p=0.01 and 0.007 respectively).

Postoperative barycentremetry parameters in scoliotics compare to a reference corridor

The percentage of patients outside the reference corridor pre- and postoperative is shown in table 12.The percentage of patients whose pre-operative values were outside the reference corridor and then inside after the surgical procedure was 38% for intersegmental moment at the upper end vertebra (OR=0.06 ; p<0.001), 52% for the intersegmental moment at the lower extremity vertebra (OR=0.07; p<0.00001), 32% for the centre of mass position at the apex (OR=0.2; p=0.02), 58% for the centre of mass position at the lower extremity vertebra (OR=0.07; p<0.00001) and 42%, 83%, 62% and 25% for the respective ratios of the coronal trunk balance for the L1 (OR=0.1 ; p=0.001), L2 (OR=0.007; p<0.00001), L3 (OR=0.05; p<0.00001) and L4 (OR=0.1; p=0.04) levels.

Table 12: Percentage of patient outside the reference corridor. Significant p-values are shown by an asterisk*.

	Preoperative	Postoperative	Odds Ratio [CI 95%]	p-value
Intersegmental moment at the upper end vertebra (N/m)	100%	62%	0.06 [0.001;0.5]	<0.001*
Intersegmental moment at the apex (N/m)	45%	24%	0.4 [0.1;1.4]	0.2
Intersegmental moment at the lower end vertebra (N/m)	90%	38%	0.07 [0.01;0.3]	<0.00001*
Center of mass position at the upper end vertebra (mm)	45%	24%	0.4 [0.1;1.3]	0.2
Center of mass position at the apex (mm)	62%	28%	0.2 [0.06;0.8]	0.02*
Center of mass position at the lower end vertebra (mm)	79%	21%	0.07 [0.01;0.3]	<0.00001*
Coronal trunk balance ratio at T12 level	34%	10%	0.2 [0.03;1]	0.06
Coronal trunk balance ratio at L1 Level	52%	10%	0.1 [0.02;0.4]	0.001*
Coronal trunk balance ratio at L2 Level	86%	3%	0.007 [0.0001; 0.06]	<0.00001*
Coronal trunk balance ratio at L3 Level	76%	14%	0.05 [0.01; 0.2]	<0.00001*
Coronal trunk balance ratio at L4 Level	31%	7%	0.1 [0.01;0.9]	0.04
Coronal trunk balance ratio at L5 Level	0%	0%	/	1

VI.4 Discussion

The advent of 3D reconstruction has made it possible to focus on the correction obtained in the axial planes with the analysis of parameters such as the intervertebral rotation or axial rotation of the vertebra. These are parameters derived from direct 3D reconstruction of the bone column. But what about the distribution of the body masses? How does the vertebra, the trunk, the waist behave in relation to the centre of gravity following a bone correction? Recently, J. Dubousset reported that the objective of a scoliotic deformity surgery was to obtain a harmony, from head to toe, of both the external envelope and the 3D bone balance (Dubousset 2020). Balance describes an equilibrium in each plane; it is called sagittal balance when considering thoracic kyphosis, cervical and lumbar lordosis, and pelvic parameters; it is called coronal balance when assessing the balance of the shoulders, the waist, the Cobb angle of a curve. In the axial plane, rotation of the vertebrae is usually considered relative to the pelvis. However, harmony includes the analysis of balance but also of the distribution of masses, in other words the centre of gravity and the 3D external shape of the whole body.

In this preliminary study, we evaluated parameters derived from the external shape reconstruction, which has been previously validated in a population of healthy subjects and scoliotic patients (Langlais et al. 2021). These markers reflect the displacement and distribution of body masses and constitute an original and modern approach to 3D spinal deformation. In turn, these masses represent the static loads which are applied to the spine in load-bearing position. Previous studies (Gorton, Young, et Masso 2012; Gardner, Berryman, et Pynsent 2021) have focused on external torso asymmetry using a surface topography device. Gardner et al. concluded that surgical correction of the spine did not systematically lead to a symmetric torso (Gardner, Berryman, et Pynsent 2021). According to the authors, there were yet undefined factors that would lead to greater post-operative torso symmetry. Barycentremetry was initially proposes by Duval Beaupère et al. with a gamma rays' scanner (Duval-Beaupère et Robain 1987). However, it was in lying position. More recently, Skalli and her team proposed barycentremetry from the biplanar radiographs taking advantage of external shape 3D reconstruction (Gajny et al. 2020) and density models (Amabile, Choisne, et al. 2016). To our knowledge, there are no studies on the postoperative evaluation of

external shape analysis and barycentremetry from low dose biplanar radiographs used in daily clinical practice.

The first important finding is that some of these parameters (i.e., intersegmental moment at all three levels studied, the centre of mass position at the apical and the inferior end vertebra, ratio of coronal trunk balance from T12 to L4) were significantly improved by the surgical correction (figure 31,32 and 33). The uncertainty of these measurements had been measured in a previous study (Langlais et al. 2021) and did not exceed 0.5 N/m for the intersegmental moment, 0.8 mm for the centre of mass position and 0.1 for the ratio of coronal trunk balance. Taking this uncertainty into account, the markers were still modified after surgery. The decrease in intersegmental moment allows us to conclude that the posteromedial multisegmented translation allowed a displacement of the apical vertebra and of the upper and lower boundary. The question remains as to which component (sagittal tilt, lateral displacement) and to what extent the translational technique allowed this change. Additionally, this procedure also brought the centre of mass closer to the apical and the lower boundary to the line of HA vertical axis (Thenard et al. 2019).

The second outcome is the correlation between the intersegmental moment at the upper and lower boundary with spinal parameters from 3D bone reconstruction. This confirms that the decrease, following surgery, of the intersegmental moment at the upper level is related to a correction of the anomalies of the frontal plane (translated by a decrease of the Cobb angle), sagittal plane (translated by an increase of the T4-T12 kyphosis, an improvement of the hypocyphosis index) but also of the axial plane (translated by a decrease of the vertebra axial rotation at the apical). As far as the lower levels are concerned, the decrease in the intersegmental moment is linked to an improvement in the thoracic kyphosis but also to a decrease in the torsion index and the intervertebral rotation at the lower boundary. The fact that the axial rotation of the apical vertebra correlates with the decrease of the intersegmental moment at the superior level and that the decrease of the torsion index improves the intersegmental moment at the inferior level reflects the importance of considering the correction of the axial plane of curvature in its entirety and not at a single level. These different correlations between the displacements in the 3 planes reinforce the

idea, demonstrated by some authors (Schlösser et al. 2014; Illés et al. 2020), that the analysis of the axial plane should be included in the initial and final evaluation of a treatment.

The third important point is that the surgical procedure allowed for several patients (outside the reference corridor in preoperative) to achieve postoperative values within this corridor and statistically significant for the intersegmental moment at the upper (38% of patients) and lower (52% of patients) boundary, for the position of the centre of mass at the apical (32% of patients) and lower level (58% of patients). It should be noted that the reference corridor was calculated in a population of subjects with an average age of 21y (from 10 to 31 y) without a history of spinal pathology (Langlais et al. 2021). The basal state of barycentremetry in scoliotic patients is not known and probably each patient has his own characteristics. The aim in future studies would be to find a body harmony of the mass displacement resulting from the 3D surgical correction rather than trying to bring the values of these parameters into a reference corridor. Finally, one of the clinical applications of this barycentric assessment is to understand possible mechanical complications (such as proximal junctional kyphosis or adding-on phenomena below the instrumented lower level). In light of these parameters, the distribution of the different forces applied above and below the arthrodesis can be assessed. Recently, Kim et al. reported in a population of 199 adults operated on for spinal deformity that post-operative assessment of odontoid-hip alignment (by measuring the OD-HA) was predictive of mechanical complications (Kim et al. 2021).

This study has some limitations. It is a barycentremetry's assessment in static positions, and the effect of the dynamic proprioceptive system on the compressive forces or the centre of gravity was not investigated, although it has been established that the dynamic proprioceptive system is affected in patients with idiopathic scoliosis (Assaiante et al. 2012). The second limitation is the small number of patients included with no difference between the different curvature locations. Finally, this study did not evaluate quality of life scores and especially self-evaluation of postoperative physical appearance. It would be important to carry out this study to verify whether the assessment of the external envelope correction by this analytical method brings satisfaction to the patients. In other words, to know if patients whose postoperative values are outside the reference corridor have a worse clinical evolution.

Nevertheless, this is an original preliminary study and to our knowledge has never been reported.

The 3D assessment of the barycenter after surgery to correct adolescent idiopathic scoliosis is promising. This is achieved by 3D reconstruction of the external envelope from low dose biplanar radiographs. The intersegmental moment of the upper and lower boundary vertebra (a parameter related to vertebral mass, lateral and sagittal displacement), the centre of mass of both apical and lower boundary vertebra (i.e. the lateral offset from the line of gravity) and the coronal trunk balance (from T12 to L4) are parameters improved by surgical correction.

VI.5 Conclusion

La correction chirurgicale améliore les paramètres issus de la reconstruction de l'enveloppe externe. La répartition et la distribution des masses changent après la correction chirurgicale. Au vu de ses résultats et de la revue de littérature présentée en seconde partie, nous nous demandons si ces changements des propriétés biomécaniques sont également détectables au niveau des disques intervertébraux lombaires.

VII - Évaluation par élastographie ultrasonore de l'*annulus fibrosus* après correction chirurgicale

Ce travail a été réalisé dans les suites de mon travail de Master II (Langlais et al. 2018) sur l'évaluation par élastographie du disque intervertébral chez les patients scoliotiques au cours duquel nous avons développé le protocole de mesure, inclut une base de données de sujets sains et commencé l'inclusion de patients en préopératoire.

Cet article a fait l'objet d'une publication dans la revue European Radiology : https://link.springer.com/article/10.1007/s00330-019-06563-4

Shear wave elastography of lumbar annulus fibrosus in adolescent idiopathic scoliosis before and after surgical intervention

VII.1 Introduction

Adolescent idiopathic scoliosis (AIS) is the main symptom of a multifactorial pathology, the etiopathogenesis of which is still unknown. According to the scoliosis research society, scoliosis is mainly characterized by a Cobb angle higher than 10° developing after 10 years of age, and it presents a high risk of progression during the growth spurt.

Beyond the Cobb angle, a parameter measurable in the patient's coronal plane, other characteristics are specific to AIS, such as a rotation of the vertebrae in the axial plane and an increased stiffness of the spine (Deviren et al. 2002). Both these aspects could be related to alterations of the intervertebral disc. Indeed, the disc likely plays a role in the scoliotic deformity: recent in vivo study showed that scoliotic discs present a stiffer *annulus fibrosus* than asymptomatic adolescents (Langlais et al. 2018). Those measurements were per- formed with shear wave elastography, a non-invasive and ultrasound-based technique that can quantitatively evaluate soft tissue mechanical properties (Gennisson et al. 2013). When conservative treatment of the deformity fails, and progression leads to severe scoliosis (Cobb angle > 50°), surgery can be necessary to avoid respiratory impairment and to improve the patient's quality of life. The most common approach is to fuse the scoliotic curve to avoid

further progression of the deformity, while leaving some spinal segments free to allow the trunk some mobility (Marks et al. 2012). Thus, while the discs within the instrumented segment almost completely lose their mobility, those outside the fusion can undergo larger strains than usual to compensate and allow the patient to perform every-day tasks. Therefore, assessing disc status may be in- formative for the surgeon when choosing which vertebral levels should be included in the instrumentation.

Magnetic resonance imaging is usually used to assess intervertebral disc. For instance, it has been shown that discs below the fusion can tend to recover hydration 2 years post-operatively (Abelin-Genevois et al. 2015) but also, in more than half the cases, undergo accelerated disc degeneration (Green et al. 2011). Still, magnetic resonance imaging remains of difficult access in clinical routine, and it does not provide information on disc mechanical properties in vivo.

The aim of this study was to determine if any change in *annulus fibrosus* mechanical properties could be detected after fusion surgery in AIS patients with shear wave elastography.

VII.2 Materials and methods

Subjects

Data were collected prospectively from the Trousseau University children's hospital within follow-up clinical routine, between November 2016 and June 2018. Twenty-five severe AIS patients were included prospectively in this study (18 girls and 7 boys, 15 ± 1.5 years old, ranging between 13 and 17 years. Cobb angle 57 ± 14°, ranging between 40 and 93 °). Fifteen AIS patients had thoracic curves, nine had thoracolumbar curves, and one a lumbar curve; according to Lenke's classification (Lenke et al. 2002), 15 patients were type A, 6 were type B, and 4 type C. All patients had indications for spine fusion surgery. Patients presenting transitional anomalies, non-idiopathic scoliosis, or antecedent connective tissue pathology or spinal surgery were excluded.

Fifty-nine asymptomatic subjects were also included as control group (36 girls and 23 boys, 13 ± 2 years old, ranging between 10 and 16 years).

Height and weight were measured for all subjects, and body mass index (BMI) was calculated. All subjects signed informed consent, as approved by the ethical committee (C.P.P Île de France IV #14 409).

Shear wave elastography

Shear wave speed (SWS) was measured with an Aixplorer (SuperSonic Imagine) and a superlinear SL 10–2 MHz probe with a previously described protocol (Vergari et al. 2014b). Briefly, patients were in supine position and the probe was placed on the abdomen to image the spine with an anterior approach. Constant pressure was applied with the probe, which allowed displacing the intestinal contents, thus improving ultrasound penetration. The aortic bifurcation was localized to determine the L4 vertebral level, and the probe was subsequently moved up or down to measure SWS at three discs levels: L3-L4, L4-L5, and L5-S1. The orientation of the probe was adjusted to be in the plane of the disc; the orientation was deemed acceptable when the *annulus* lamellae were visible, and a reliable shear wave image was obtained (i.e., an image with little to no localized saturation of the color chart or absent signal, and a constant color chart in time).

Protocol

Measurements were performed preoperatively for all AIS patients, and they were repeated 3 months after surgery in 13 patients and 1 year after surgery in the remaining 12 patients. No patients were lost at follow-up, and surgery was performed blinded to SWS results. For each measurement, three 10-s clips of elastography were acquired, corresponding to about 30 elastographic images. Images were processed in custom software developed in MATLAB (The MathWorks) to select the *annulus fibrosus* in each image and calculate the corresponding average SWS. Images with missing signal or saturation were discarded. Then, the SWSs measured in the remaining images were averaged to obtain a single SWS value for each measurement (Vergari et al. 2014b). All measurements and processing were performed by two trained operators, while a third blinded operator verified the processing.

Statistics

Non-parametric statistical tests were used because not all variables were normally distributed (Lilliefors normality test). Kruskal-Wallis tests were used to compare the three

vertebral levels and the four groups (asymptomatic, preop, 3 months postop, 1 year postop). Correlations were analyzed with Spearman's rank test. Significance was $p < 0.05$. Analyses were performed in MATLAB 2016b (The MathWorks)

VII.3 Results

Figure 34 shows examples of echographic and elastographic images at all disc levels considered. Figure 35 reports SWS in *annulus fibrosus* at the three disc levels for the four groups (asymptomatic, preop AIS, 3 months postop, and 1 year postop). Within each group, no difference was observed between disc levels ($p > 0.05$), so figure 35 also reports values for pooled levels; when pooling all levels, SWS was 3.1 ± 0.5 m/s in asymptomatic subjects and significantly higher in preop AIS, at 4.0 ± 0.5 m/s ($p < 0.0001$). Three months postop, SWS decreased to 3.5 ± 0.3, and it further decreased to 3.3 ± 0.4 m/s after 1 year. Preop SWS was significantly higher than in asymptomatic patients at all disc levels ($p < 0.0001$). The SWS decrease after 3 months postop was not significant, but it became significant after 1 year at all disc levels ($p < 0.0001$), when SWS was similar to that of asymptomatic controls ($p > 0.05$). Three months postop, only 4 patients had slightly in- creased their SWS by 0.1 m/s in average, while the rest decreased by 0.7 m/s. One year postop, only one patient appeared to increase her SWS by 0.2 m/s, while the rest decreased by 0.8 m/s. A normality corridor can be defined based on the asymptomatic population as the 5–95% quantiles, which results as the range 2.3 and 3.8 m/s. Before surgery, 44% of the measured discs were above this corridor (and none was below). Three months after surgery, 26% were above the corridor, and this percentage decreased to 10% 1 year postop.

Thoracic (SWS = 3.8 ± 0.4) and thoracolumbar AIS patients (SWS = 3.9 ± 0.4) showed similar SWS ($p > 0.05$); the only patient with a lumbar curve showed an average SWS of 5.1 m/s, which was the highest value observed. Patients which were classified as Lenke type C ($n = 4$, corresponding to 12 discs) showed significantly higher SWS (4.4 ± 0.7 m/s) than B-type (3.7 ± 0.6 m/s, $p = 0.001$) and A-type patients (3.8 ± 0.4 m/s, $p = 0.04$). Still, all three types had significantly higher SWS than asymptomatic subjects ($p < 0.0001$).

Asymptomatic patients showed no correlation between SWS and age, height, weight, or BMI. AIS patients only showed a weak positive correlation preop with age (rho = 0.3, p = 0.007), but not postop. A weak correlation was also observed between SWS (all disc levels pooled) and Cobb angle (figure 35, Spearman's rho = − 0.4, p = 0.05). When com- paring SWS in AIS patients with the 95% normality corridor of asymptomatic subjects (shaded area in figure 36), it can be noticed that all patients are in the top half of the normality corridor and that 52% of them (13 patients) are above it.

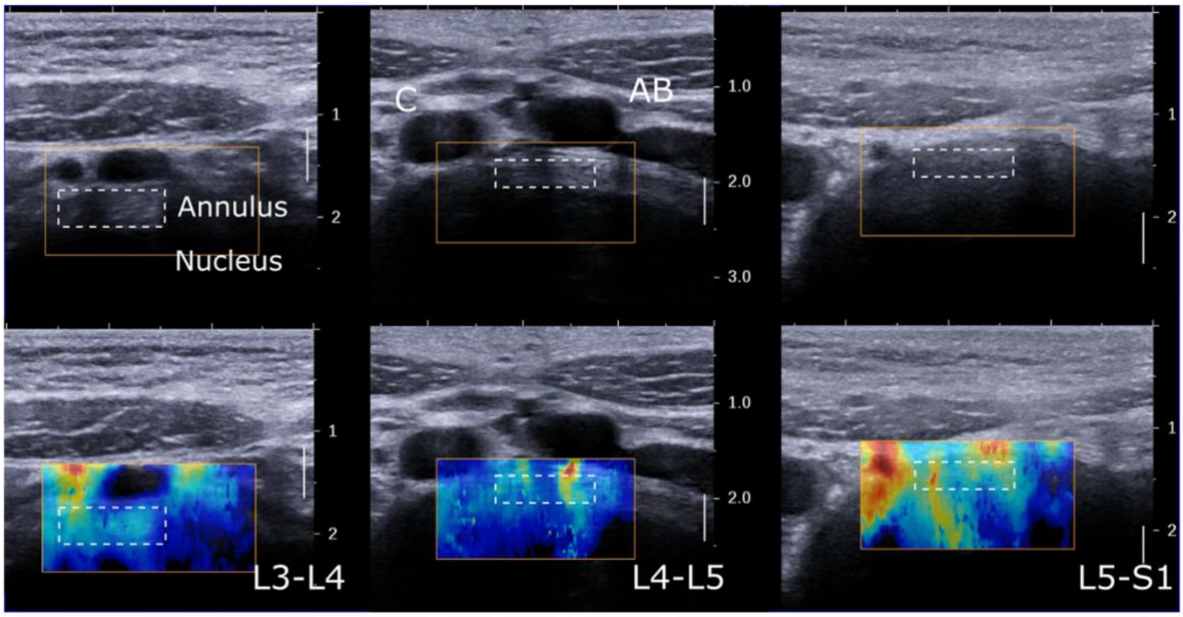

Figure 34: Example of *annulus fibrosus* echography and shear wave elastography at L3-L4, L4-L5, and L5-S1 disc levels. Nucleus appears hypoechoic. Aortic bifurcation (AB) and inferior vena cava (C) are visible at the L4-L5 level. Dashed line rectangles show placement of region of interest for shear wave speed measurement.

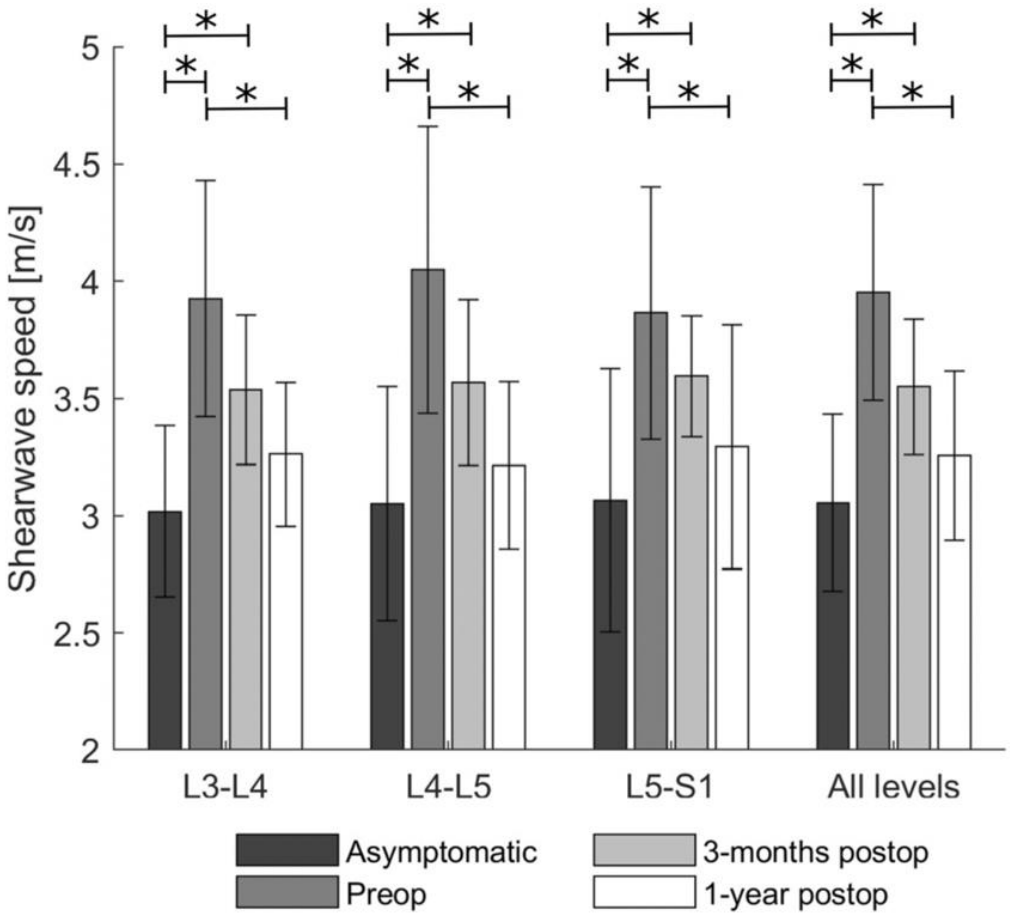

Figure 35: Shear wave speed (SWS) of the *annulus fibrosus* at L3-L4, L4-L5, and L5-S1 disc levels (average ± standard deviation), and all levels pooled. Comparison between asymptomatic subjects, preoperative adolescent idiopathic scoliosis patients, and 3-month and 1-year post surgery patients. Preop measurements were significantly higher than in asymptomatic subjects and 1 year postop ($p < 0.001$, Kruskal-Wallis test), while 1 year postop was significantly lower than preop in all disc levels ($p < 0.001$).

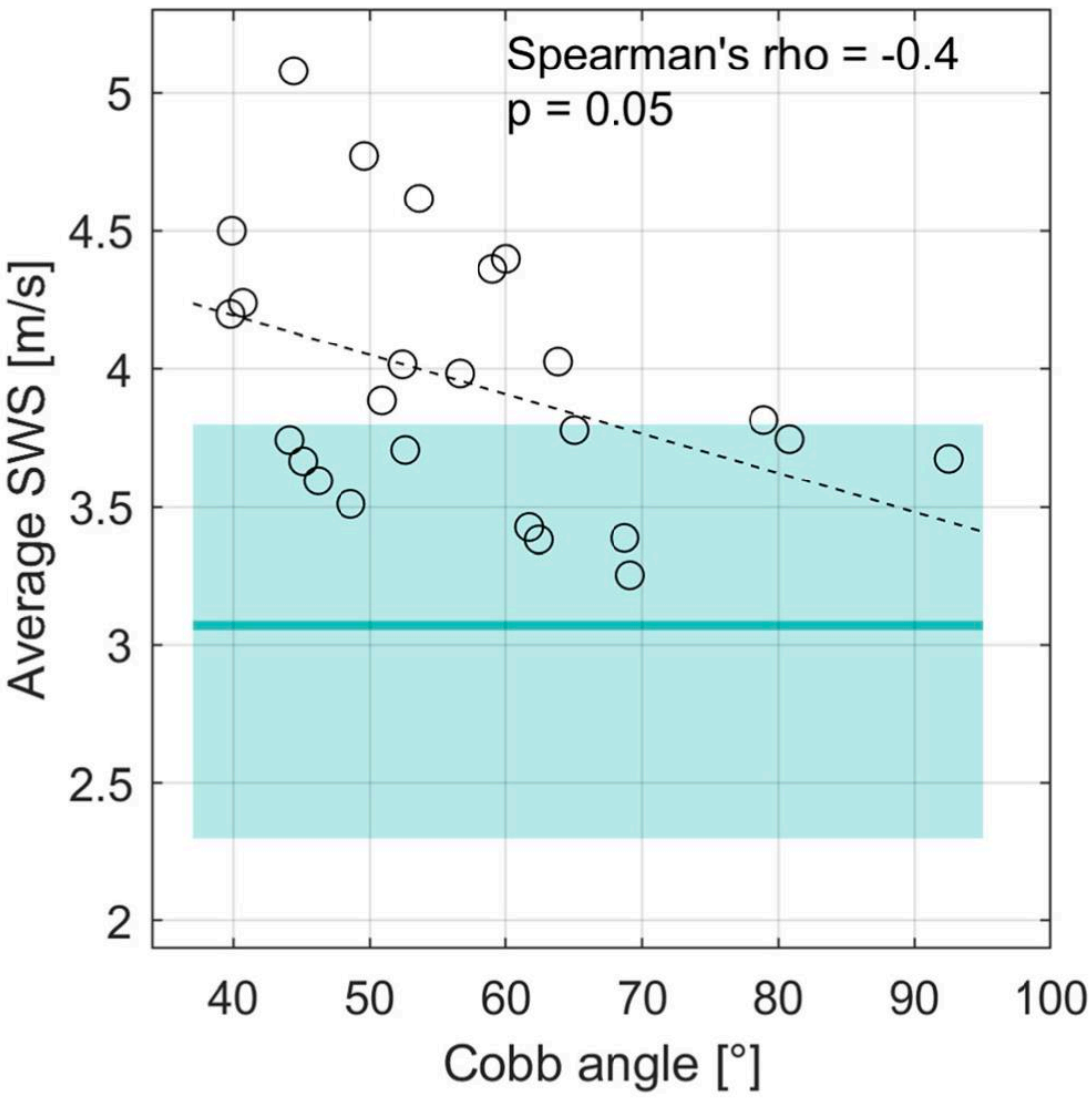

Figure 36: Relationship between Cobb angle and the average shear wave speed (SWS) of disc levels between L3-L4 and L5-S1 (Spearman's rho = − 0.4, p = 0.05). The dashed line is a linear regression between variables, while the horizontal line and the shaded area represent the average and 95% normality corridor of asymptomatic subjects, respectively.

VII.4 Discussion

In this study, scoliotic intervertebral disc was assessed preoperatively and postoperatively, for the first time, by shear wave elastography. A higher SWS is associated to a stiffer tissue; indeed, SWS can be directly related to the tissue's shear modulus (μ) and Young's modulus (E) by the following relationship: $SWS = \sqrt{\mu/\rho} \approx \sqrt{3E/\rho}$, where ρ is the tissue mass density. This relationship allows calculating the shear modulus from SWS, but it is only valid under several assumptions, such as tissue homogeneity, non-dispersivity, and non-compressibility (Bercoff, Tanter, et Fink 2004; Deffieux et al. 2011). Since biological tissues rarely satisfy these assumptions, only SWS is reported in this work. Results confirm previous measurements reporting that scoliotic *annulus fibrosus* shows higher SWS, but they also show that the *annulus* start normalizing 3 months after surgery and can attain normal values 1 year later. Surgery aims at straightening and fusing the scoliotic curve, but there is still no consensus on the choice of which vertebrae should be included in the fusion. On the one hand, long fusion will better stabilize the spine while on the other hand, shorter instrumentation improves trunk mobility (Fischer et Kim 2011). In particular, the choice of the last instrumented vertebra is important to avoid adjacent disc disease or degeneration (Ilharreborde et al. 2009; Abelin-Genevois et al. 2015), but again, no universal rule exists. Shear wave elastography is a rapid and non-invasive measurement which can be performed at bedside; potentially, it could play a key role in helping the surgeon choosing the last instrumented level. Moreover, it could be potentially employed to detect early a degeneration of the adjacent disc postoperatively. Future work should aim at including larger cohorts to analyze more in detail those discs adjacent to the lower junctional vertebra (defining the lower end of the scoliotic curve), to the stable vertebra (the most closely bisected by a vertically directed central sacral line) and the neutral disc (vertebra with the least axial rotation) (O'Brien et al. 2008). These vertebrae are critical in the assessment of spinal deformities, and there- fore, their adjacent discs could present specific characteristics. Future work could also assess the feasibility of standing disc elastography, which could be informative on disc changes when loaded, while intraoperative elastography could provide a strong validation of the measurement, which would not be affected by the surrounding soft tissues, although anterior approach is rare in scoliosis surgery.

The main limitation of the present study is that the cohort was not large enough to perform a sub-analysis on disc levels adjacent to instrumentation: only 5 patients were fused down to a vertebra below L3; thus, only 5 discs adjacent to the instrumentation were measured, and only 4 patients (16 discs) were type C. Nevertheless, results suggest that deformity in the lumbar region further affects the intervertebral discs, although lumbar discs ap- pear stiffer than asymptomatic ones even when the deformity if limited to the thoracic region (A-type patients and thoracic curves).

In the proposed protocol, vertebral level was determined relative to the aortic bifurcation; however, this landmark is at the L4 vertebral level only in 64% of the population (Deswal, Tamang, et Bala 2014). Other means exist for robust determination of the level at which the elastography is performed, especially in preoperative patients. First of all, patients usually undergo magnetic resonance imaging, which allows locating the aortic bifurcation relative to vertebral level. Second, standing radiography is routinely performed, which shows the relationship between the iliac crests, which can be easily located during ultrasonography, and the spinal levels. Finally, it is possible to localize with ultrasound the lowest visible disc and move upwards to find the following discs. Therefore, with a combination of these methods, a robust identification of the imaged disc level is possible.

A limit intrinsic to the technique is that measurements are performed with an anterior approach, which does not allow accessing the thoracic discs. Thoracic curves still showed high SWS in lumbar discs, indicating that disc alteration reaches outside the curve. Nevertheless, the only lumbar patient included showed the highest SWS measured in this study; while no conclusion can be drawn on a single measurement, it does not appear too speculative to hypothesize that those discs within or adjacent to the curve can more affected than others by altered mechanical properties.

Finally, postprocessing is performed in MATLAB, and the processing of a single patient (i.e., three films times three discs) takes about 10 min. This might not yet be compatible with clinical routine, but more sophisticated techniques could be employed to speed up processing time, for instance based on machine learning for automatic ROI selection and tracking. Acquiring a large number of elastographic images allows averaging SWS on a relatively long period (about 30 s), thus smoothing potential periodical variations due to respiration or arterial pulsation. Reproducibility of shear wave elastography in lumbar *annulus fibrosus* is 0.5 m/s, in terms of

95% confidence interval (Vergari et al. 2016), which is smaller than the difference between asymptomatic and AIS subjects measured in this study (3.1 ± 0.4 m/s versus 4.0 ± 0.5, respectively), and smaller than the postoperatively decrease of SWS (− 0.7 m/s at 1 year). This confirms that the difference between the two popuations is clinically relevant. Although most discs normalized their SWS 1 year postop, they did so at different rates; future studies should aim at establishing a relationship between preoperative disc SWS, its short-term change postoperatively, and the longer term clinical outcome.

SWS tended to decrease with higher Cobb angles. This is surprising because AIS patients have higher SWS than asymptomatic controls, so an increase of SWS with curve severity could be expected. However, more severe patients would have been treated by bracing more aggressively and for longer time than less severe patients. It is possible that bracing influenced disc hydration, and therefore its mechanical properties as estimated by shear wave elastography. This hypothesis could be tested on a group of mild scoliotic patients before and during brace treatment.

In conclusion, this study confirmed previous shear wave elastography assessment of scoliotic discs, reporting that *annulus fibrosus* is stiffer in AIS. Moreover, data shows that *annulus* started normalizing 3 months after surgery and had attained normal SWS 1 year postop. Further work should be based on larger cohorts allowing for more in-depth analysis on key disc levels (relative to the scoliotic curve). However, these results are promising, since they show that shear wave elastography can assess alterations of the scoliotic *annulus fibrosus* and their change in time after surgery.

VII.5 Conclusion

Cette étude a confirmé les résultats de l'étude précédente et que l'évaluation par élastographie de l'*annulus fibrosus* lombaire a montré qu'il existait une altération structurelle chez les patients scoliotiques. Cette dernière étude objective une diminution des valeurs des vitesses d'ondes de cisaillements (ce qui traduit une diminution de ces altérations biomécaniques) après une chirurgie de correction et fusion vertébrale à partir du troisième mois et confirmé à un an postopératoire. Ces résultats sont prometteurs, car ils confirment

que l'élastographie ultrasonore de l'*annulus fibrosus* lombaire est un examen utile, accessible et non invasive pouvant aider le clinicien à l'évaluation thérapeutique.

VIII - Conclusion générale et perspective

L'avènement de l'analyse personnalisée tridimensionnelle de la colonne vertébrale a permis de développer de nombreux paramètres biomécaniques aidant le clinicien au diagnostic et à l'évaluation thérapeutique dans sa pratique quotidienne. Pour l'aide au diagnostic, un marqueur biomécanique d'aggravation (soit l'indice de sévérité) a été développé mais se compose uniquement de paramètres issus de la reconstruction osseuse. Quant à l'évaluation thérapeutique, de nombreux travaux se sont intéressés sur la correction chirurgicale de ces paramètres osseux. Dans la revue de la littérature, nous avons rapporté de nouveaux paramètres évaluant l'alignement global, l'asymétrie du pli de taille ou la barycentremétrie d'un patient scoliotique. Néanmoins, aucune étude n'avait été réalisée sur leur possible rôle dans la prédiction d'une scoliose progressive ou leur possible caractère réversible après une correction chirurgicale. Enfin, nous avons exposé que l'analyse par élastographie ultrasonore de l'*annulus fibrosus* lombaire pourrait être un paramètre de progression d'une scoliose idiopathique mais aucune évaluation postopératoire n'avait été réalisée.

L'objectif de cette thèse était de rechercher et d'évaluer de nouveaux paramètres biomécaniques issus de l'analyse 3D de l'alignement global et de la reconstruction de l'enveloppe externe contribuant à l'aide au diagnostic d'une scoliose progressive. Dans un second temps, cette thèse a permis l'analyse de ces paramètres et de l'*annulus fibrosus* lombaire par élastographie ultrasonore après une correction et fusion vertébrale postérieure.

Le premier point est que l'analyse précoce de l'alignement global (soit la mesure de l'OD-HA) suggère que c'est un potentiel paramètre d'aggravation d'une scoliose idiopathique. L'ajout de l'analyse coronale de cette mesure à l'indice de sévérité améliore les performances de l'indice et en particulier pour les scolioses thoraciques.

Le second point est que l'analyse de la reconstruction de l'enveloppe externe chez les adolescents porteurs d'une scoliose idiopathique est réalisable, pertinente et prometteuse dans l'aide au diagnostic mais également dans l'évaluation thérapeutique. La position du centre masse de la vertèbre sommet semble être perturbée à un stade précoce et l'ajout du

moment intersegmentaire de la vertèbre sommet améliore les performances de l'indice de sévérité dans les scolioses thoraciques. Après correction chirurgicale, les valeurs de l'asymétrie du pli de taille et des paramètres liés au barycentre sont améliorés et corrélés en partie à la correction du plan axial.
Enfin, l'évaluation de l'*annulus fibrosus* lombaire par élastographie a confirmé que cet outil permettait de dépister les perturbations biomécaniques de l'*annulus fibrosus* et que ces altérations étaient réversibles jusqu'au moins un an après la correction chirurgicale.

L'analyse de la littérature et des travaux de cette thèse ont montré qu'il existait plusieurs paramètres prédicteurs de la progression d'une scoliose. Il est important de souligner que ces paramètres isolés ne sont pas suffisants pour déterminer le caractère progressif d'une courbure mais nous devons les combiner. Cela traduit le caractère complexe et multifactoriel d'une scoliose qui ne présente pas les mêmes caractéristiques. En effet, chaque sujet a ses spécificités et chaque courbure a ses caractéristiques. Dans certain cas, la barycentremétrie peut être altérée précocement alors que dans d'autre cas le dépistage précoce peut reposer sur un trouble de l'alignement ou une altération des propriétés biomécaniques du disque intervertébral.

Cependant cette thèse a permis de montrer l'intérêt de l'analyse tridimensionnelle précoce de l'alignement, de l'asymétrie du pli de taille et de la barycentremétrie dans la prise en charge d'une scoliose idiopathique et la pertinence de l'utilisation de l'élastographie ultrasonore pour évaluer les altérations biomécaniques de l'*annulus fibrosus*. Les principaux avantages de ces nouvelles méthodes d'analyse sont liés aux caractères utiles, quantitatifs, objectifs, fiables, accessibles en routine clinique et non invasifs des mesures.
Ces travaux ouvrent des perspectives de recherche importantes. Nous pouvons donner comme exemple la validation à grande échelle de l'ajout de certains paramètres spécifiques dans l'indice de sévérité, une meilleure compréhension des complications mécaniques liées à la distribution des masses postopératoire ou l'évaluation des altérations biomécaniques de l'*annulus fibrosus* en fonction de sa localisation par rapport à la courbure (c'est-à-dire dans la courbure, au niveau jonctionnel inférieur, dans la contre-courbure ou en zone neutre). L'une des limitations à une utilisation en routine clinique, afin d'apporter au clinicien tous les

éléments importants à sa prise en charge, est le temps des reconstructions de l'enveloppe externe. Également, nous n'avons pas abordé dans cette thèse la composante dynamique que ce soit dans l'évaluation de l'alignement, du barycentre ou des altérations de l'*annulus fibrosus*. Les travaux sont actifs au sein de l'institut pour aborder ces problématiques.

Néanmoins, dès à présent, le clinicien peut s'aider de l'alignement coronal global d'un patient dans la décision de la mise en place d'un traitement précoce, essayer d'obtenir une harmonie des masses dans sa correction chirurgicale et s'efforcer d'améliorer la correction du plan horizontal, dont cette thèse a contribué à mettre en relief l'importance.

IX - Bibliographie

Abelin-Genevois, Kariman, Erik Estivalezes, Jerome Briot, Annick Sévely, Jerome Sales de Gauzy, et Pascal Swider. 2015. « Spino-Pelvic Alignment Influences Disc Hydration Properties after AIS Surgery: A Prospective MRI-Based Study ». *European Spine Journal* 24 (6):1183-90.

Adam, Clayton J., Geoffrey N. Askin, et Mark J. Pearcy. 2008. « Gravity-Induced Torque and Intravertebral Rotation in Idiopathic Scoliosis ». *Spine* 33 (2): E30-37.

Altaf, Farhaan, Alexander Gibson, Zaher Dannawi, et Hilali Noordeen. 2013. « Adolescent Idiopathic Scoliosis ». *BMJ (Clinical Research Ed.)* 346 (avril): f2508.

Alzakri, Abdulmajeed, Claudio Vergari, M. Van den Abbeele, Olivier Gille, Wafa Skalli, et Ibrahim Obeid. 2019. « Global Sagittal Alignment and Proximal Junctional Kyphosis in Adolescent Idiopathic Scoliosis ». *Spine Deformity* 7 (2): 236-44.

Amabile, Celia, Hélène Pillet, Virginie Lafage, Cédric Barrey, Jean-Marc Vital, et Wafa Skalli. 2016a. « A New Quasi-Invariant Parameter Characterizing the Postural Alignment of Young Asymptomatic Adults ». *European Spine Journal* 25 (11): 3666-74.

Amabile, Celia, Julie Choisne, Agathe Nérot, Hélène Pillet, et Wafa Skalli. 2016b. « Determination of a New Uniform Thorax Density Representative of the Living Population from 3D External Body Shape Modeling ». *Journal of Biomechanics* 49 (7): 1162-69.

Assaiante, Christine, Sophie Mallau, Jean-Luc Jouve, Gérard Bollini, et Marianne Vaugoyeau. 2012. « Do Adolescent Idiopathic Scoliosis (AIS) Neglect Proprioceptive Information in Sensory Integration of Postural Control? » Édité par Paul L. Gribble. *PLoS ONE* 7 (7): e40646.

Barrey, Cédric, Sabina Champain, Sophie Campana, Aymen Ramadan, Gilles Perrin, et Wafa Skalli. 2012. « Sagittal Alignment and Kinematics at Instrumented and Adjacent Levels after Total Disc Replacement in the Cervical Spine ». *European Spine Journal: Official Publication of the European Spine Society, the European Spinal Deformity Society, and the European Section of the Cervical Spine Research Society* 21 (8): 1648-59.

Bercoff, Jérémy, Mickaël Tanter, et Mathias Fink. 2004. « Supersonic Shear Imaging: A New Technique for Soft Tissue Elasticity Mapping ». *IEEE Transactions on Ultrasonics, Ferroelectrics, and Frequency Control* 51 (4): 396-409.

Berthonnaud, Eric, Joannès Dimnet, Pierre Roussouly, et Hubert Labelle. 2005. « Analysis of the Sagittal Balance of the Spine and Pelvis Using Shape and Orientation Parameters ». *Journal of Spinal Disorders & Techniques* 18 (1): 40-47.

Blondel, B., V. Pomero, B. Moal, V. Lafage, J.-L. Jouve, P. Tropiano, G. Bollini, R. Dumas, et E. Viehweger. 2012. « Sagittal Spine Posture Assessment: Feasibility of a Protocol Based on Intersegmental Moments ». *Orthopaedics & Traumatology, Surgery & Research: OTSR* 98 (1):

Bolzinger, Manon, Isabelle Bernardini, Camille Thevenin Lemoine, Adeline Gallini, Franck Accadbled, et Jérôme Sales de Gauzy. 2021. « Monitoring Adolescent Idiopathic Scoliosis by

Measuring Ribs Prominence Using Surface Topography Device ». *Spine Deformity* 9 (5): 1349-54.

Boyer, Laure, Jesse Shen, Stefan Parent, Samuel Kadoury, et Carl-Eric Aubin. 2018. « Accuracy and Precision of Seven Radiography-Based Measurement Methods of Vertebral Axial Rotation in Adolescent Idiopathic Scoliosis ». *Spine Deformity* 6 (4): 351-57.

Castelein, René M., Saba Pasha, Jack Cy Cheng, et Jean Dubousset. 2020. « Idiopathic Scoliosis as a Rotatory Decompensation of the Spine ». *Journal of Bone and Mineral Research: The Official Journal of the American Society for Bone and Mineral Research* 35 (10): 1850-57.

Cheng, Jack C., René M. Castelein, Winnie C. Chu, Aina J. Danielsson, Matthew B. Dobbs, Theodoros B. Grivas, Christina A. Gurnett, et al. 2015. « Adolescent Idiopathic Scoliosis ». *Nature Reviews. Disease Primers* 1 (septembre): 15030.

Clavel, Louis, Valérie Attali, Isabelle Rivals, Marie-Cécile Niérat, Pierantonio Laveneziana, Philippe Rouch, Thomas Similowski, et Baptiste Sandoz. 2020. « Decreased Respiratory-Related Postural Perturbations at the Cervical Level under Cognitive Load ». *European Journal of Applied Physiology* 120 (5): 1063-74.

Clement, R. Carter, Jason Anari, Carrie E. Bartley, Tracey P. Bastrom, Ronit Shah, Divya Talwar, et Vidyadhar V. Upasani. 2020. « What Are Normal Radiographic Spine and Shoulder Balance Parameters among Adolescent Patients? » *Spine Deformity* 8 (4): 621-27.

Coonrad, R. W., G. A. Murrell, G. Motley, E. Lytle, et L. A. Hey. 1998. « A Logical Coronal Pattern Classification of 2,000 Consecutive Idiopathic Scoliosis Cases Based on the Scoliosis Research Society-Defined Apical Vertebra ». *Spine* 23 (12): 1380-91.

Courvoisier, Aurélien, Xavier Drevelle, Jean Dubousset, et Wafa Skalli. 2013. « Transverse Plane 3D Analysis of Mild Scoliosis ». *European Spine Journal* 22 (11): 2427-32.

Courvoisier, Aurélien, Christophe Garin, Raphaël Vialle, et Rémi Kohler. 2015. « The Change on Vertebral Axial Rotation after Posterior Instrumentation of Idiopathic Scoliosis ». *Child's Nervous System* 31 (12): 2325-31.

Dalal, Aliasgar, Vidyadhar V. Upasani, Tracey P. Bastrom, Burt Yaszay, Suken A. Shah, Harry L. Shufflebarger, et Peter O. Newton. 2011. « Apical Vertebral Rotation in Adolescent Idiopathic Scoliosis: Comparison of Uniplanar and Polyaxial Pedicle Screws ». *Journal of Spinal Disorders & Techniques* 24 (4): 251-57.

Dalleau, G., M. Damavandi, P. Leroyer, C. Verkindt, C. H. Rivard, et P. Allard. 2011. « Horizontal Body and Trunk Center of Mass Offset and Standing Balance in Scoliotic Girls ». *European Spine Journal: Official Publication of the European Spine Society, the European Spinal Deformity Society, and the European Section of the Cervical Spine Research Society* 20 (1): 123-28.

Damavandi, Mohsen, Georges Dalleau, Georgios Stylianides, Charles-Hilaire Rivard, et Paul Allard. 2013. « Head and Trunk Mass and Center of Mass Position Estimations in Able-Bodied and Scoliotic Girls ». *Medical Engineering & Physics* 35 (11): 1607-12.

Deffieux, Thomas, Jean-Luc Gennisson, Jeremy Bercoff, et Mickael Tanter. 2011. « On the Effects of Reflected Waves in Transient Shear Wave Elastography ». *IEEE Transactions on Ultrasonics, Ferroelectrics, and Frequency Control* 58 (10): 2032-35.

Dempster, WT. 1955. « Space requirements of the seated operator: geomet- rical, kinematic, and mechanical aspects of the body with special reference to the limbs. », Wright-Patterson Air Force Base. OH: Wright Air Development Center.

Deswal, Arvind, Binod Kumar Tamang, et Anju Bala. 2014. « Study of Aortic- Common Iliac Bifurcation and Its Clinical Significance ». *Journal of Clinical and Diagnostic Research: JCDR* 8 (7): AC06-08.

Deviren, Vedat, Sigurd Berven, Frank Kleinstueck, James Antinnes, Jason A. Smith, et Serena S. Hu. 2002. « Predictors of Flexibility and Pain Patterns in Thoracolumbar and Lumbar Idiopathic Scoliosis ». *Spine* 27 (21): 2346-49.

Diebo, Bassel G., Jeffrey J. Varghese, Renaud Lafage, Frank J. Schwab, et Virginie Lafage. 2015. « Sagittal Alignment of the Spine: What Do You Need to Know? » *Clinical Neurology and Neurosurgery* 139 (décembre): 295-301.

Dubousset, J. 1999. « Les scolioses dites idiopathiques. Définition-pathologie-classification-étiologie. [Idiopathic scoliosis. Definition-pathology-classification-etiology]. », nº183(4): 699-704.

Dubousset, J., G. Charpak, W. Skalli, G. Kalifa, et J.-Y. Lazennec. 2007. « [EOS stereo-radiography system: whole-body simultaneous anteroposterior and lateral radiographs with very low radiation dose] ». *Revue De Chirurgie Orthopedique Et Reparatrice De L'appareil Moteur* 93 (6 Suppl): 141-43.

Dubousset, Jean. 2020. « Past, Present, and Future in Pediatric Spinal Surgery ». *Annals of Translational Medicine* 8 (2): 36.

Duval-Beaupère, G. 1970. « [Maturation indices in the surveillance of scoliosis] ». *Revue De Chirurgie Orthopedique Et Reparatrice De L'appareil Moteur* 56 (1): 59-76.

Duval-Beaupère, G. 1992. « Rib Hump and Supine Angle as Prognostic Factors for Mild Scoliosis ». *Spine* 17 (1): 103-7

.

Duval-Beaupère, G., et T. Lamireau. 1985. « Scoliosis at Less than 30 Degrees. Properties of the Evolutivity (Risk of Progression) ». *Spine* 10 (5): 421-24.

Duval-Beaupère, G., et G. Robain. 1987. « Visualization on Full Spine Radiographs of the Anatomical Connections of the Centres of the Segmental Body Mass Supported by Each Vertebra and Measured in Vivo ». *International Orthopaedics* 11 (3): 261-69.

Duval-Beaupère, G., C. Schmidt, et P. Cosson. 1992. « A Barycentremetric Study of the Sagittal Shape of Spine and Pelvis: The Conditions Required for an Economic Standing Position ». *Annals of Biomedical Engineering* 20 (4): 451-62.

Faro, Frances D., Michelle C. Marks, Jeffrey Pawelek, et Peter O. Newton. 2004. « Evaluation

of a Functional Position for Lateral Radiograph Acquisition in Adolescent Idiopathic Scoliosis ». *Spine* 29 (20): 2284-89.

Ferrero, Emmanuelle, Pierre Guigui, Marc Khalifé, Robert Carlier, Antoine Feydy, Adrien Felter, Virginie Lafage, et Wafa Skalli. 2021. « Global Alignment Taking into Account the Cervical Spine with Odontoid Hip Axis Angle (OD-HA) ». *European Spine Journal: Official Publication of the European Spine Society, the European Spinal Deformity Society, and the European Section of the Cervical Spine Research Society* 30 (12): 3647-55.

Fischer, Charla R., et Yongjung Kim. 2011. « Selective Fusion for Adolescent Idiopathic Scoliosis: A Review of Current Operative Strategy ». *European Spine Journal: Official Publication of the European Spine Society, the European Spinal Deformity Society, and the European Section of the Cervical Spine Research Society* 20 (7): 1048-57.

Gajny, Laurent, Shahin Ebrahimi, Claudio Vergari, Elsa Angelini, et Wafa Skalli. 2019. « Quasi-Automatic 3D Reconstruction of the Full Spine from Low-Dose Biplanar X-Rays Based on Statistical Inferences and Image Analysis ». *European Spine Journal* 28 (4): 658-64.

Gajny, Laurent, Léopold Robichon, Eleonora Pinto, Thibault Hernandez, Raphaël Vialle, et Wafa Skalli. 2020. « 3D Reconstruction of Adolescent Scoliotic Trunk Shape from Biplanar X-Rays: A Feasibility Study ». *Computer Methods in Biomechanics and Biomedical Engineering: Imaging & Visualization* 8 (3): 245-51.

Gangnet, N., V. Pomero, R. Dumas, W. Skalli, et J.-M. Vital. 2003. « Variability of the Spine and Pelvis Location with Respect to the Gravity Line: A Three-Dimensional Stereoradiographic Study Using a Force Platform ». *Surgical and Radiologic Anatomy* 25 (5-6): 424-33.

Gardner, Adrian, Fiona Berryman, et Paul Pynsent. 2021. « The Use of Statistical Modelling to Identify Important Parameters for the Shape of the Torso Following Surgery for Adolescent Idiopathic Scoliosis ». *Journal of Anatomy* 239 (3): 602-10.

Gennisson, J.-L., T. Deffieux, M. Fink, et M. Tanter. 2013. « Ultrasound Elastography: Principles and Techniques ». *Diagnostic and Interventional Imaging* 94 (5): 487-95.

Gille, Olivier, Nicolas Champain, Abdelkrim Benchikh-El-Fegoun, Jean-Marc Vital, et Wafa Skalli. 2007. « Reliability of 3D Reconstruction of the Spine of Mild Scoliotic Patients ». *Spine* 32 (5): 568-73.

Gómez Cristancho, David Camilo, Gabriela Jovel Trujillo, Iván Felipe Manrique, Juan Carlos Pérez Rodríguez, Roberto Carlos Díaz Orduz, et Miguel Enrique Berbeo Calderón. 2022. « Neurological Mechanisms Involved in Idiopathic Scoliosis. Systematic Review of the Literature ». *Neurocirugia (English Edition)*, mars, S2529-8496(22)00018-1.

Gorton, George E., Megan L. Young, et Peter D. Masso. 2012. « Accuracy, Reliability, and Validity of a 3-Dimensional Scanner for Assessing Torso Shape in Idiopathic Scoliosis »: *Spine* 37 (11): 957-65.

Green, Daniel W., Thomas W. Lawhorne, Roger F. Widmann, Christopher K. Kepler, Caitlin Ahern, Douglas N. Mintz, Bernard A. Rawlins, Stephen W. Burke, et Oheneba Boachie-Adjei. 2011. « Long-Term Magnetic Resonance Imaging Follow-up Demonstrates Minimal

Transitional Level Lumbar Disc Degeneration after Posterior Spine Fusion for Adolescent Idiopathic Scoliosis ». *Spine* 36 (23): 1948-54.

Grivas, Theodoros B., Elias Vasiliadis, Vasilios Mouzakis, Constantinos Mihas, et Georgios Koufopoulos. 2006. « Association between Adolescent Idiopathic Scoliosis Prevalence and Age at Menarche in Different Geographic Latitudes ». *Scoliosis* 1 (mai): 9.

Groisser, Benjamin N., Howard J. Hillstrom, Ankush Thakur, Kyle W. Morse, Matthew Cunningham, M. Timothy Hresko, Ron Kimmel, Alon Wolf, et Roger F. Widmann. 2022. « Reliability of Automated Topographic Measurements for Spine Deformity ». *Spine Deformity* 10 (5): 1035-45.

Guo, Xia, W W. Chau, Christina W. Y. Hui-Chan, Catherine S. K. Cheung, William W. N. Tsang, et Jack C. Y. Cheng. 2006. « Balance Control in Adolescents With Idiopathic Scoliosis and Disturbed Somatosensory Function »: *Spine* 31 (14): E437-40.

Hasegawa, Kazuhiro, et Jean Felix Dubousset. 2022. « *Cone of Economy with the Chain of Balance*-Historical Perspective and Proof of Concept ». *Spine Surgery and Related Research* 6 (4): 337-49.

Hernandez, Thibault, Thomas Thenard, Claudio Vergari, Leopold Robichon, Wafa Skalli, et Raphaël Vialle. 2018. « Étude du déséquilibre postural frontal dans la scoliose idiopathique : l'étude barycentremétrique confirme-t-elle les données de l'examen clinique ? » *Revue de Chirurgie Orthopédique et Traumatologique* 104 (5): 442-48.

Hong, Albert, Neha Jaswal, Lindsey Westover, Eric C. Parent, Marc Moreau, Douglas Hedden, et Samer Adeeb. 2017. « Surface Topography Classification Trees for Assessing Severity and Monitoring Progression in Adolescent Idiopathic Scoliosis ». *Spine* 42 (13): E781-87.

Hu, Zongshan, Claudio Vergari, Laurent Gajny, Gene Chi-Wai Man, Kwong-Hang Yeung, Zhen Liu, Tsz-Ping Lam, et al. 2022. « An analysis on the determinants of head to pelvic balance in a Chinese adult population ». *Quantitative Imaging in Medicine and Surgery* 12 (4): 2311-20.

Huber, Maxime, Guillaume Gilbert, Julien Roy, Stefan Parent, Hubert Labelle, et Delphine Périé. 2016. « Sensitivity of MRI Parameters within Intervertebral Discs to the Severity of Adolescent Idiopathic Scoliosis: MRI in Adolescent Idiopathic Scoliosis ». *Journal of Magnetic Resonance Imaging* 44 (5): 1123-31.

Humbert, L., J.A. De Guise, B. Aubert, B. Godbout, et W. Skalli. 2009. « 3D Reconstruction of the Spine from Biplanar X-Rays Using Parametric Models Based on Transversal and Longitudinal Inferences ». *Medical Engineering & Physics* 31 (6): 681-87.

Ilharreborde, Brice, Emmanuelle Ferrero, Marianne Alison, et Keyvan Mazda. 2016. « EOS Microdose Protocol for the Radiological Follow-up of Adolescent Idiopathic Scoliosis ». *European Spine Journal: Official Publication of the European Spine Society, the European Spinal Deformity Society, and the European Section of the Cervical Spine Research Society* 25 (2): 526-31.

Ilharreborde, Brice, Etienne Morel, Keyvan Mazda, et Mark B. Dekutoski. 2009. « Adjacent

Segment Disease after Instrumented Fusion for Idiopathic Scoliosis: Review of Current Trends and Controversies ». *Journal of Spinal Disorders & Techniques* 22 (7): 530-39.

Ilharreborde, Brice, Jean Sebastien Steffen, Eric Nectoux, Jean Marc Vital, Keyvan Mazda, Wafa Skalli, et Ibrahim Obeid. 2011. « Angle Measurement Reproducibility Using EOS Three-Dimensional Reconstructions in Adolescent Idiopathic Scoliosis Treated by Posterior Instrumentation ». *Spine* 36 (20): E1306-1313.

Illés, Tamás S., Stig M. Jespersen, Pieter Reynders, Fabien Lauer, Jean Charles Le Huec, et Jean F. Dubousset. 2020. « Axial Plane Characteristics of Thoracic Scoliosis and Their Usefulness for Determining the Fusion Levels and the Correction Technique ». *European Spine Journal* 29 (8): 2000-2009.

Illés, Tamás S., Francois Lavaste, et Jean F. Dubousset. 2019. « The Third Dimension of Scoliosis: The Forgotten Axial Plane ». *Orthopaedics & Traumatology: Surgery & Research* 105 (2): 351-59.

Jaremko, Jacob L., Philippe Poncet, Janet Ronsky, James Harder, Jean Dansereau, Hubert Labelle, et Ronald F. Zernicke. 2002. « Indices of Torso Asymmetry Related to Spinal Deformity in Scoliosis ». *Clinical Biomechanics (Bristol, Avon)* 17 (8): 559-68.

Jung, Ji-Yong, Eun-Jong Cha, Kyung-Ah Kim, Yonggwan Won, Soo-Kyung Bok, Bong-Ok Kim, et Jung-Ja Kim. 2015. « Influence of Pelvic Asymmetry and Idiopathic Scoliosis in Adolescents on Postural Balance during Sitting ». *Bio-Medical Materials and Engineering* 26 Suppl 1: S601-610.

Karam, Mohamad, Ismat Ghanem, Claudio Vergari, Nour Khalil, Maria Saadé, Céline Chaaya, Ali Rteil, et al. 2022. « Global Malalignment in Adolescent Idiopathic Scoliosis: The Axial Deformity Is the Main Driver ». *European Spine Journal: Official Publication of the European Spine Society, the European Spinal Deformity Society, and the European Section of the Cervical Spine Research Society* 31 (9): 2326-38.

Kim, Kwang-Ryeol, Jean-Charles Le Huec, Hyun-Jun Jang, Sung-Hyun Noh, Jeong-Yoon Park, Yoon Ha, Sung-Uk Kuh, et al. 2021. « Which Is More Predictive Value for Mechanical Complications: Fixed Thoracolumbar Alignment (T1 Pelvic Angle) Versus Dynamic Global Balance Parameter (Odontoid-Hip Axis Angle) ». *Neurospine* 18 (3): 597-607.

Kobielarz, Magdalena, Sylwia Szotek, Maciej Głowacki, Joanna Dawidowicz, et Celina Pezowicz. 2016. « Qualitative and Quantitative Assessment of Collagen and Elastin in Annulus Fibrosus of the Physiologic and Scoliotic Intervertebral Discs ». *Journal of the Mechanical Behavior of Biomedical Materials* 62 (septembre): 45-56.

Kouwenhoven, Jan-Willem M., et René M. Castelein. 2008. « The Pathogenesis of Adolescent Idiopathic Scoliosis: Review of the Literature ». *Spine* 33 (26): 2898-2908.

Labelle, H., J. Dansereau, C. Bellefleur, et J. C. Jéquier. 1995. « Variability of Geometric Measurements from Three-Dimensional Reconstructions of Scoliotic Spines and Rib Cages ». *European Spine Journal: Official Publication of the European Spine Society, the European Spinal Deformity Society, and the European Section of the Cervical Spine Research Society* 4 (2): 88-94.

Lamerain, Mayalen, Manon Bachy, Arnaud Dubory, Reda Kabbaj, Caroline Scemama, et Raphaël Vialle. 2017. « All-Pedicle Screw Fixation With 6-Mm-Diameter Cobalt-Chromium Rods Provides Optimized Sagittal Correction of Adolescent Idiopathic Scoliosis ». *Clinical Spine Surgery* 30 (7): E857-63.

Langlais, T, et J Sales de Gauzy. 2019. « Scoliose idiopathique (adultes exclus) », Appareil Locomoteur, Encyclopédie médico-chirurgicale

Langlais, T, C Vergari, R Pietton, J Dubousset, W Skalli, et R Vialle. 2018. « Shear-Wave Elastography Can Evaluate Annulus Fibrosus Alteration in Adolescent Scoliosis. » *Eur Radiol* 28: 2830-37.

Langlais, T, C Vergari, F Xavier, M Al Hawsawi, L Gajny, R Vialle, W Skalli, et R Pietton. 2022. « 3D Quasi-Automatic Spine Length Assessment Using Low Dose Biplanar Radiography after Surgical Correction in Thoracic Idiopathic Scoliosis. » *Med Eng Phys* 99: 103735.

Langlais, T, R Vialle, et J Sales de Gauzy. 2020. « Traitement chirurgical des scolioses idiopathiques », Technique chirurgicale, Encyclopédie médico-chiururgicale

Langlais, Tristan, Claudio Vergari, Grégoire Rougereau, Laurent Gajny, Ayman Assi, Ismat Ghanem, Jean Dubousset, Raphaël Vialle, Raphaël Pietton, et Wafa Skalli. 2021. « Balance, Barycentremetry and External Shape Analysis in Idiopathic Scoliosis: What Can the Physician Expect from It? » *Medical Engineering & Physics* 94 (août): 33-40.

Lee, Choon Sung, Chang Ju Hwang, Hyung Seo Jung, Dong-Ho Lee, Jae Woo Park, Jae Hwan Cho, Jae Jun Yang, et Sehan Park. 2020. « Association Between Vertebral Rotation Pattern and Curve Morphology in Adolescent Idiopathic Scoliosis ». *World Neurosurgery* 143 (novembre): e243-52.

Legaye, J., et G. Duval-Beaupere. 2008. « Gravitational Forces and Sagittal Shape of the Spine. Clinical Estimation of Their Relations ». *International Orthopaedics* 32 (6): 809-16.

Legaye, Jean, et Ginette Duval-Beaupere. 2017. « Influence of a Variation in the Position of the Arms on the Sagittal Connection of the Gravity Line with the Spinal Structures ». *European Spine Journal: Official Publication of the European Spine Society, the European Spinal Deformity Society, and the European Section of the Cervical Spine Research Society* 26 (11): 2828-33.

Lenke, Lawrence G., Randal R. Betz, David Clements, Andrew Merola, Thomas Haher, Thomas Lowe, Peter Newton, Keith H. Bridwell, et Kathy Blanke. 2002. « Curve Prevalence of a New Classification of Operative Adolescent Idiopathic Scoliosis: Does Classification Correlate with Treatment? » *Spine* 27 (6): 604-11.

Lion, Alexis, Thierry Haumont, Gérome C. Gauchard, Sylvette R. Wiener-Vacher, Pierre Lascombes, et Philippe P. Perrin. 2013. « Visuo-Oculomotor Deficiency at Early-Stage Idiopathic Scoliosis in Adolescent Girls ». *Spine* 38 (3): 238-44.

Lonstein, J. E. 1994. « Adolescent Idiopathic Scoliosis ». *Lancet (London, England)* 344 (8934): 1407-12.

Lonstein, J. E., et J. M. Carlson. 1984. « The Prediction of Curve Progression in Untreated Idiopathic Scoliosis during Growth ». *The Journal of Bone and Joint Surgery. American Volume* 66 (7): 1061-71.

Marks, Michelle, Peter O. Newton, Maty Petcharaporn, Tracey P. Bastrom, Suken Shah, Randal Betz, Baron Lonner, et Firoz Miyanji. 2012. « Postoperative Segmental Motion of the Unfused Spine Distal to the Fusion in 100 Patients with Adolescent Idiopathic Scoliosis ». *Spine* 37 (10): 826-32.

Michalik, R., H. Siebers, J. Eschweiler, V. Quack, M. Gatz, T. Dirrichs, et M. Betsch. 2019. « Development of a New 360-Degree Surface Topography Application ». *Gait & Posture* 73 (septembre): 39-44.

Mínguez, María Fe, Mateo Buendía, Rosa M. Cibrián, Rosario Salvador, Manuel Laguía, Antonio Martín, et Francisco Gomar. 2007. « Quantifier Variables of the Back Surface Deformity Obtained with a Noninvasive Structured Light Method: Evaluation of Their Usefulness in Idiopathic Scoliosis Diagnosis ». *European Spine Journal: Official Publication of the European Spine Society, the European Spinal Deformity Society, and the European Section of the Cervical Spine Research Society* 16 (1): 73-82.

Larouche Guilbert M, Raison M, Fortin C, et Achiche S. 2019. « Development of a Multibody Model to Assess Efforts along the Spine for the Rehabilitation of Adolescents with Idiopathic Scoliosis ». *Journal of Musculoskeletal & Neuronal Interactions* 19 (1).

Nachemson, A. L., et L. E. Peterson. 1995. « Effectiveness of Treatment with a Brace in Girls Who Have Adolescent Idiopathic Scoliosis. A Prospective, Controlled Study Based on Data from the Brace Study of the Scoliosis Research Society ». *The Journal of Bone and Joint Surgery. American Volume* 77 (6): 815-22.

Nault, Marie-Lyne, Paul Allard, Sébastien Hinse, Richard Le Blanc, Olivier Caron, Hubert Labelle, et Heydar Sadeghi. 2002. « Relations between Standing Stability and Body Posture Parameters in Adolescent Idiopathic Scoliosis ». *Spine* 27 (17): 1911-17.

Nault, Marie-Lyne, Marie Beauséjour, Marjolaine Roy-Beaudry, Jean-Marc Mac-Thiong, Jacques de Guise, Hubert Labelle, et Stefan Parent. 2020. « A Predictive Model of Progression for Adolescent Idiopathic Scoliosis Based on 3D Spine Parameters at First Visit ». *Spine* 45 (9): 605-11.

Nault, Marie-Lyne, Jean-Marc Mac-Thiong, Marjolaine Roy-Beaudry, Jacques deGuise, Hubert Labelle, et Stefan Parent. 2013. « Three-Dimensional Spine Parameters Can Differentiate between Progressive and Nonprogressive Patients with AIS at the Initial Visit: A Retrospective Analysis ». *Journal of Pediatric Orthopedics* 33 (6): 618-23.

Nault, Marie-Lyne, Stefan Parent, Philippe Phan, Marjolaine Roy-Beaudry, Hubert Labelle, et Michèle Rivard. 2010. « A Modified Risser Grading System Predicts the Curve Acceleration Phase of Female Adolescent Idiopathic Scoliosis ». *The Journal of Bone and Joint Surgery. American Volume* 92 (5): 1073-81.

Negrini, S, S Donzelli, J Wynes, et F Zaina. 2018. « 2016 SOSORT guidelines: orthopaedic

and rehabilitation treatment of idiopathic scoliosis during growth - PubMed ». 2018.

Nérot, Agathe, Julie Choisne, Célia Amabile, Christophe Travert, Hélène Pillet, Xuguang Wang, et Wafa Skalli. 2015. « A 3D Reconstruction Method of the Body Envelope from Biplanar X-Rays: Evaluation of Its Accuracy and Reliability ». *Journal of Biomechanics* 48 (16): 4322-26.

O'Brien, MF, TR Kulklo, KM Blanke, et LG Lenke. 2008. « Radiographic measurement manual. », Spinal deformity study group (SDSG), Medtronic Sofamor Danek USA, Inc.

Pasha, Saba, Patrick J. Cahill, John P. Dormans, et John M. Flynn. 2016. « Characterizing the Differences between the 2D and 3D Measurements of Spine in Adolescent Idiopathic Scoliosis ». *European Spine Journal: Official Publication of the European Spine Society, the European Spinal Deformity Society, and the European Section of the Cervical Spine Research Society* 25 (10): 3137-45.

Patias, Petros, Theodoros B. Grivas, Angelos Kaspiris, Costas Aggouris, et Evangelos Drakoutos. 2010. « A Review of the Trunk Surface Metrics Used as Scoliosis and Other Deformities Evaluation Indices ». *Scoliosis* 5 (juin): 12.

Perdriolle, R. 1979. « La scoliose: son étude tridimensionnelle. », Maloine, Paris

Pesenti, S., J.-L. Jouve, C. Morin, S. Wolff, J. Sales de Gauzy, A. Chalopin, A. Ibnoulkhatib, et al. 2015. « Evolution of Adolescent Idiopathic Scoliosis: Results of a Multicenter Study at 20 Years' Follow-Up ». *Orthopaedics & Traumatology, Surgery & Research: OTSR* 101 (5): 619-22.

Pialasse, Jean-Philippe, Martin Descarreaux, Pierre Mercier, Jean Blouin, et Martin Simoneau. 2015. « The Vestibular-Evoked Postural Response of Adolescents with Idiopathic Scoliosis Is Altered ». *PloS One* 10 (11): e0143124.

Pialasse, Jean-Philippe, Pierre Mercier, Martin Descarreaux, et Martin Simoneau. 2017. « A Procedure to Detect Abnormal Sensorimotor Control in Adolescents with Idiopathic Scoliosis ». *Gait & Posture* 57 (septembre): 124-29.

Pomero, V., F. Lavaste, G. Imbert, et W. Skalli. 2004. « A Proprioception Based Regulation Model to Estimate the Trunk Muscle Forces ». *Computer Methods in Biomechanics and Biomedical Engineering* 7 (6): 331-38.

Rebeyrat, Guillaume, Wafa Skalli, Rami Rachkidi, Hélène Pillet, Abir Massaad, Joe Mehanna, Karl Semaan, Eddy Saad, Ismat Ghanem, et Ayman Assi. 2022. « Assessment of Dynamic Balance during Walking in Patients with Adult Spinal Deformity ». *European Spine Journal: Official Publication of the European Spine Society, the European Spinal Deformity Society, and the European Section of the Cervical Spine Research Society* 31 (7): 1736-44.

Richards, B. Stephens, Robert M. Bernstein, Charles R. D'Amato, et George H. Thompson. 2005. « Standardization of Criteria for Adolescent Idiopathic Scoliosis Brace Studies: SRS Committee on Bracing and Nonoperative Management ». *Spine* 30 (18): 2068-75; discussion 2076-2077.

Risser, J. C. 1958. « The Iliac Apophysis; an Invaluable Sign in the Management of Scoliosis ». *Clinical Orthopaedics* 11: 111-19.

Sandoz, Baptiste, Sébastien Laporte, Wafa Skalli, et David Mitton. 2010. « Subject-Specific Body Segment Parameters' Estimation Using Biplanar X-Rays: A Feasibility Study ». *Computer Methods in Biomechanics and Biomedical Engineering* 13 (6): 649-54.

Schlösser, Tom P. C., Marijn van Stralen, Rob C. Brink, Winnie C. W. Chu, Tsz-Ping Lam, Koen L. Vincken, René M. Castelein, et Jack C. Y. Cheng. 2014. « Three-Dimensional Characterization of Torsion and Asymmetry of the Intervertebral Discs versus Vertebral Bodies in Adolescent Idiopathic Scoliosis ». *Spine* 39 (19): E1159-1166.

Schmid, Samuel L., F. M. Buck, T. Böni, et M. Farshad. 2016. « Radiographic Measurement Error of the Scoliotic Curve Angle Depending on Positioning of the Patient and the Side of Scoliotic Curve ». *European Spine Journal: Official Publication of the European Spine Society, the European Spinal Deformity Society, and the European Section of the Cervical Spine Research Society* 25 (2): 379-84.

Schwab, Frank, Virginie Lafage, Reid Boyce, Wafa Skalli, et Jean-Pierre Farcy. 2006. « Gravity Line Analysis in Adult Volunteers: Age-Related Correlation with Spinal Parameters, Pelvic Parameters, and Foot Position ». *Spine* 31 (25): E959-967.

Skalli, Wafa, Claudio Vergari, Eric Ebermeyer, Isabelle Courtois, Xavier Drevelle, Remi Kohler, Kariman Abelin-Genevois, et Jean Dubousset. 2017. « Early Detection of Progressive Adolescent Idiopathic Scoliosis: A Severity Index ». *Spine* 42 (11): 823-30.

Stagnara, P., et P. Queneau. 1953. « [Developmental scolioses during the period of growth; clinical and radiological aspects and therapeutic considerations] ». *Revue De Chirurgie Orthopedique Et Reparatrice De L'appareil Moteur* 39 (3-4): 378-452.

Steffen, Jean-Sebastien, Ibrahim Obeid, Nicolas Aurouer, Olivier Hauger, Jean-Marc Vital, Jean Dubousset, et Wafa Skalli. 2010. « 3D Postural Balance with Regard to Gravity Line: An Evaluation in the Transversal Plane on 93 Patients and 23 Asymptomatic Volunteers ». *European Spine Journal: Official Publication of the European Spine Society, the European Spinal Deformity Society, and the European Section of the Cervical Spine Research Society* 19 (5): 760-67.

Steib, Jean-Paul, Raphaël Dumas, David Mitton, et Wafa Skalli. 2004. « Surgical Correction of Scoliosis by in Situ Contouring: A Detorsion Analysis ». *Spine* 29 (2): 193-99.

Stokes, I. A., H. Spence, D. D. Aronsson, et N. Kilmer. 1996. « Mechanical Modulation of Vertebral Body Growth. Implications for Scoliosis Progression ». *Spine* 21 (10): 1162-67.

Tan, Ken-Jin, Maung Maung Moe, Rose Vaithinathan, et Hee-Kit Wong. 2009. « Curve Progression in Idiopathic Scoliosis: Follow-up Study to Skeletal Maturity ». *Spine* 34 (7): 697-700.

Thenard, Thomas, Claudio Vergari, Thibault Hernandez, Raphael Vialle, et Wafa Skalli. 2019. « Analysis of Center of Mass and Gravity-Induced Vertebral Axial Torque on the Scoliotic Spine by Barycentremetry ». *Spine Deformity* 7 (4): 525-32.

Vergari, C, L Gajny, I Courtois, E Ebermeyer, K Abelin-Genevois, Y Kim, T Langlais, et al. 2019. « Quasi-Automatic Early Detection of Progressive Idiopathic Scoliosis from Biplanar Radiography: A Preliminary Validation. » *Eur Spine J* 28: 1970-76.

Vergari, C, W Skalli, K Abelin-Genevois, JC Bernard, Z Hu, JCY Cheng, WCW Chu, et al. 2021. « Effect of Curve Location on the Severity Index for Adolescent Idiopathic Scoliosis: A Longitudinal Cohort Study. » *Eur Radiol* 31: 8488-97.

Vergari, Claudio, Guillaume Dubois, Raphael Vialle, Jean-Luc Gennisson, Mickael Tanter, Jean Dubousset, Philippe Rouch, et Wafa Skalli. 2016. « Lumbar Annulus Fibrosus Biomechanical Characterization in Healthy Children by Ultrasound Shear Wave Elastography ». *European Radiology* 26 (4): 1213-17.

Vergari, Claudio, Mohammad Karam, Raphael Pietton, Raphael Vialle, Ismat Ghanem, Wafa Skalli, et Ayman Assi. 2020. « Spine Slenderness and Wedging in Adolescent Idiopathic Scoliosis and in Asymptomatic Population: An Observational Retrospective Study ». *European Spine Journal* 29 (4): 726-36.

Vergari, Claudio, Philippe Rouch, Guillaume Dubois, Dominique Bonneau, Jean Dubousset, Mickael Tanter, Jean-Luc Gennisson, et Wafa Skalli. 2014a. « Intervertebral Disc Characterization by Shear Wave Elastography: An in Vitro Preliminary Study ». *Proceedings of the Institution of Mechanical Engineers. Part H, Journal of Engineering in Medicine* 228 (6): 607-15.

Vergari, Claudio, Philippe Rouch, Guillaume Dubois, Dominique Bonneau, Jean Dubousset, Mickael Tanter, Jean-Luc Gennisson, et Wafa Skalli. 2014b. « Non-Invasive Biomechanical Characterization of Intervertebral Discs by Shear Wave Ultrasound Elastography: A Feasibility Study ». *European Radiology* 24 (12): 3210-16. https://doi.org/10.1007/s00330-014-3382-8.

Vergari, Claudio, Wafa Skalli, Kariman Abelin-Genevois, Jean-Claude Bernard, Zongshan Hu, Jack Chun Yiu Cheng, Winnie Chiu Wing Chu, et al. 2022. « Spine Slenderness Is Not an Early Sign of Progression in Adolescent Idiopathic Scoliosis ». *Medical Engineering & Physics* 108 (octobre): 103879.

Vidal, Christophe, Keyvan Mazda, et Brice Ilharreborde. 2016. « Sagittal Spino-Pelvic Adjustment in Severe Lenke 1 Hypokyphotic Adolescent Idiopathic Scoliosis Patients ». *European Spine Journal: Official Publication of the European Spine Society, the European Spinal Deformity Society, and the European Section of the Cervical Spine Research Society* 25 (10): 3162-69.

Villemure, I., C. E. Aubin, G. Grimard, J. Dansereau, et H. Labelle. 2001. « Progression of Vertebral and Spinal Three-Dimensional Deformities in Adolescent Idiopathic Scoliosis: A Longitudinal Study ». *Spine* 26 (20): 2244-50.

Violas, Philippe, Erik Estivalezes, Jérome Briot, Jérome Sales de Gauzy, et Pascal Swider. 2007. « Quantification of Intervertebral Disc Volume Properties below Spine Fusion, Using Magnetic Resonance Imaging, in Adolescent Idiopathic Scoliosis Surgery ». *Spine* 32 (15): E405-412.

Vital, J. M., et J. Senegas. 1986. « Anatomical Bases of the Study of the Constraints to Which the Cervical Spine Is Subject in the Sagittal Plane. A Study of the Center of Gravity of the Head ». *Surgical and Radiologic Anatomy: SRA* 8 (3): 169-73.

W, Skalli, Zeller Rd, Miladi L, Bourcereau G, Savidan M, Lavaste F, et Dubousset J. 2006. « Importance of Pelvic Compensation in Posture and Motion after Posterior Spinal Fusion Using CD Instrumentation for Idiopathic Scoliosis ». *Spine* 31 (12).

Weinstein, Stuart L., Lori A. Dolan, James G. Wright, et Matthew B. Dobbs. 2013. « Effects of Bracing in Adolescents with Idiopathic Scoliosis ». *The New England Journal of Medicine* 369 (16): 1512-21.

Will, Ryan E., Ian A. Stokes, Xing Qiu, Matthew R. Walker, et James O. Sanders. 2009. « Cobb Angle Progression in Adolescent Scoliosis Begins at the Intervertebral Disc ». *Spine* 34 (25): 2782-86.

Yu, Jing, Jeremy C. T. Fairbank, Sally Roberts, et Jill P. G. Urban. 2005. « The Elastic Fiber Network of the Anulus Fibrosus of the Normal and Scoliotic Human Intervertebral Disc ». *Spine* 30 (16): 1815-20.

Yu, Jing, Peter C. Winlove, Sally Roberts, et Jill P. G. Urban. 2002. « Elastic Fibre Organization in the Intervertebral Discs of the Bovine Tail ». *Journal of Anatomy* 201 (6): 465-75.

X - Publications dans des revues à comité de lecture scientifique réalisées avec le laboratoire de l'Institut de Biomécanique Humaine Georges Charpak dans le cadre des années de doctorat

- **Analyse sagittale du cintrage manuel des tiges dans la correction par translation postérieure concave des scolioses thoraciques idiopathiques de l'adolescent (Lenke 1 et 3)**

  Langlais T, Bouy A, Gauthier E, Mainard N, Skalli W, Vergari C, Vialle R

  Orthopaedics & Traumatology: Surgery & Research (2022)

- **Spine slenderness is not an early sign of progression in adolescent idiopathic scoliosis**

  Vergari C, Skalli W, Abelin- Genevois K, Bernard JC, Hu Z, Cheng JCY, Chu WCW, Assi A, Karam M, Ghanem I, Bassani T, Galbusera F, Sconfienza LM, Brayda-Bruno M, Courtois I, Ebermeyer E, Vialle R, Langlais T, Dubousset J

  Medical Engineering and Physics (2022)

- **Changes in quantitative elastography assessment of the adjacent lumbar disc after segmental fixation of the spine : a case description of a burst fracture of L4**

  Pietton R, Vialle R, Laurent R, Skalli W, Vergari C, Langlais T

  Quantitative Imaging in Medecine and Surgery (2022)

- **3D quasi-automatic spine length assessment using low dose biplanar radiography after surgical correction in thoracic idiopathic scoliosis**

  Langlais T, Vergari C, Xavier F, Al Hawsawi M, Gajny L, Vialle R, Skalli W, Pietton R

  Medical Engineering and Physics (2022)

- **Estimating pulmonary function after surgery for adolescent idiopathic scoliosis using biplanar radiographs of the chest with 3D reconstruction**

  Pietton R, Bouloussa H, Langlais T, Taytard J, Beydon N, Skalli W , Vergari C, Vialle R

  Bone and Joint Journal (2022)

- **Balance, barycentremetry and external shape analysis in idiopathic scoliosis: What can the physician expect from it?**

  Langlais T, Vergari C, Rougereau G, Gajny L, Assi A, Ghanem I, Dubousset J, Vialle R, Pietton R, Skalli W

  Medical Engineering and Physics (2021)

- **Effect of curve location on the severity index for adolescent idiopathic scoliosis: a longitudinal cohort study**

  Vergari C, Skalli W, Abelin- Genevois K, Bernard JC, Hu Z, Cheng JCY, Chu WCW, Assi A, Karam M, Ghanem I, Bassani T, Galbusera F, Sconfienza LM, Brayda-Bruno M, Courtois I, Ebermeyer E, Vialle R, Langlais T, Dubousset J

  European Radiology (2021)

- **Towards a predictive simulation of brace action in adolescent idiopathic scoliosis**

  Vergari C, Chen Z, Robichon L, Corutois I, Ebermeyer E, Vialle R, Langlais T, Pietton R, Skalli W

  Computer Methods in Biomechanics and Biomedical Engineering (2020)

- **Biomechanical evaluation of intercostal muscles in healthy children and adolescent idiopathic scoliosis: A preliminary study**

  Pietton R, David M, Hisaund A, Langlais T, Skalli W, Vialle R, Vergari C.

  Ultrasound in Medicine and Biology (2020)

- **Shear wave elastography of lumbar annulus fibrosus in adolescent idiopathic scoliosis before and after surgical intervention**

  Vergari C, Chanteux L, Pietton R, Langlais T, Vialle R, Skalli W

  European Radiology (2019)

- **Microstructural characterization of annulus fibrosus by ultrasonography: a feasibility study with an in vivo and in vitro approach**

Langlais T, Desprairies P, Pietton R, Rohan PY, Dubousset J, Meakin JR, Winlove PC, Vialle R, Skalli W, Vergari C

Biomechanics and Modeling in Mechanobiology (2019)

- **Quasi-automatic early detection of progressive idiopathic scoliosis from biplanar radiography: a preliminary validation**

  Vergari C, Gajny L, Courtois I, Ebermeyer E, Abelin- Genevois K, Kim Y, Langlais T, Vialle R, Assi A, Ghanem I, Dubousset J, Skalli W

  European Spine Journal (2019)

- **Shear-wave elastography can evaluate annulus fibrosus alteration in adolescent scoliosis**

  Langlais T, Vergari C, Pietton R, Dubousset J, Skalli W, Vialle R

  European Radiology (2018)

HESAM UNIVERSITÉ

Arts et Métiers Sciences et Technologies

Tristan Langlais

Recherche de paramètres biomécaniques améliorant le diagnostic et l'évaluation thérapeutique d'une scoliose idiopathique de l'adolescent

Résumé : L'avènement de l'analyse personnalisée tridimensionnelle non invasif de la colonne vertébrale a permis de développer de nombreux paramètres biomécaniques mais certains restent à évaluer. L'objectif de cette thèse était d'évaluer le rôle possible de ces paramètres dans la prédiction d'une scoliose progressive et d'étudier leurs variations après une correction chirurgicale.
Un trouble de l'alignement global précoce semble être un potentiel paramètre de progression et plus particulièrement la mesure coronale dans les scolioses thoraciques. La barycentremétrie est perturbée à un stade précoce et les propriétés liées à la vertèbre sommet (le centre de masse ou son moment intersegmentaire) semblent être prédicteur d'une progression d'une courbure thoracique. Ces perturbations biomécaniques liées à l'asymétrie du pli de taille et du barycentre sont réversibles après traitement chirurgical et sont corrélées à la correction du plan axial. Enfin, les perturbations biomécaniques de l'*annulus fibrosus* lombaire sont détectables par l'élastographie ultrasonore et sont réversibles après une correction chirurgicale.
Les résultats sont prometteurs et démontrent l'intérêt de l'analyse tridimensionnelle de l'alignement, de l'asymétrie du pli du taille, du barycentre et de l'utilisation de l'élastographie dans la prise en charge de la scoliose idiopathique. Ces travaux ouvrent des perspectives de recherche et une application clinique importante avec comme exemple la validation à grande échelle de l'ajout de paramètres spécifiques dans l'indice de sévérité ou une meilleure planification de la correction chirurgicale.

Mots-clés : Scoliose idiopathique, Courbure progressive, Arthrodèse, Radiographies biplanaires, Barycentremétrie, Enveloppe externe, Reconstruction 3D, Annulus fibrosus

Biomechanical parameter research improving diagnosis and therapeutic evaluation of adolescent idiopathic scoliosis

Summary: The advent of custom three-dimensional and non-invasive spinal analysis has led to the development of many biomechanical parameters, but some remain to be assessed. The purpose of this thesis was to assess the potential role of these parameters in predicting progressive scoliosis and to study their variations after surgical correction.
Early global alignment disorders appear to be a potential parameter of progression and especially coronal measurement in thoracic scoliosis. Barycentremetry is disrupted at an early stage and the properties related to the apical vertebra (the center of mass or its intersegmental moment) appear to predict a progression of a thoracic curvature. The coronal trunk balance and the barycenter-related biomechanical disturbances are reversible after surgical treatment and correlate with axial plane correction. Finally, biomechanical disturbances of the *annulus fibrosus* lumbar are detectable by ultrasonic elastography and are reversible after surgical correction.
The findings are promising and demonstrate the value of three-dimensional analysis of alignment, coronal trunk balance, barycenter and the use of elastography in the management of idiopathic scoliosis. This work provides prospects for research and important clinical application, such as large-scale validation of the inclusion of selected parameters in the severity index or better planning of surgical correction.

Keywords : Idiopathic scoliosis, Progressive curvature, Arthrodesis, Biplanar radiographs, Barycentremetry, External enveloppe, 3D reconstruction, Annulus fibrosus